St. Anthony Falls Hydraulic Laboratory
University of Minnesota

Project Report No. 214

MIXING OF THE METRO WASTEWATER TREATMENT PLANT

EFFLUENT WITH THE MISSISSIPPI RIVER BELOW ST. PAUL

by

Heinz G. Stefan

TABLE OF CONTENTS

MIXING OF THE METRO WWTP EFFLUENT

WITH THE MISSISSIPPI RIVER IN SUMMER

SUMMARY

As a result of this study the following description of the Metro
Wastewater Treatment Plant (WWTP) effluent zone in the Mississippi River
below St. Paul can be given:

● The shape and the size of the mixing zone changes with season.
  Only summer conditions were analyzed specifically.

● The longest mixing zone can be expected in fall or spring when the
  mixing is controlled by transverse spreading under neutrally
  buoyant conditions. Such conditions may also exist at very high
  flows during other seasons.

● Between June and August the Metro WWTP effluent plunges below the
  water surface before reaching the end of the diverging outlet chan-
  nel. The process also occurs in May and ends sometime in Sep-
  tember. The effluent water therefore enters the Mississippi River
  as a submerged flow (underflow). Water temperatures and higher
  dissolved solids content in the effluent relative to the oncoming
  Mississippi River water are the cause of the plunging phenomenon
  and the underflow.

● The river becomes vertically stratified below the outlet due to the
  sinking of the effluent into the deepest part of the river main
  channel.

● The spread of the effluent underflow across the river bottom during
  June, July and August appears essentially completed within 0.3
  miles or less from the outlet, the actual distance depending on
  river flow rate. An analysis of the initial transverse spreading
  process (nearfield) has not been made.

● The most appropriate model for the summer Metro WWTP effluent
  mixing zone is therefore a model which considers the plunging,
  transverse underflow and vertical mixing in the river.

1

- The stratified river is vertically mixed by two mechanisms:

  (a) turbulence induced by shear on the river bed and secondary flow due to channel irregularities, and

  (b) barge traffic (tug boats, barge tows).

- To accomplish complete vertical mixing by turbulent shear flow a distance of approximately 0.8 miles or more, dependent on river flow rate, is required. At river flow rates below an estimated 5,000 cfs shear induced vertical mixing becomes very slow and the mixing zone can become several miles long.

- Barge traffic mixes the stratified river very effectively. The passage of three barge tows appears sufficient to reduce vertical water quality differentials to natural values or the values within measurement accuracy.

- An approximate frequency of one barge tow per hour was observed on weekdays. At that frequency the effluent mixing zone will not exceed an approximate length of 1.3 miles below the outlet.

- Under existing conditions barge traffic controls the length of the mixing zone in the summer when river flows are below 6,000 cfs, whereas for river flows above 20,000 cfs mixing is predominantly by shear flow. Between 6,000 and 20,000 cfs, both processes make significant contributions.

- Figure IX-1 gives the best current estimate of the Metro WWTP effluent mixing zone in summer. Further studies of vertical mixing in the Mississippi River are recommended to refine the result.

I. OBJECTIVE

The objective of this study was to provide qualitative and quantitative information on the mixing between the Metro WWTP effluent and the Mississippi River under summer flow conditions. The objective was accomplished in four steps:

1) Identification of effluent mixing processes.

2) Theoretical analysis of significant processes and formulation of alternative mixing zone models.

3) Collection of field data in the Mississippi River in July and August 1982.

4) Estimation of summer mixing zone lengths.

II. MIXING ZONE CONCEPT

The mixing zone can be thought of as that portion (volume) of the river necessary to achieve dilution of the effluent water to specified levels of concentration. The size of the mixing zone can be observed by lines (surfaces) of equal concentration (isopleths) or equal temperature (isotherms) as illustrated in Figure II-1. The concentrations (e.g. of chloride) or temperatures are excess values over and above those in the river upstream from the discharge. As effluent water and river mix, excess concentrations or excess temperatures diminish. The size, shape, length or width of the mixing zone depend on the value of excess concentration or temperature chosen as the limit of the mixing zone.

A mixing zone model describes the location of the isopleths as a function of river and outlet channel geometry, river flow, and effluent flow conditions. The development of the model takes into consideration the processes listed in the next section.

3

Waste Water Discharge

River

Mixing
Zone

A

A

Surface Isopleth
or Isotherm

Isopleth or
Isotherm
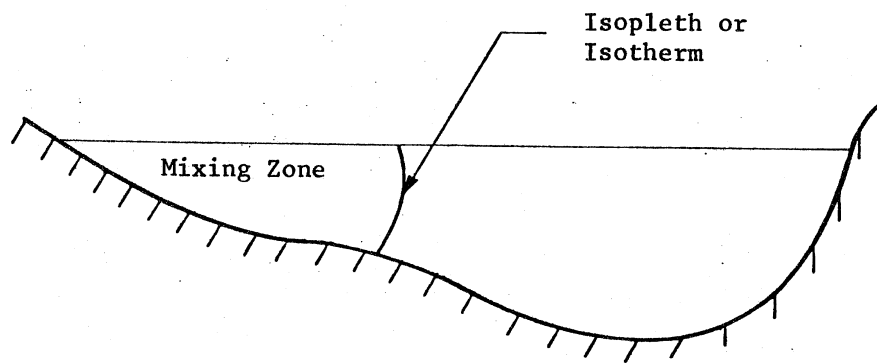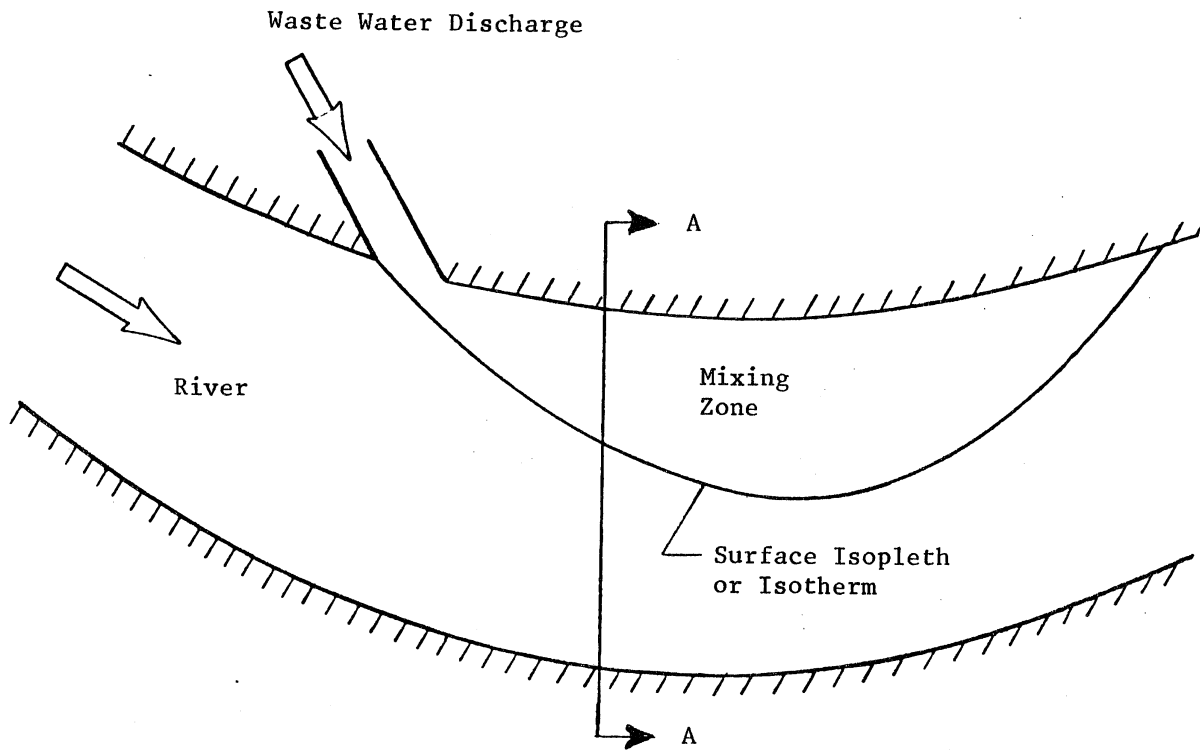
Mixing Zone

Section A - A

Fig. II-1. Schematic view of a mixing zone below an
effluent outlet into a river.

4

III. MIXING PROCESSES

A side channel discharge such as that from the Metro WWTP into the Mississippi River interacts with the river flow in several ways before the two become fully mixed. Among the flow and mixing processes generally to be considered are:

(a) Jet effects due to the momentum of the discharge.

(b) Lateral displacement of river flow by the effluent input. Conservation of mass requires that the streamlines in the river are displaced towards the center to make room for the effluent flow rate in the river (Fig. III-1).

(c) Downstream advection by the river flow.

(d) Transverse turbulent mixing due to bed shear and secondary flow in the river.

(e) Buoyant spreading caused by the density difference between effluent water and river water. The density depends on water temperature and total solids content (Fig. III-2).

(f) Vertical turbulent mixing by the river due to bed shear.

(g) Mixing by tug boats and barge traffic.

To facilitate the analysis it can be considered that some of the above processes occur in sequence. Schematic subdivisions of the mixing regimes downstream from a shore located effluent source are shown in Figs. III-3 and III-4; these figures present alternatives. The sequence shown in Fig. III-3 is typical for a nonbuoyant or weakly buoyant discharge. For strongly buoyant flow, the sequence shown in Fig. III-4 is more appropriate.

Effluent models are usually subdivided into a NEARFIELD and a FARFIELD. In the nearfield the mixing and dilution are influenced by effluent conditions. In the farfield, the mixing is passive and imposed by the river conditions. The nearfield is represented by Region 1 in Figs. III-3 and III-4; the farfield is given by Regions 3 and 4. Region 2 is a transition and will be incorporated into the nearfield.

5
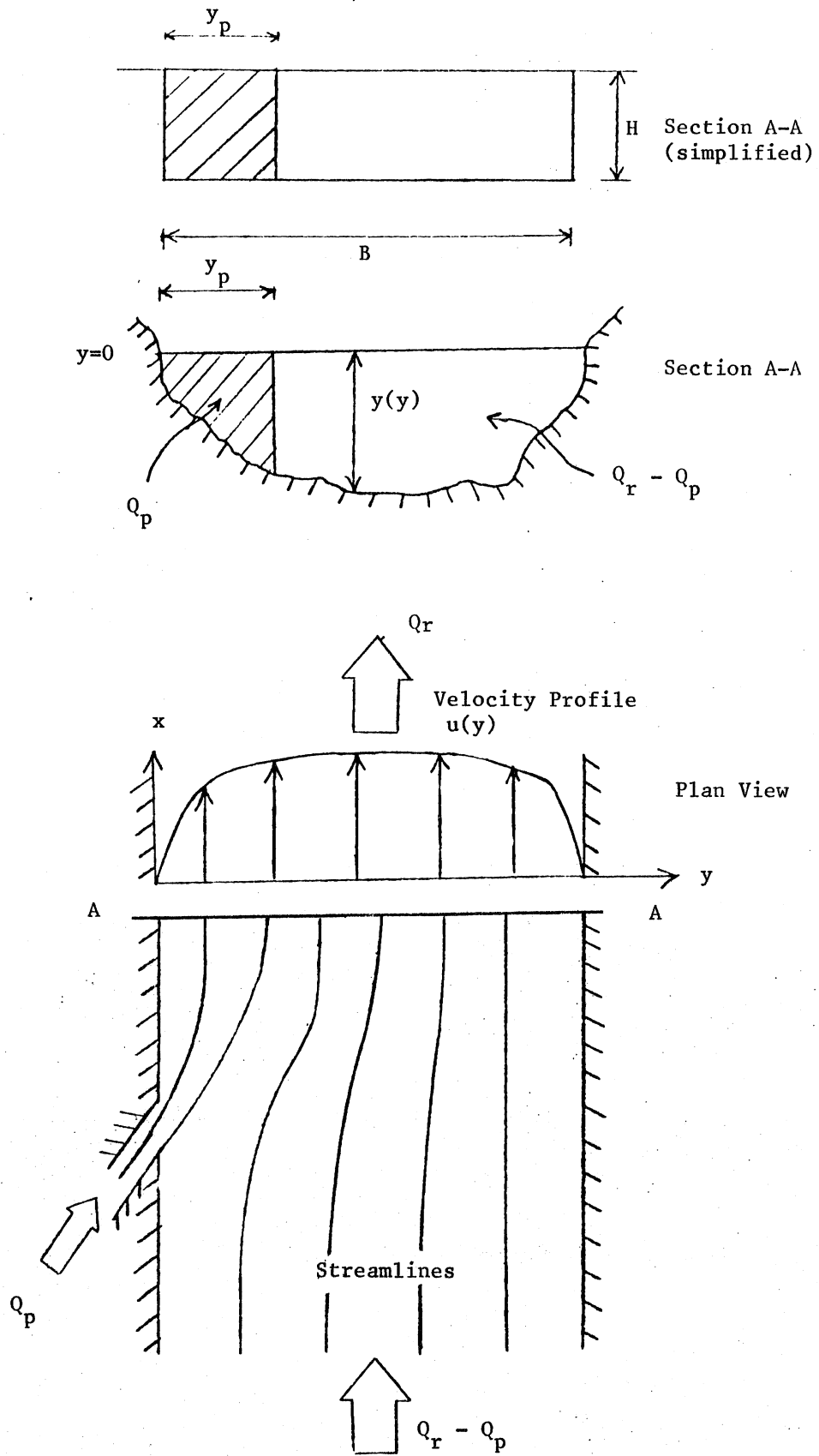
Fig. III-1. Streamlines and displacement width y_p near side channel effluent outlet. Q_r = river flow rate, Q_p = plant effluent discharge.
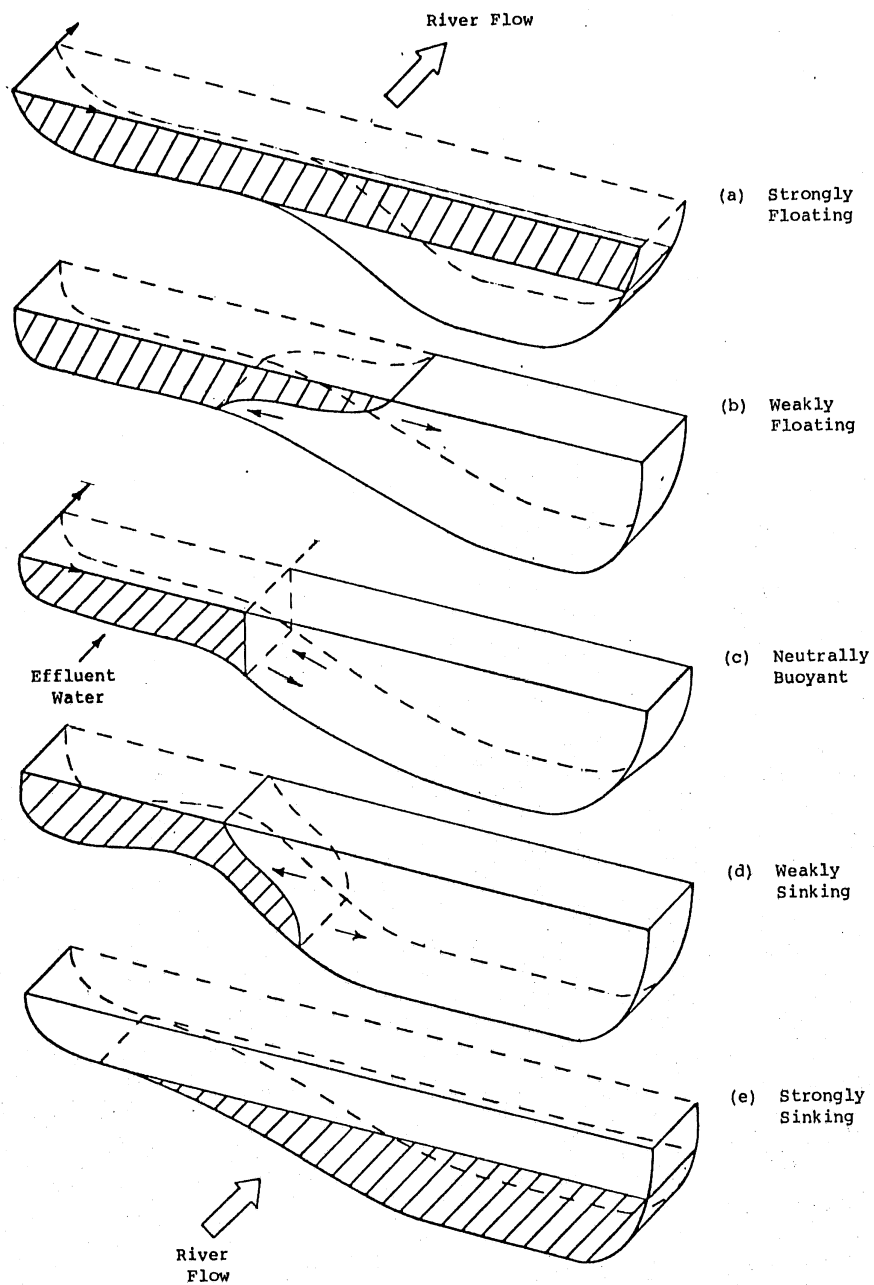
Fig. III-2. Effects of effluent water buoyancy on transverse
spreading and vertical stratification. Effluent
discharge is on the left bank. Cross sections
shown are some distance downstream from the outlet.

Vertically
Completely
Mixed

Transversely
Completely
Mixed

Streamflow

Region 1

8

Region 2

Region 3

Region 4

Waste
Water

Jet and
Displace -
ment Effects

Vertically
Stratified

Vertically Well-Mixed
Transverse Concentration Gradients

Well-Mixed
Cross Section.
Longitudinal
Concentration
Gradients Only

Fig. III-3. Mixing regions downstream from an effluent source with weak buoyancy.
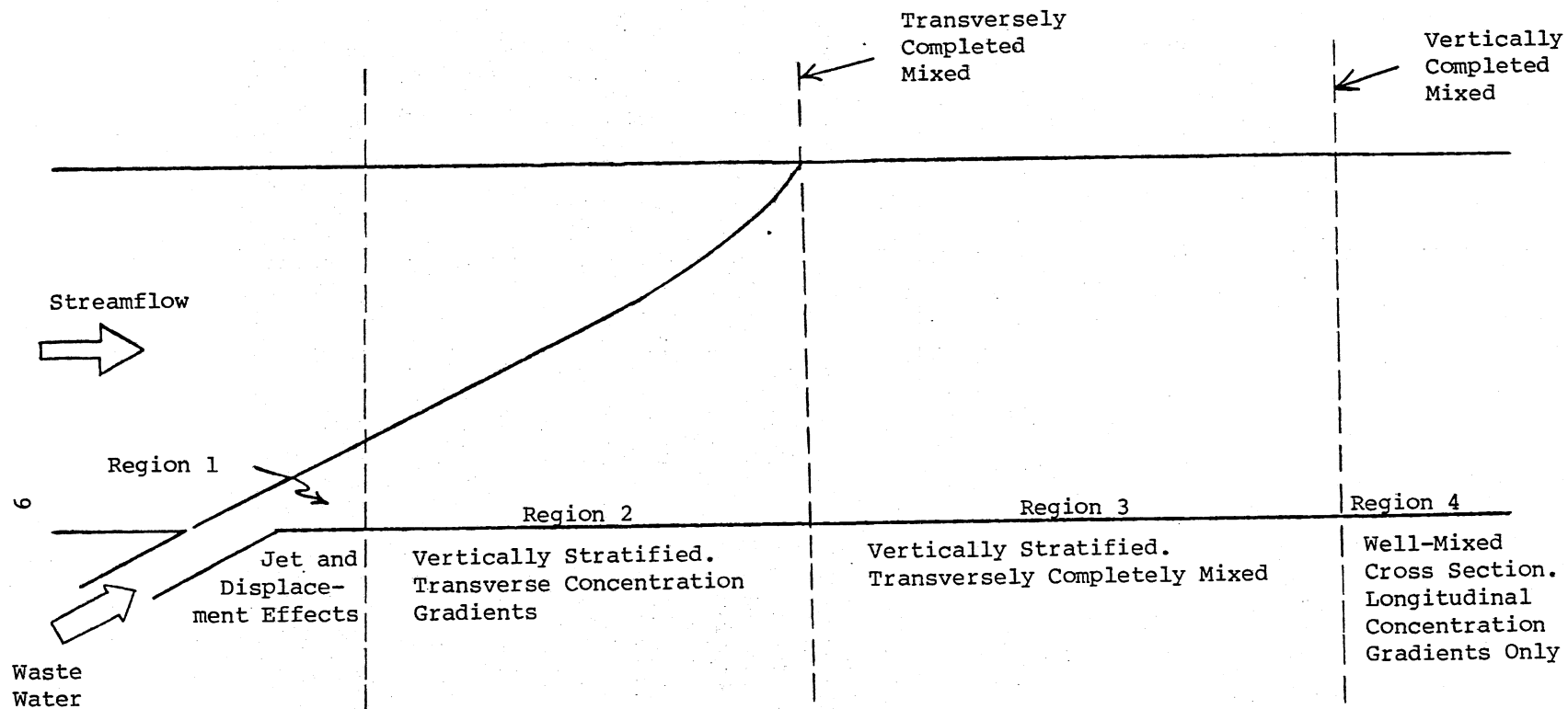
Fig. III-4. Mixing regions downstream from an effluent source with strong buoyancy.
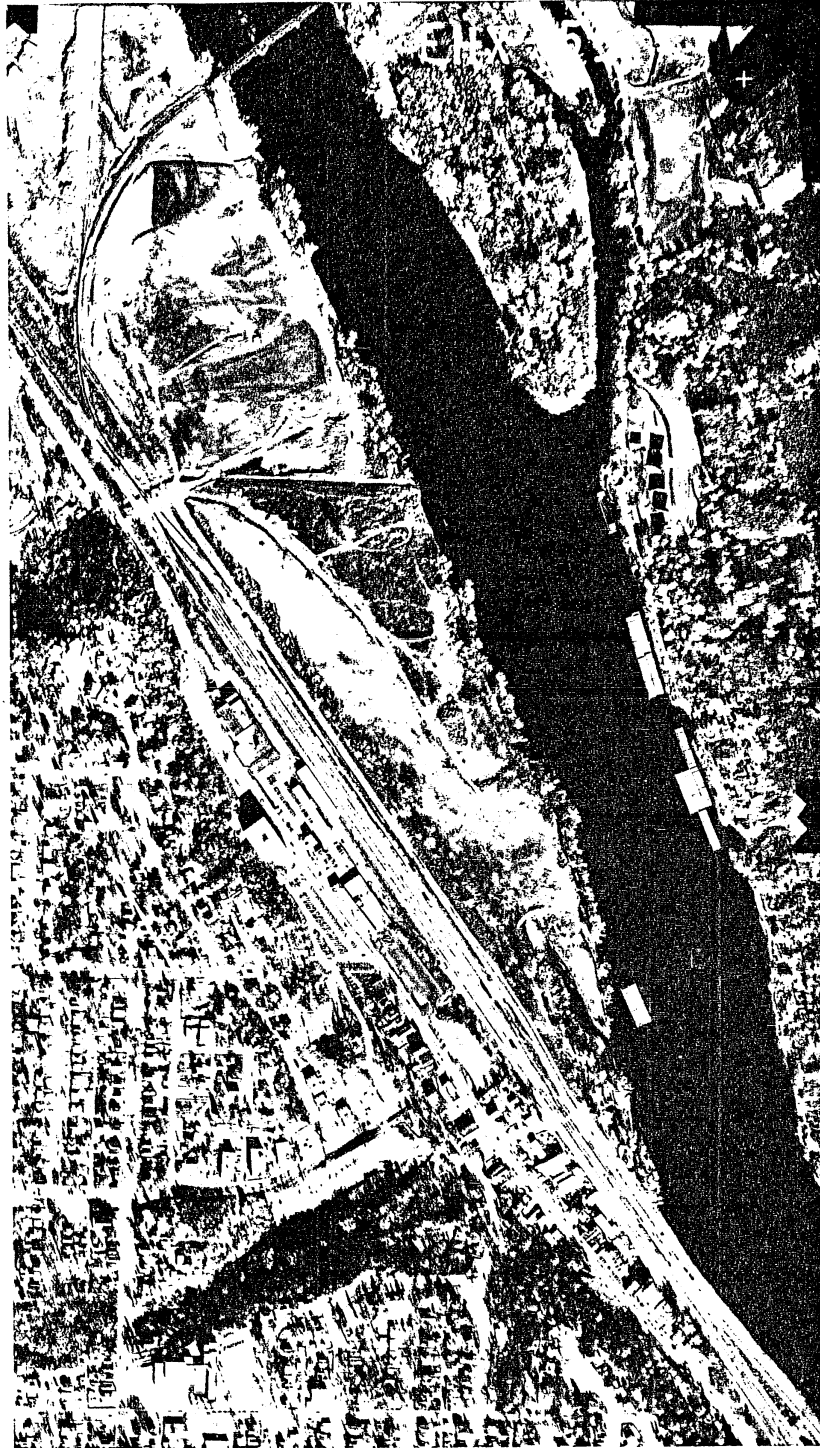
Fig. IV-2. Aerial view showing vicinity of discharge.

TABLE IV-1 - Mississippi River Flows (cfs) at St. Paul

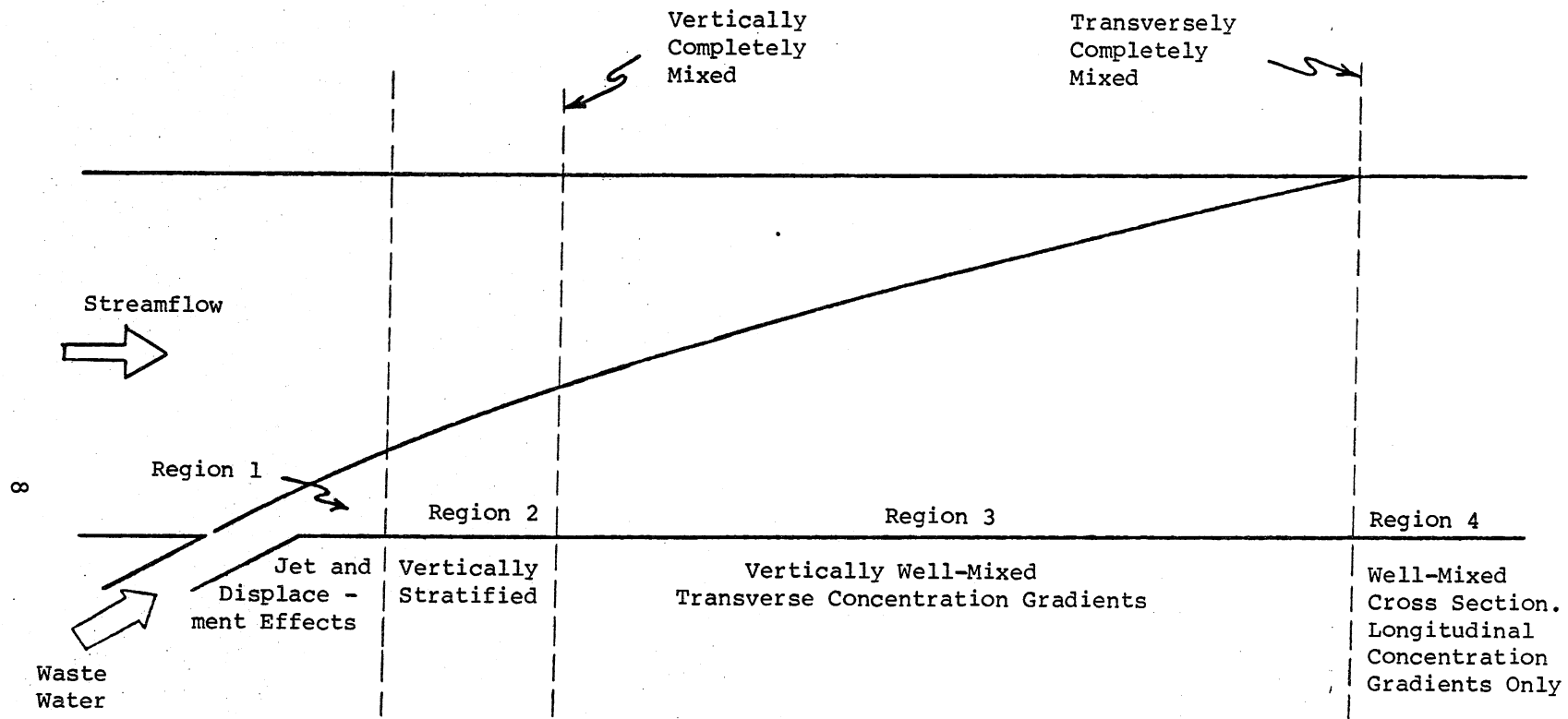|	June			July			August			September		
	MIN	AVG	MAX	MIN	AVG	MAX	MIN	AVG	MAX	MIN	AVG	MAX
1971	12400	15800	19000	8280	15290	20200	2880	4530	8240	1690	2195	2840
1972	15300	19220	22000	11000	21030	48600	19000	27050	42600	2910	3650	4440
1973	8200	14940	23800	3780	6110	8350	5710	7825	9340	4160	5809	7460
1974	16200	29200	39400	6070	8757	1590	4460	6645	8580	2810	3658	4520
1975	20000	26970	39400	10200	24170	38900	5460	7137	10800	5750	6265	7460
1976	2680	3190	4050	1610	2564	3980	723	1440	1850	821	1153	1650
1977	3450	5671	9590	2870	4173	6530	1480	2508	7670	4980	6211	8420
1978	15900	19530	22800	15800	22640	29700	8700	11970	16200	11100	13340	15600
1979	16700	24320	33600	16700	23460	33000	16500	21400	35100	7740	18190	36200
1980	6110	15680	23000	3670	5395	8670	3100	4295	6120	4900	7418	10900
Hist. Avg.		19150			15380			8250			7601	

13
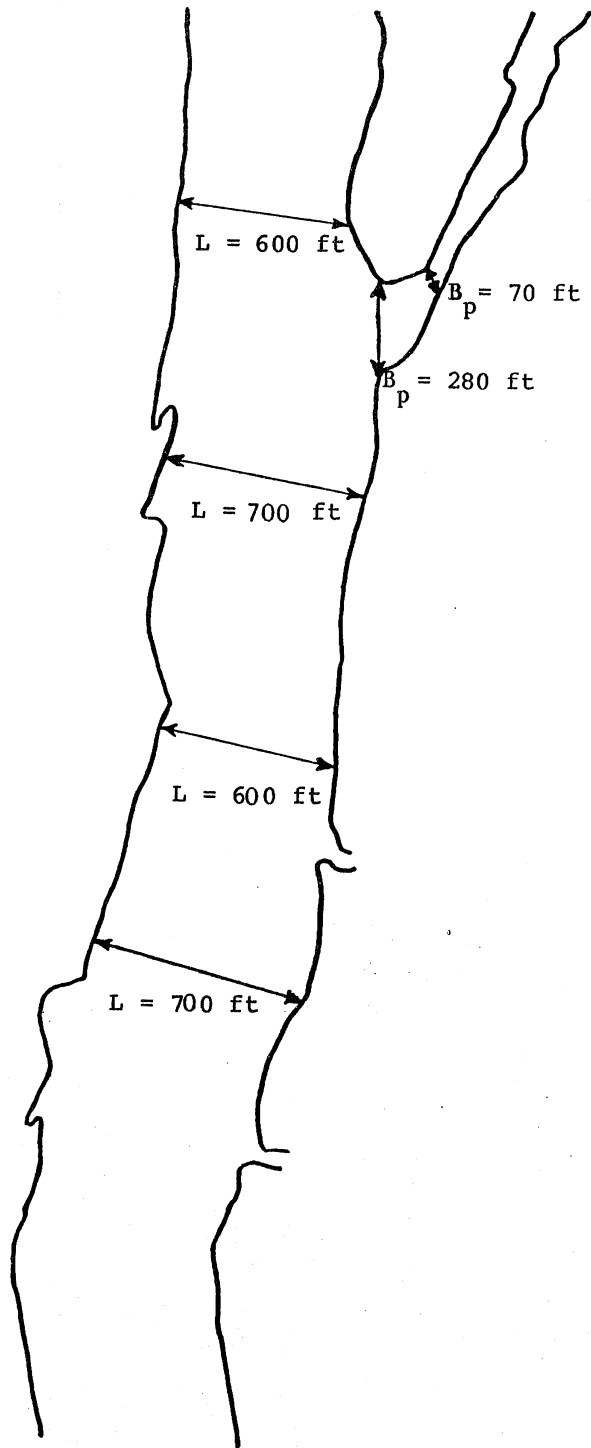
Fig. IV-3. Distances as scaled from Photo EHX-55 (taken
            11-19-76). Scale on Photo: 1" - 735'.

14

TABLE IV-2 - Metro WWTP Effluent Flows (mgd)

	June			July			August			September		
1978	MIN	AVG	MAX	MIN	AVG	MAX	MIN	AVG	MAX	MIN	AVG	MAX
1978	180	242	346	200	292	371	167	250	335	163	230	496
1979	191	254	338	173	221	321	165	242	414	169	242	471
1980	170	237	420	146	190	224	156	198	276	152	197	364
1981	197	233	347	178	230	343	193	241	391	186	224	272
Avg.		242			233			233			223	

Four Month Avg. = 233 mgd = 360 cfs

Fig. IV-4. Typical water temperatures.

TABLE IV-3 — Mean Monthly Water Temperatures and Water Densities

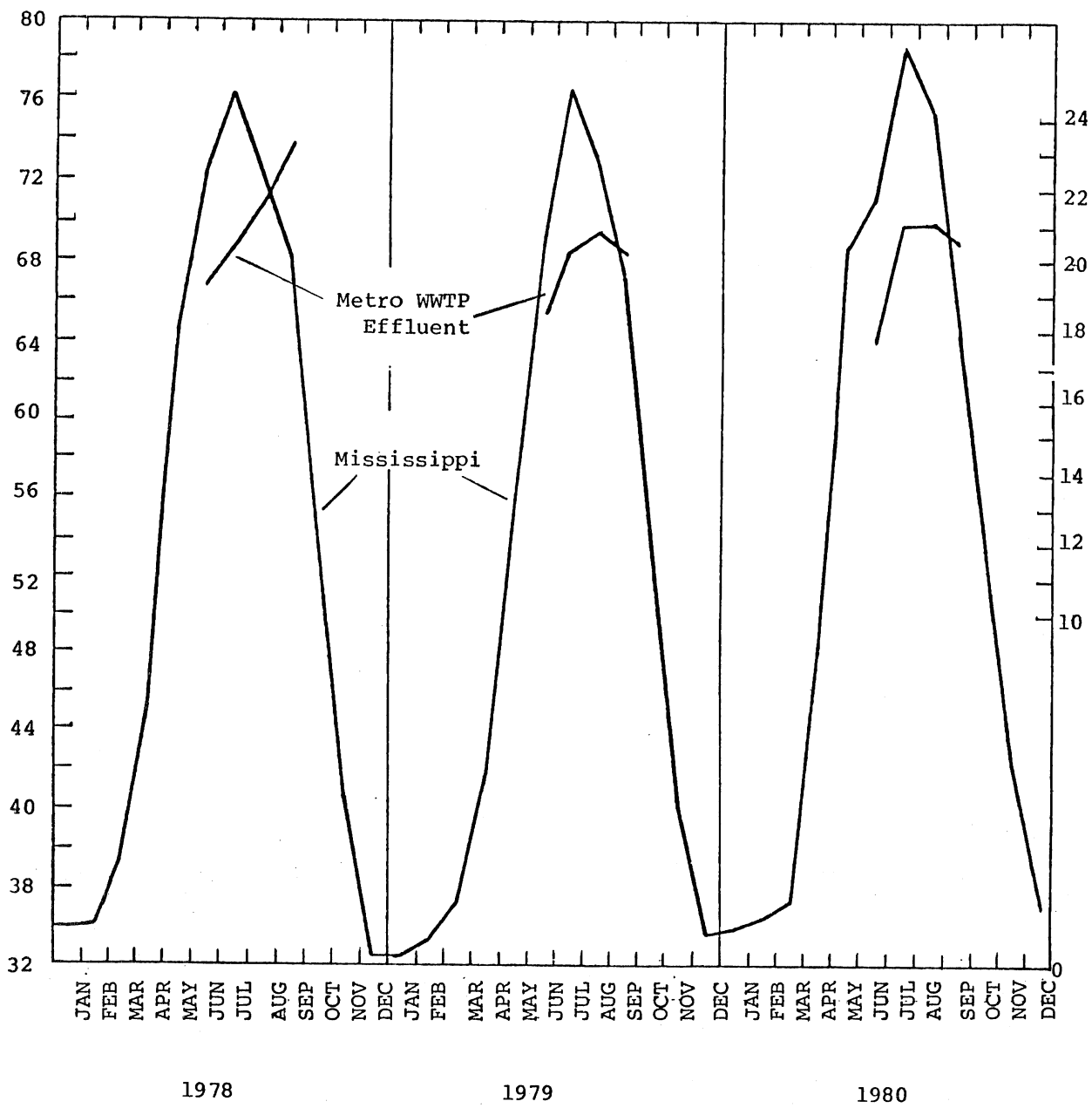| | Mississippi River — St. Paul (UM 829.4 & UM 826.8) | | | | | | Metro WWTP Effluent | | | | |
| | T | ρ_T | TDS | $\Delta\rho_{TDS}$ | ρ_r | | T | ρ_T | TDS | $\Delta\rho_{TDS}$ | ρ_p[1] | $\rho_p - \rho_r$ |
	(°C)	(g/cm^3)	(mg/ℓ)	(g/cm^3)	(g/cm^3)		(°C)	(g/cm^3)	(mg/ℓ)	(g/cm^3)	(g/cm^3)	(g/cm^3)
1978												
Jun	21.42	.99793					19.21	.99839				.00046
Jul	24.48	.99720					20.36	.99815				.00125
Aug	24.17	.99728					21.73	.99787				.00059
Sep	20.17	.99819					23.34	.99750				-.00069
1979												
Jun	20.61	.99811					18.46	.99853				.00043
Jul	24.50	.99720					20.28	.99817				.00097
Aug	22.07	.99778					20.94	.99804				.00026
Sep	19.50	.99831					20.33	.99817				-.00016
1980												
Jun	21.8	.99784	375	.00029	.99813		17.93	.99864	600**	.00046	.99910	.00097
Jul	26.19	.99676	330	.00025	.99701		20.91	.99804	550*	.00042	.99846	.00145
Aug	23.78	.99737	280	.00021	.99758		21.21	.99798	620*	.00047	.99845	.00087
Sep	18.84	.99847	280	.00021	.99868		20.37	.99815	600**	.00046	.99861	-.00007

[1] $\rho_p = \rho_T + \Delta\rho_{TDS}$, where ρ_T = density dependent on temperature

$\Delta\rho_{TDS}$ = density increment due to total dissolved solids

*TDS based on 1980 sample data.

**TDS based on estimates from 1982 field surveys.

17

$$\Delta\rho_{TDS} = \frac{\rho_S - \rho_T}{\rho_T} C \approx (.75)C \qquad\qquad\qquad (IV-1)$$

where ρ_S = density of dissolved solids

   C = concentration of total dissolved solids (kg/ℓ)

1980 TDS data was available. The sum of the density dependent on temperature and the density increment due to suspended solids produced the calculated density $\rho = \rho_T + \Delta\rho_{TDS}$. The column $\rho_p - \rho_r$ is the difference between the Metro WWTP effluent density and the Mississippi River water density upstream from the discharge.

   As a measure of the effluent buoyancy, outlet channel densimetric Froude numbers have been calculated (Table IV-4). (The outlet densimetric Froude number is defined in Section V, Eq. 3).

TABLE IV-4 - Buoyancy of Effluenct in Outlet Channel

	$\Delta\rho = \rho_p - \rho_r$	Q_p		Concrete Section		River Bank Section	
				U_p	F_p*	U_p	F_p*
	(g/cm^2)	(mgd)	(cfs)	(ft/s)	(-)	(ft/s)	(-)
Jun	0.00097	242	374	1.03	2.9**	.089	0.13
Jul	0.00145	233	360	0.99	2.3**	.086	0.10
Aug	0.00087	233	360	0.99	3.0**	.086	0.13
Sep	0.00007	223	345	0.95	-31.6***	-.082	-0.45

WSEL = 687.2 above MSL

In Concrete Section: H_p = 4 ft, B_p = 91 ft, A_p = 364 ft^2

At River Bank: H_p = 15 ft, B_p = 280 ft, A_p = 4200 ft^2 (Fig. IV-3)

*Outlet densimetric Froude number defined by Eq. V-3.

**Sinking plume.

***Rising plune.

V. MODEL FORMULATION

The mathematical description of riverine flow and mixing processes can be attempted at different levels of sophistication. The options range from the fully three-dimensional transport equations to totally empirical equations. The selection is a function of the objectives, and the availability of data. This study is exploratory in nature because of funding limitations.

Steady-state, and basically two-dimensional models were formulated. Consideration was given to the main processes listed in Section III.

A. Nearfield

1. Jet effects

The outlet channel widens (diffuses) considerably before reaching the river (Fig. IV-2). Field observations made in the summers of 1976 and 1982 indicate that the effluent discharge velocity relative to the river flow velocity is so small that jet effects are insignificant.

2. Displacement

The transverse displacement y_p for a neutrally buoyant discharge shown in Fig. III-1 can be estimated given the river flow Q_r, the plant discharge Q_p , the river cross section, and the velocity distribution. The width occupied by the effluent water y_p is given by the relationship

$$Q_p = \int_o^{y_p} \overline{u}(y) \; h(y)dy \qquad (V-1)$$

For a rectangular river cross section of width B, mean depth H, and mean flow velocity U, the displacement width y_p is approximated as

$$\frac{y_p}{B} = \frac{Q_p}{Q_r} \qquad (V-2)$$

where $\overline{u}(y)$ = depth averaged velocity = $\dfrac{1}{H} \int_o^H u(x,y,z)dy$

$H(y)$ = river depth

20

Equation V-1 is used in the absence of any buoyancy effects. For a plunging flow the displacement y_p has no meaning. Instead the underflow must be analyzed as shown in the next section. Dilution in the nearfield can be incorporated by increasing Q_p by a dilution factor.

3. Buoyancy effects in the outlet channel or near the outlet

When the effluent buoyancy is negative, the effluent flow becomes a plunging flow (underflow) as shown in Fig. III-2d; if buoyancy is positive a surface flow (overflow) occurs as shown in Fig. III-2b. In the summer, effluent buoyancy from the Metro WWTP is negative (Table IV-3). The densimetric Froude number of the effluent in the outlet channel is a measure of the strength of buoyancy. The densimetric Froude number is defined as

$$ F = U_p (g' H_p)^{-1/2} \tag{V-3a} $$

with

$$ g' = \left| \frac{\rho_p - \rho_r}{\rho_r} \right| g \tag{V-3b} $$

where U_p = mean effluent velocity,

H_p = mean effluent channel depth,

ρ = water density of the effluent (subscript p) and the river

(subscript r), respectively, and

g = acceleration of gravity

Laboratory experiments of plunging flows in diffusers have shown that the effluent flow becomes a plunging flow at a critical value $F = F_c$. A typical critical value for F_c is from 0.55 to 1.0. We shall use $F_c = 1.0$.

The critical Froude number criterion can be used to determine if the effluent from the Metro WWTP will be sinking before reaching the river. Outlet densimetric Froude numbers have been shown in Table IV-4. According to those values, the effluent must sink somewhere in the outlet channel diffuser from June through August, but not always in September. Such sinking has indeed been observed at the Metro WWTP outlet in the summer.

After the effluent has left the mouth of the effluent channel, it will tend to spread transversely across the river (Region 2, Fig. III-4). In the initial phase of this process, buoyancy is important. The Metro WWTP effluent has positive buoyancy in winter and negative buoyancy in summer. Buoyancy causes increased spreading, near the river bottom if negative, and on the water surface if positive. Buoyancy will therefore tend to produce stratification in the river.

21

The transverse spreading velocity v of the buoyant underflow in summer (overflow in winter) is that of a stationary front as studied in saltwater intrusion (salt water wedge) and other estuarine problems. Because the underflow (overflow) discharges into the river, the river flow causes the front to become oblique (Fig. V-1). The author knows of no reliable oblique front studies to estimate the value of v . Instead, information for straight fronts has to be used.

The spreading velocity of a front can be estimated from

$$v = k \sqrt{g' h} \qquad\qquad (V\text{-}4)$$

where v = transverse spreading velocity of the underflow,

g' = local densimetric acceleration of gravity,

h = thickness of underflow, and

k = coefficient.

The value of g' must take into consideration the dilution of the effluent. The densities used to calculate $g' = (\rho_u - \rho_r / \rho_r)g$ are local values.

At this time no nearfield model (Regions 1 and 2) will be formulated. The farfield analysis requires, however, that the effluent plume at the end of the nearfield is specified. Therefore two different nearfield approximations, depending on the strength of the effluent buoyancy were made:

(a) The size of the effluent plume at the end of the nearfield is estimated from Eqs. V-1 and V-2. The effluent does not plunge or float before it reaches the river. The plant effluent rate Q_p can be increased to account for dilution at the outlet. At the end of the nearfield, the flow is vertically well mixed. This situation is illustrated in Figs. III-1, III-2c, and V-1.

(b) The effluent flow plunges in the outlet channel (strong buoyancy) and spreads across the river bed over the entire river width. At the end of the nearfield, the flow is vertically stratified but without gradients in transverse directions (Figs. V-2 and III-2e). An accurate determination of the oblique front of the underflow in the river is not possible until the exact river bottom topography near the outlet has been surveyed and dilution rates at the front have been determined. However, measurements of depth and density of the underflow at the end of the outlet channel diffuser indicate an initial transverse spreading velocity on the order of 0.2 ft/s.
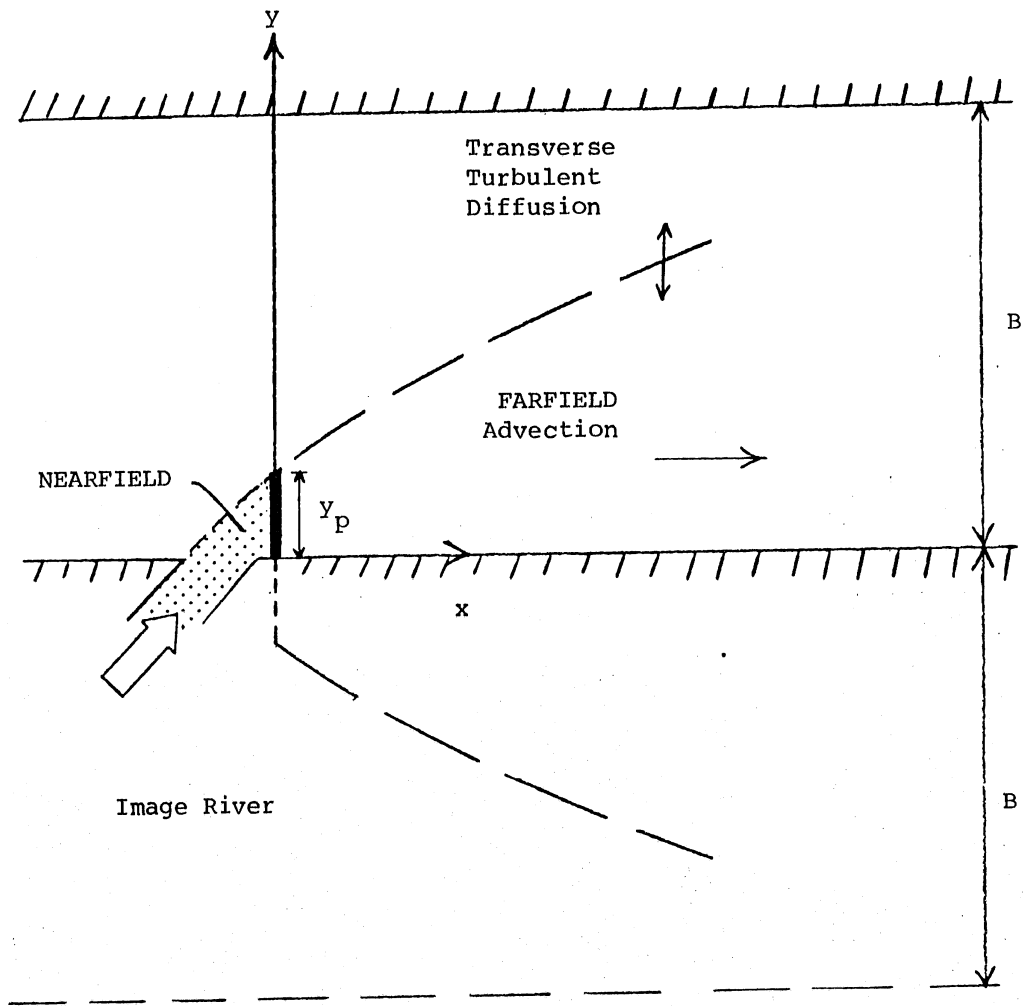
22

Fig. V-1. 2-D Advective and transverse turbulent spreading of an effluent below a line source (plan view). Flow is vertically well mixed.
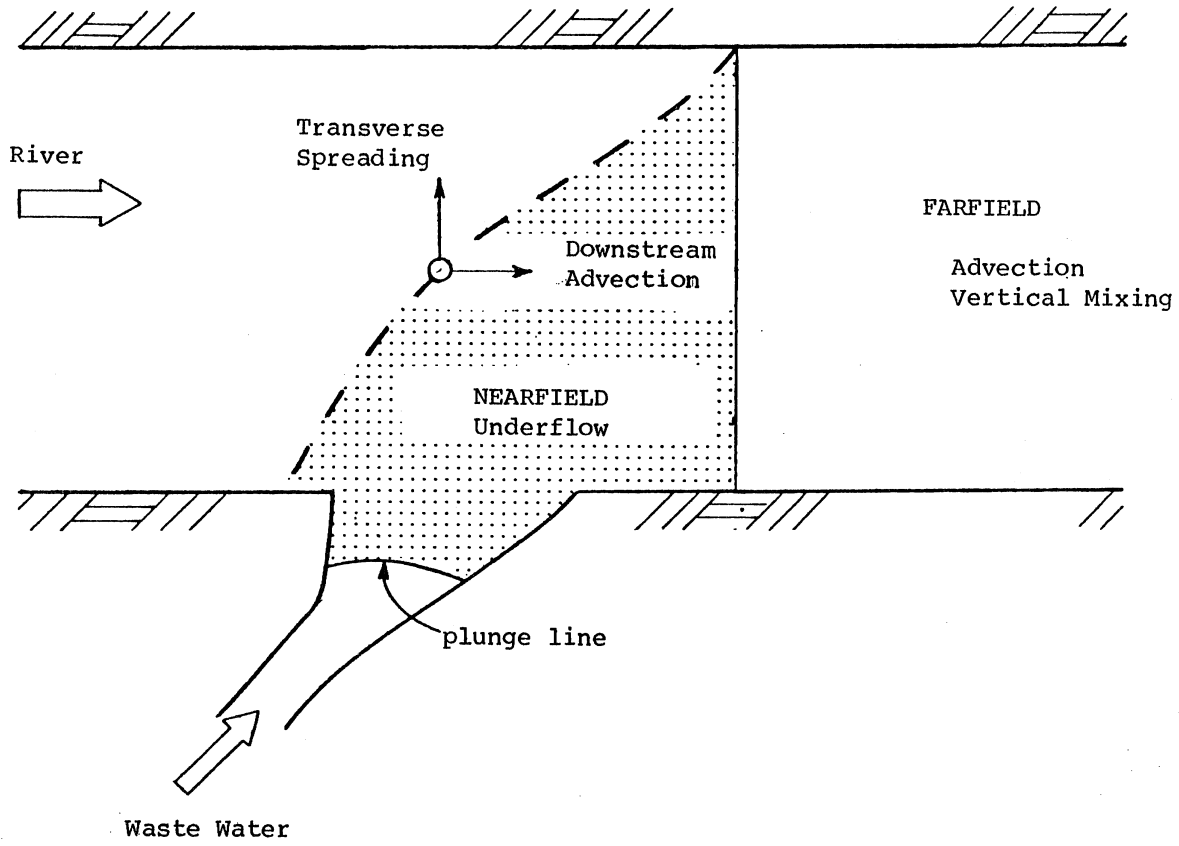
23

Fig. V-2. Plan view of underflow into the river.

B. Farfield

In accordance with the two nearfield concepts, two groups of farfield models were considered. One model is two-dimensional in the horizontal and assumes well mixed conditions in the vertical. This occurs when the effluent is only weakly buoyant. It is a model of Region 3 in Fig. III-3. This model shall be referred to as the "Horizontal Mixing Zone Model." The other group of models is two-dimensional in a vertical plane and considers the vertical mixing in the presence of a vertical density gradient. It represents Region 3 in Fig. III-4 and shall be referred to as the "Vertical Mixing Zone Model."

Horizontal mixing zone models are more frequently applicable to rivers and shall be described first.

1. Horizontal Mixing Zone Model

If the effluent flow remains vertically well mixed in the river the field of concentrations can be described by a 2-D advection/diffusion equation. Advection is in the downstream direction and turbulent diffusion in the transverse direction as shown in Fig. V-1. The transverse turbulent diffusion coefficient may at first be estimated from available equations but needs ultimately to be evaluated from field data because the river is very irregular, winding, and modified by wing dams and dredged areas. Allowance can be made for effects of buoyancy by appropriate selection of the transverse turbulent diffusion coefficient. This farfield model describes Region 3 in Fig. III-3 with an allowance for Regions 1 and 2 by appropriate upstream conditions, e.g. as shown in Fig. V-2.

The basic equation which describes the steady-state field of concentrations is

$$0 = -\frac{\partial}{\partial x}(uhC) - \frac{\partial}{\partial y}(vhC) + \frac{\partial}{\partial x}\left(D_x h \frac{\partial C}{\partial x}\right) + \frac{\partial}{\partial y}\left(D_y h \frac{\partial C}{\partial y}\right) - KCh \qquad (V-5)$$

where $C(x,y)$ = concentration (ML^{-3})

x = coordinate in the main direction of river flow (L)

y = coordinate transverse to river flow (L)

$u(x,y)$ = longitudinal (x-dir.) river flow velocity (LT^{-1})

$v(x,y)$ = transverse (y-dir.) river flow velocity component (LT^{-3})

$h(x,y)$ = local river depth (L)

$D_x(x,y)$ = longitudinal turbulent diffusion coefficient ($L^2 T^{-1}$)

$D_y(x,y)$ = transverse turbulent diffusion coefficient ($L^2 T^{-1}$)

K = first order reaction rate coefficient

The foregoing equation describes the transport of material in a river including the effects of advection (flow) in longitudinal and transverse direction, transverse and longitudinal turbulent diffusion, and loss of material by a first order reaction. Since there can be no mass transport through the river banks, the boundary conditions may be expressed as

$$\frac{\partial C}{\partial y}\bigg/_{y=0} = 0 \qquad \text{and} \qquad \frac{\partial C}{\partial y}\bigg/_{y=B(x)} = 0$$

where $y=0$ and $y=B(x)$ are the locations of the river banks.

The effluent source can be represented as a point source for large river to effluent flow ratios, or as a transverse line source for smaller river to effluent flow ratios (Fig. V-1).

Equation V-5 can be solved analytically or numerically. If detailed information on river depths $h(x,y)$, flow velocities $u(x,y)$ and $v(x,y)$, is available, a numerical solution is appropriate. An analytical solution is feasible with additional simplifying assumptions. We shall give several such solutions for first estimates.

a. Closed form concentration distribution functions for the mixing zone in a river of constant depth and width

To solve Eq. V-5 analytically, substantial simplifications are necessary: all morphometric and river flow values must be described as average values, i.e. H = mean river depth, B = mean river width, U = $Q(BH)^{-1}$ = mean flow velocity, and D_y = D = mean transverse turbulent diffusion coefficient. Transverse velocity v = 0; then Eq. V-5 becomes

$$0 = -U\frac{\partial C}{\partial x} + D\frac{\partial^2 C}{\partial y^2} - KC \qquad (V-6)$$

The outlet (effluent discharge) can be approximated by a source of total strength W (mass per unit time).

(1) Single Point Source in unconfined flow

The simplest model representation of the effluent channel is a single point source of strength W located at $x=0$ and $y=0$ and discharging into a river flow rate Q_r. The solution of Eq. V-6 for a point source located at the river bank $y=0$ is

$$C = \frac{WB}{Q_r(4\pi Dx/U)^{1/2}} \exp\left(\frac{-y^2 U}{4Dx} - K\frac{x}{U}\right) \qquad y \geqslant 0 \qquad (V-7)$$

In this solution, C is the concentration in the mixing zone in excess of
ambient concentration in river. In addition to the simplification of river
geometry, the solution assumes that the river is infinitely wide and that
the waste discharge W is with zero transverse displacement width in the
river ($y_p = 0$ in Fig. V-1). The solution accounts for the boundary con-
dition

$$\frac{\partial C}{\partial y}\bigg/_{y=0} = 0$$

(2) Point Source with river bank effects (images)

For a finite river width B, the effect of both river banks ($\partial C/\partial y$
= 0 at y=0 and y=B) can be accounted for by the method of superposition.
To this end, imaginary discharge point sources are located at y = 2nB,
where n is an integer from $-\infty$ to $+\infty$.

It is useful to define the dimensionless parameters

$$C_o = \frac{W}{Q_r} \qquad\qquad\qquad\qquad (V-8)$$

$$x' = \frac{xD}{UB^2} \qquad\qquad\qquad\qquad (V-9)$$

$$y' = y/B \qquad\qquad\qquad\qquad (V-10)$$

$$K' = \frac{KB^2}{D} \qquad\qquad\qquad\qquad (V-11)$$

If the real effluent source of strength W is located at y=0, x=0
(shoreline), superposition gives the downstream concentration distribution
as

$$\frac{C}{C_o} = \frac{1}{(\pi x')^{1/2}} \left\{ \sum_{n=-\infty}^{\infty} \text{exp} [-(y' - 2n)^2/4x'] \right\} \exp(-K' x') \qquad (V-12)$$

From Eq. V-12 concentrations at both river banks (y'=0 and y'=1.0) can
be calculated as a function of distance x' (Fig. V-3). It is found that
the concentrations at the banks are within 10% of the fully mixed river
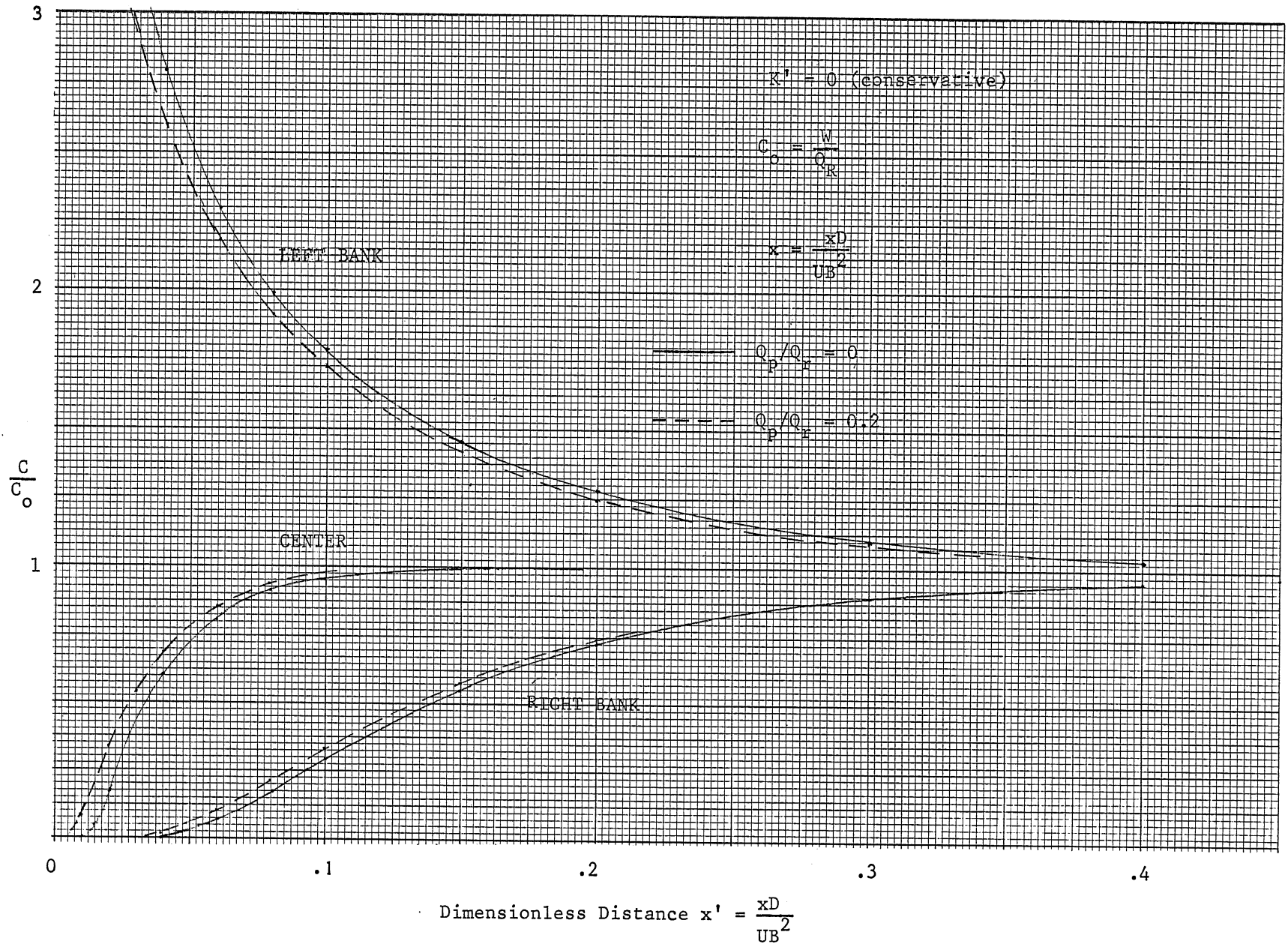value C_o at a distance x'= 0.3 or within 4% at x'= 0.4.

27

Fig. V-3. Normalized concentration versus distance – conservative substance.
Transverse mixing zone model.

$$x_{90\%} = 0.3 \frac{UB^2}{D} \tag{V-13}$$

$$x_{96\%} = 0.4 \frac{UB^2}{D} \tag{V-14}$$

(3) Virtual outlet model

To account for the transverse displacement of river water, buoyancy and other outlet effects, one can consider that the outlet is located at a virtual distance x_v upstream from the real outlet. A method to estimate x_v (Schatzmann and Naudascher, 1980) considers that x_v is a function

$$\frac{x_v}{H} = f \ (Q_E^* \ , \ S) \tag{V-15}$$

where Q_E^* and S are dimensionless numbers defined as

$$S = \frac{\overline{\rho} \ \dfrac{Q}{UH^2}}{\left(\dfrac{D}{UB}\right)^2 \left(\dfrac{B}{H}\right)^2 \left(\dfrac{U}{gH}\right)^2} = \frac{\Delta\rho}{\rho} \ \frac{Q_p Hg}{U \ D^2} \tag{V-16}$$

and

$$Q_E^* = \frac{p}{UH^2} \tag{V-17}$$

The stability parameter "S" relates the effluent buoyancy forces to turbulence of the river flow. The parameter Q_E^* is a non-dimensional volume flux emitted by a virtual reference source.

By introducing the virtual source concept, problems of side channel discharges can be reduced to the simpler problem of a point discharge. The relationship (Eq. V-15) has been established experimentally for 90° discharges and is available in form of a chart. The Metro WWTP discharges at a 22° angle. A function (Eq. V-15) appropriate for that angle is not available at this time.

(4) Line source with river bank effects (images)

If the effluent discharge is a significant portion of the river flow, the transverse displacement width y_p is large. A line source perpendicular to the river flow and equal in length to the displacement width (Fig. V-1) is therefore a better representation than a point source.

The concentration distribution in the coordinate system of Fig. V-1 is

$$C(x,y) = \exp(-Kx/U) \int_{-\infty}^{\infty} \frac{f(\eta)}{\sqrt{4\pi Dx/U}} \exp\left[\frac{-(y-\eta)^2}{4Dx/U}\right] d\eta \qquad (V-18)$$

The strength of the line source $f(\eta)$ has to equal the total discharge. Therefore

$$f(\eta) = C_p = W/y_p, \text{ along the line source and} \qquad (V-19)$$

$$f(\eta) = 0, \text{ outside the line source.}$$

C_p = plant effluent concentration.

The method of superposition (image sources) can be used again to account for the streambanks (Fig. V-4). $f(\eta) = C_p$ will be applied at

$$2nB - y_p \leqslant \eta \leqslant 2nB + y_p$$

where n=0, ±1, ±2 ... At all other values of η , $f(\eta)$ will be zero.

An analytical solution of the integral can be developed by setting

$$u = \frac{y-\eta}{\sqrt{4Dx/U}} \qquad (V-20)$$

The integral can be transformed to

$$C(x,y) = \frac{p}{\sqrt{\pi}} \int_{+\infty} e^{-u^2} du \qquad (V-21)$$

30

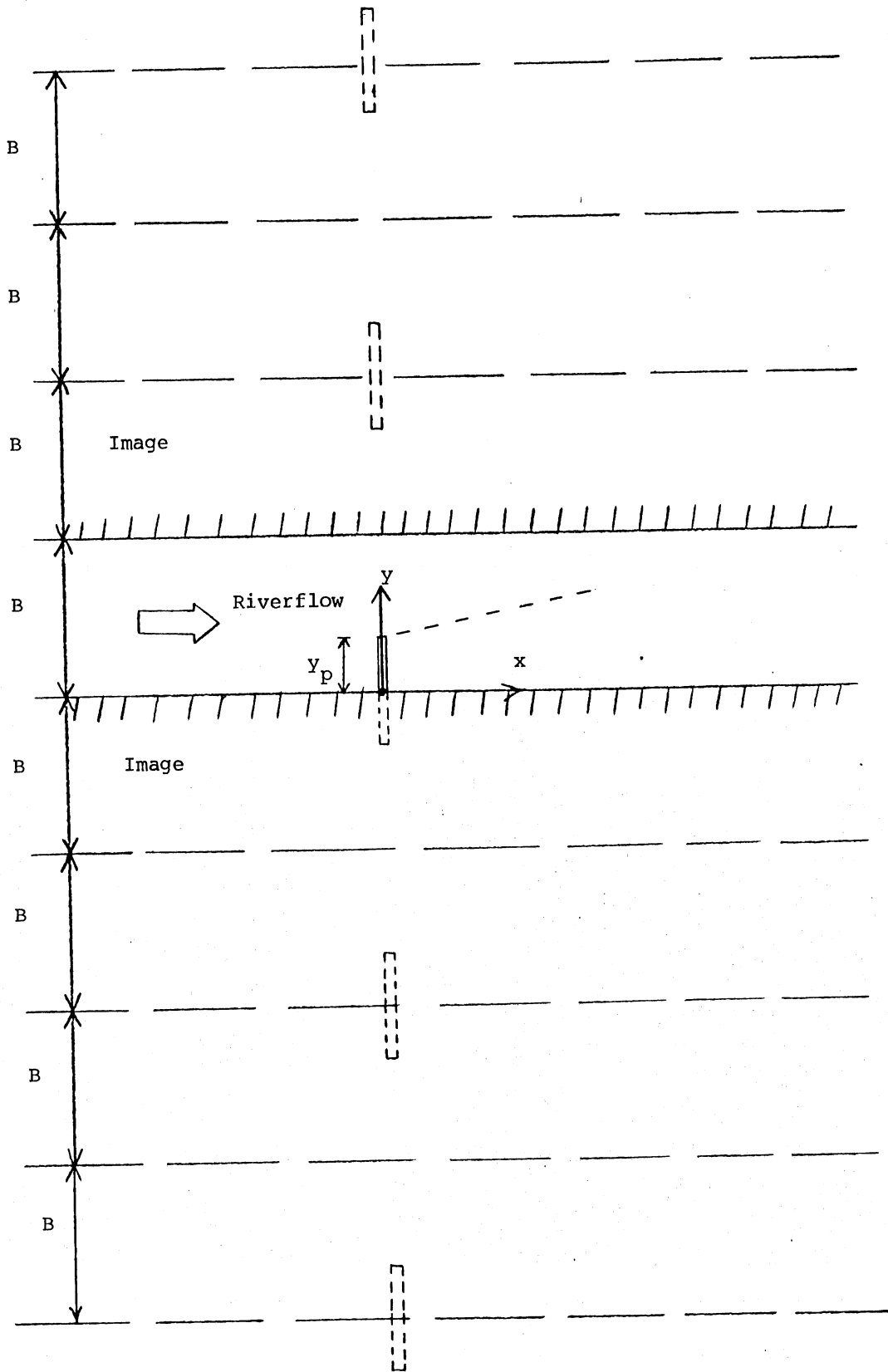Fig. V-4. Line source and image sources.

31

$$C_p \neq 0 \quad \text{between} \quad u_1 = \frac{y - 2nB + y_p}{\sqrt{4Dx/U}} \quad \text{and}$$

$$u_2 = \frac{y - 2nB - y_p}{\sqrt{4Dx/U}}$$

$$\text{With} \qquad \int_0^z e^{-u^2} \, du = \frac{\sqrt{\pi}}{2} \, \text{erf}(z) \tag{V-22}$$

$$C(x,y) = \frac{C_p}{2} \sum_{n=+\infty}^{-\infty} \left\{ \text{erf} \left[\frac{y - 2nB - y_p}{\sqrt{4Dx/U}} \right] - \text{erf} \left[\frac{y - 2nB + y_p}{\sqrt{4Dx/U}} \right] \right\} \exp\left(-\frac{Kx}{U} \right) \tag{V-23}$$

With dimensionless parameters from Eqs. V-9, V-10, and V-11.

$$\frac{C(x,y)}{C_p} = \frac{1}{2} \exp(-K'x') \left\{ \sum_{n=-\infty}^{\infty} \text{erf} \frac{y' + 2n + y_p'}{\sqrt{4x'}} - \text{erf} \frac{y' + 2n - y_p'}{\sqrt{4x'}} \right\} \tag{V-24}$$

Plots are given in Fig. V-2 for a conservative material (K=0) and an effluent to river flow ratio $Q_p/Q_r = 0.2$.

A comparison between point source and line source representations near the outlet is given in Fig. V-5. Beyond x' = 0.14 the differences between point source and line source predictions are less than 5 percent. Only in the immediate vicinity of the outlet does the line source give a more representative solution, as is shown in Fig. V-5.

A loss of material can change the concentration distribution in the mixing zone significantly. A plot of C/C_0 values for a loss rate K' = $KB^2/D = 1.0$ is shown in Fig. V-6. The corresponding values for K' = 0 were given in Fig. V-2.

b. Stream tube model

A rectangular cross-section approximates the Mississippi River below the MWTP rather poorly. The river cross section often has a deep navigable part and a shallow portion near one of the banks. There are submerged groins (wing dams) to slow down the flow in the shallow parts. The areas between the wingdams are often filled in by sediment deposits. There has been substantial dredging to maintain the 9 ft navigation channel or to provide barge parking spaces along the river banks. Downstream velocities are fastest in the deepest sections and slow to zero near the shores.
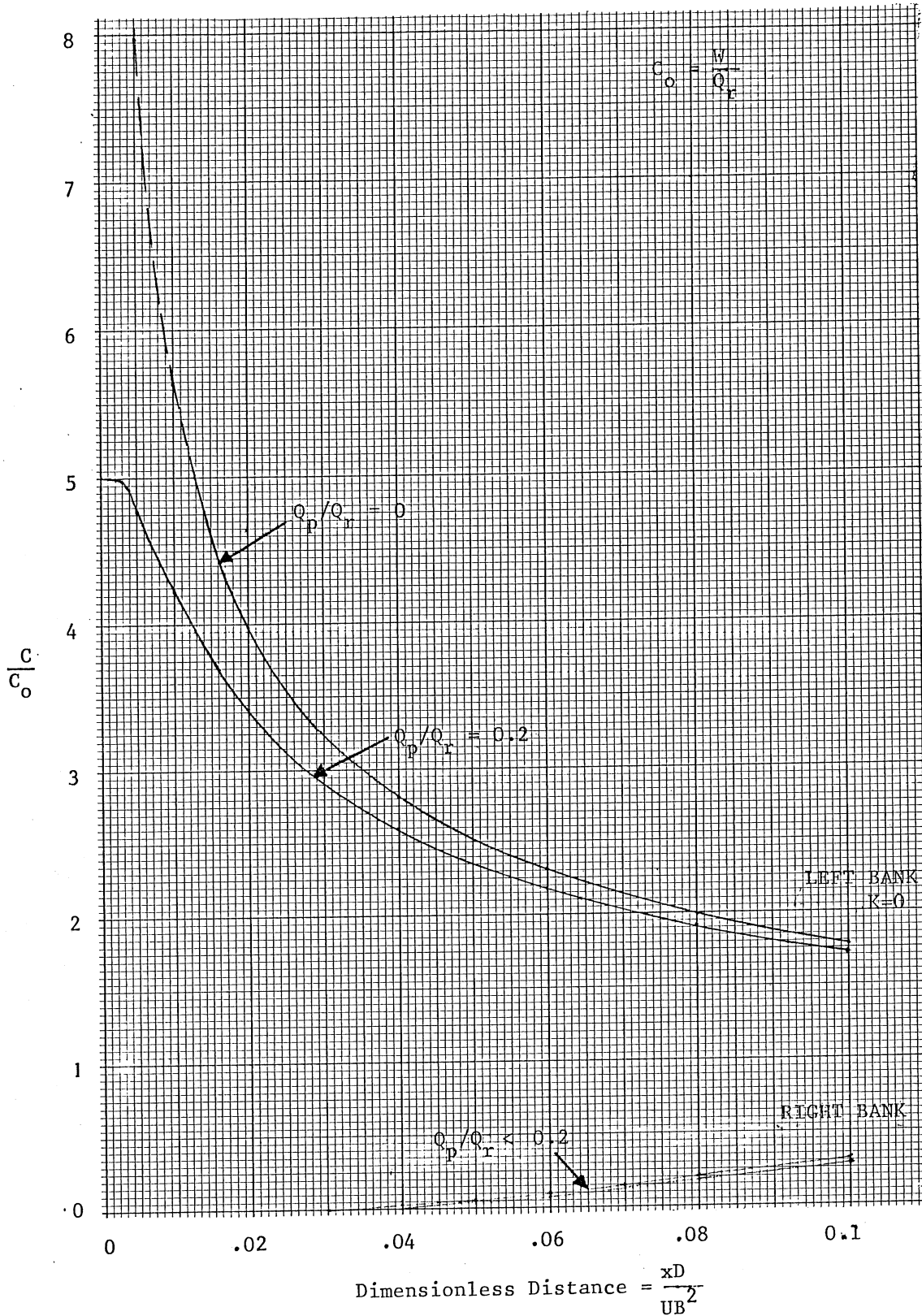
32

$$C_o = \frac{W}{Q_r}$$

$\frac{C}{C_o}$

$\frac{Q_p}{Q_r} = 0$

$\frac{Q_p}{Q_r} = 0.2$

LEFT BANK
K=0

RIGHT BANK

$\frac{Q_p}{Q_r} < 0.2$

Dimensionless Distance $= \frac{xD}{UB^2}$

Fig. V-5. Normalized concentration versus distance near the outlet for conservative substance. Transverse mixing zone model.

33

$$K' = \frac{KB^2}{D} = 1.0$$

$$C_0 = \frac{W}{QR}$$

$$x' = \frac{xD}{UB^2}$$

$$\frac{Q_0}{Q} = 0$$

LEFT BANK

CENTER

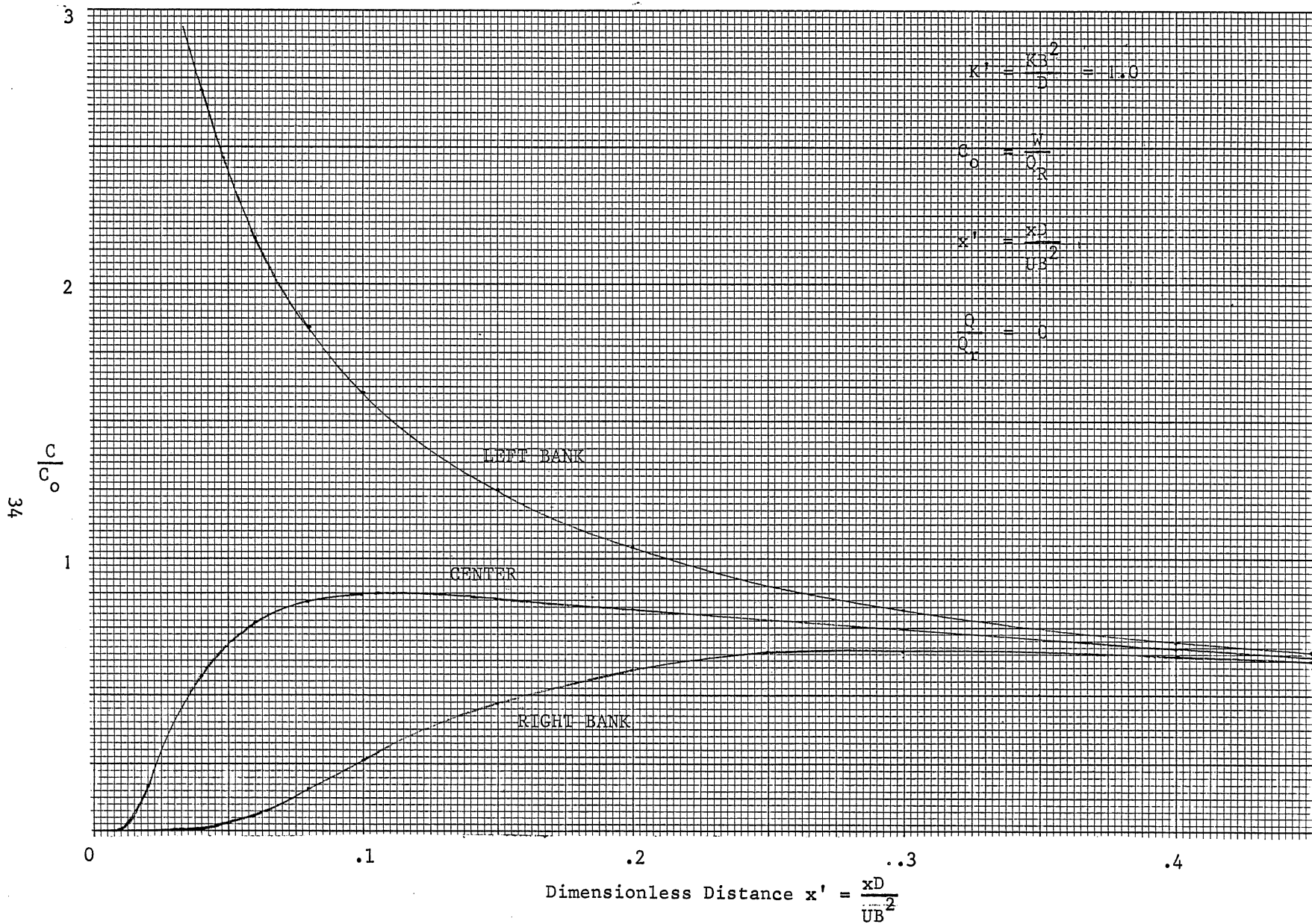RIGHT BANK

Dimensionless Distance $x' = \dfrac{xD}{UB^2}$

Fig. V-6. Normalized concentration versus distance for nonconservative substance.

An approximation of the "Horizontal Mixing Zone" can be obtained by the methods outlined in Section B.1. The approximation will have to suffice until the actual river cross sections, local flow velocities, and transverse mixing coefficients have been evaluated. If river geometry and velocity distributions are known, a better procedure for mixing zone analysis is the cumulative discharge method. The cumulative discharge is defined as

$$q(y) = \int_0^y h \, \bar{u} \, dy \, , \tag{V-25}$$

where
$$\bar{u(y)} = \frac{1}{h(y)} \int_0^h u(x,y,z)dz \tag{V-26}$$

is the depth averaged flow velocity. The value of $q(y)$ varies from zero at one bank to the total flow rate Q_r at the other.

For steady-state conditions, the depth integrated equation for transverse diffusion is

$$h\bar{u} \, \frac{\partial C}{\partial x} = \frac{\partial}{\partial y} \left(hD \, \frac{\partial C}{\partial y} \right) - KCh \tag{V-27}$$

or

$$\frac{\partial C}{\partial x} = \frac{\partial}{\partial q} \left(h^2 \, \bar{u}D \, \frac{\partial C}{\partial q} \right) - \frac{KC}{\bar{u}} \tag{V-28}$$

The expression $h^2 \, \bar{u}D$ is treated as a constant "diffusion factor" and the solution of Eq. V-28 is given in the x-q coordinate system.

Replacing the transverse coordinate y by the cumulative flow rate q renders it possible to account for the streamline pattern in the river section, including the effects of locally variable depth and velocity. Each value of q is associated with a streamline, and the coordinate system shifts sideways in a cross section as the streamlines do. (See Fig. V-7.)

With $D_r = h^2\bar{u}D$ and $K_r = K/\bar{u}$ treated as constants Eq. V-28 takes the form

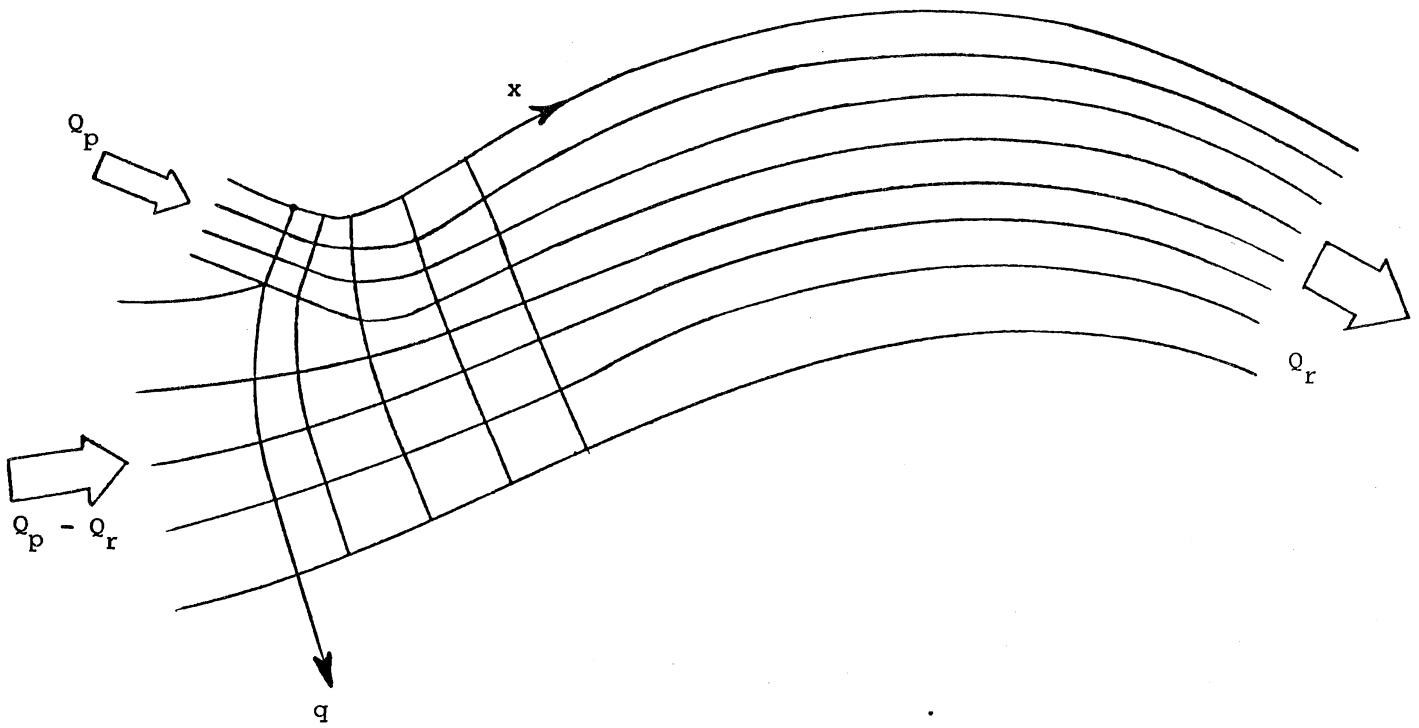$$\frac{\partial C}{\partial x} = D_r \frac{\partial^2 C}{\partial q^2} - K_r C \tag{V-29}$$

Fig. V-7. The x-q coordinate system used in the
cumulative discharge method.

Analytical solutions similar to Eq. V-12 and V-24 can be given if the following substitutions are made: D_r for D/U, K_r for K/U, and q for y. For the line source solution, the displacement width y_p must be found from Eq. V-1.

An analytical solution in terms of x and q for a single point source on one bank of a very wide stream is derived from Eq. V-7 as

$$\frac{C}{C_o} = \frac{Q_r}{(4\pi D_r x)^{1/2}} \exp\left(\frac{-q^2}{4D_r x} - K_r x\right) \tag{V-30}$$

For a point source on one bank of a river of width B, Eq. V-12 yields

$$\text{with} \quad x^* = \frac{x D_r}{Q_r^2} \tag{V-31}$$

$$q^* = \frac{q}{Q_r} \tag{V-32}$$

$$C_o = \frac{W}{Q_r} \tag{V-8}$$

$$K^* = \frac{K_r Q_r^2}{D_r U} \tag{V-33}$$

$$\frac{C}{C_o} = \frac{\exp(-K^* x^*)}{(\pi x^*)^{1/2}} \sum_{n=-\infty}^{\infty} \left\{ \exp\left[-(q^* - 2n)^2/4x^* - K^* x^*\right] \right. \tag{V-34}$$

For a line source, Eq. V-24 can be transformed similarly. To use the equations $C(x,q)$, in the x-q coordinate system, the function $q(y)$ must be evaluated for many river cross sections and D_r must be estimated.

c. Numerical mixing zone model concept

If D_r and K_r in Eq. V-29 cannot be treated as constants, a numerical solution to the equation

$$-\frac{\partial C}{\partial x} + \frac{\partial}{\partial q}\left(D_r \frac{\partial C}{\partial q}\right) - K_r C = 0 \tag{V-35}$$
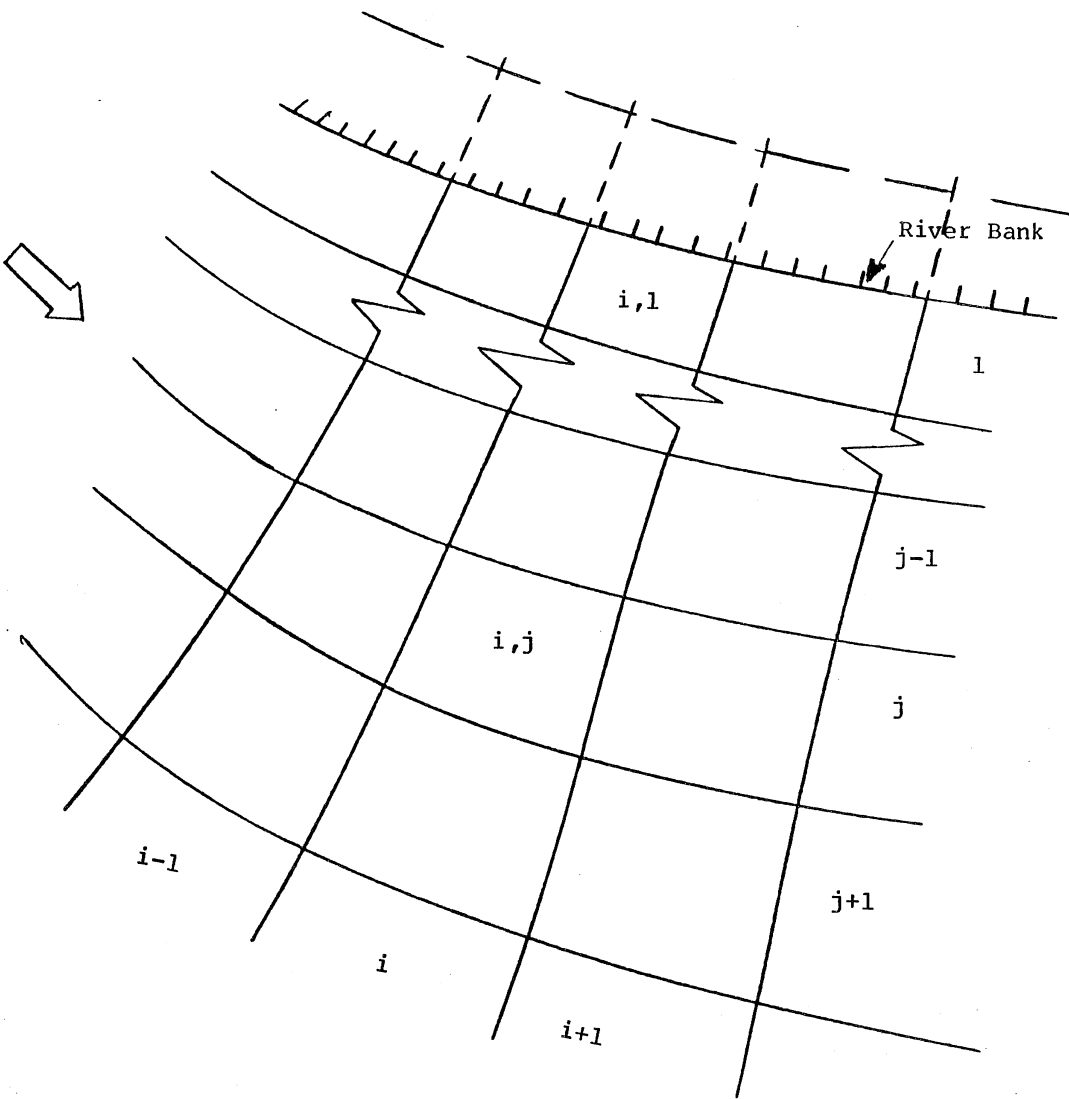
Fig. V-8. The i,j grid system used in the finite difference
numerical mixing zone model.

must be sought. Using a grid system as shown in Fig. V-7, an implicit finite difference form of Eq. V-35 can be formulated. The concentration at the midpoint of each grid $C_{i,j}$, as shown in Fig. V-8, can be computed from the numerical scheme.

With the finite difference expressions

$$\frac{\partial C}{\partial x} = \frac{C_{i,j} - C_{i-1,j}}{4x_{i,j}} \tag{V-36}$$

$$\left.\frac{\partial C}{\partial q}\right|_{j+1 \to j} = \frac{C_{i,j+1} - C_{i,j}}{1/2(\Delta q_{i,j+1} + \Delta q_{i,j})} \tag{V-37}$$

$$\frac{\partial}{\partial q}\left(D_r \frac{\partial C}{\partial q}\right) = \left[\frac{(C_{i,j+1} - C_{i,j})(D_{i,j+1} \cdot D_{i,j})^{1/2}}{1/2(\Delta q_{i,j+1} + \Delta q_{i,j-1})}\right. \tag{V-38}$$

$$\left. - \frac{(C_{i,j} - C_{i,j-1})(D_{i,j} \cdot D_{i,j+1})^{1/2}}{1/2(\Delta q_{i,j} - \Delta q_{i,j-1})}\right]\frac{1}{\Delta q_{i,j}}$$

$$K_r C = K_{r i,j} C_{i,j}$$

The finite difference equation then is

$$a\, C_{i,j+1} + b\, C_{i,j} + c\, C_{i,j-1} + d = 0 \tag{V-39}$$

where

$$a = \frac{k_{i,j+1}}{\Delta q_{i,j}} \tag{V-40}$$

$$b = -\frac{1}{\Delta x_{ij}} - \frac{k_{i,j+1}}{\Delta q_{i,j}} - \frac{k_{i,j}}{\Delta q_{i,j}} - K_{r i,j} \tag{V-41}$$

$$c = \frac{k_{i,j}}{\Delta q_{i,j}} \tag{V-42}$$

$$d = \frac{C_{i-1,j}}{\Delta x_{ij}} \qquad \qquad \text{(V-43)}$$

$$\text{with} \qquad k_{i,j+1} = \frac{(D_{i,j+1} \, D_{i,j})^{1/2}}{1/2(\Delta q_{i,j+1} + \Delta q_{i,j})} \qquad \qquad \text{(V-44)}$$

$$k_{i,j} = \frac{(D_{i,j} \, D_{i,j-1})^{1/2}}{1/2(\Delta q_{i,j} + \Delta q_{i,j-1})} \qquad \qquad \text{(V-45)}$$

where j = stream tube number, with $1 < j < N$ and
          N = total number of streamtubes including the effluent discharge.

Equations V-36, V-37, and V-38 represent but one of several possible ways to transform the differential Eq. V-35 into a finite difference equation and ultimately a set of linear equations (Eq. V-39) which can be solved on a computer.

Boundary conditions must be specified along the river banks and at the upstream end of the flow field. The upstream condition simply consists of known concentrations (effluent concentrations or river concentrations). Along the river banks transverse fluxes are zero, or $\partial C/\partial q = 0$. To achieve this, an additional (dummy) streamtube can be imagined outside each bank with the same concentrations as those in the first streamtube in the river. Any transverse differentials between the two streamtubes will then be effectively zero.

2. Vertical Mixing Zone Model

Vertical mixing is envisioned as the result of a vertical turbulent exchange process which can be described by a turbulent diffusion equation in a vertical plane.

$$0 = - \frac{\partial}{\partial z} (VbC) - \frac{\partial}{\partial x} (ubC) + \frac{\partial}{\partial x} \left(D_x b \, \frac{\partial C}{\partial x} \right) + \frac{\partial}{\partial z} \left(D_z b \, \frac{\partial C}{\partial z} \right) - KCb \qquad \text{(V-46)}$$

Equation V-46 is similar to Eq. V-5, except that mixing in the vertical z-plane instead of the horizontal y-plane is considered. The river width b takes the place of the depth h . Concentration is considered uniform in the horizontal plane.

The concentration profile at the beginning of the farfield will typically show a vertical gradient in concentration resulting from the previously discussed plunging underflow from the WWTP plant into the river.

Using mean flow velocity U, mean river width B, mean vertical turbulent eddy exchange coefficient D_z, Eq. V-46 can be simplified to

$$0 = -U \frac{\partial C}{\partial x} + D_z \frac{\partial^2 C}{\partial z} - KC \qquad (V-47)$$

An analytical solution of this equation can be found if the initial (upstream) concentration distribution is approximated by a step function (Fig. V-9). The solution must account for zero vertical mixing through the river bottom and the water surface, and for the initial underflow layer thickness z_p. The predicted concentration distribution can be derived from Eq. V-24 if the following substitutions are made:

$$K' = \frac{KH^2}{D_z} \qquad (V-48)$$

$$\text{for } y' \text{ use} \quad z' = \frac{z}{H} \qquad (V-49)$$

$$\text{for } y' \text{ use} \quad z'_p = \frac{z_p}{H} \qquad (V-50)$$

$$x' = \frac{xD_z}{UH^2} \qquad (V-51)$$
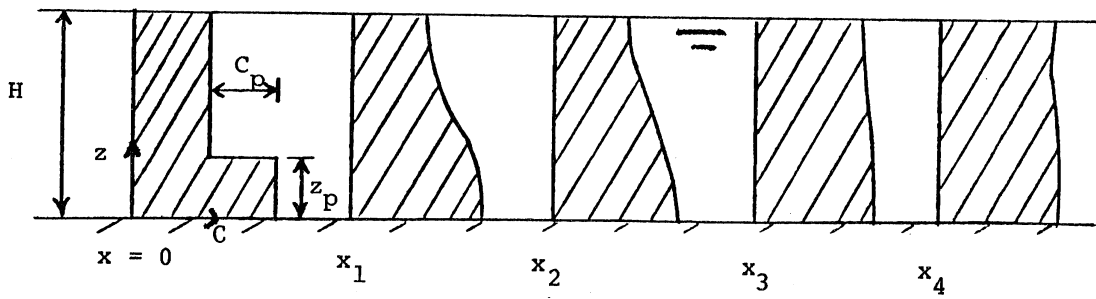
Then Eq. V-24 becomes

$$\frac{C(x,z)}{C_p} = \frac{1}{2} \exp(-K'x') \left\{ \sum_{n=-\infty}^{\infty} \text{erf} \frac{z'+2n+z_p}{\sqrt{4x'}} - \text{erf} \frac{z'+2n-z_p}{\sqrt{4x'}} \right\} \qquad (V-52)$$

Figures V-2, V-4 and V-5 are also applicable if "left bank" is replaced by "river bottom" and "right bank" by "water surface."

An estimate for the length of the mixing zone limited by vertical mixing is

$$x_{90\%} = 0.3 \frac{UH^2}{D_z} \qquad (V-53)$$

$$x_{96\%} = 0.4 \frac{UH^2}{D_z} \qquad (V-54)$$

41

V-9. Changes in vertical concentration profiles over
the length of the mixing zone (schematic).

VI. MISSISSIPPI RIVER FLOW AND MIXING CHARACTERISTICS

A. Effluent and Mississippi River Flow Rates

Design flow rates are Q_r = 1760 cfs for the river and Q_p = 251 mgd (387 cfs) for the mean monthly plant effluent. Typical summer river flow rates are summarized in Table IV-1; effluent flows are summarized in Table IV-2.

B. Mississippi River geometry, WS Elevations, Flow Velocities

The river geometry is taken from a 1972 flood plain mapping study conducted by the Minnesota Department of Natural Resources in cooperation with several other agencies. The river geometry between RM 835.3 and 828 is used (Stations 38 and 78 of that study). There has been little or no dredging in that river since 1972. However, aggradation of the river bed and minor shifts in the main channel have occurred in portions of the river since 1972 according to soundings by Owen, Ayres & Associates, Inc., Madison, Wisconsin, for the Corps of Engineers, St. Paul District in July 1981. Unfortunately depths were recorded only up to 16 ft; therefore the data of the 1981 survey could not be used in this study. Operating curves for Pool No. 2 prescribe the WS elevations given in the table below.

TABLE VI-1. Water Surface Elevations in Pool No. 2

Flow Rate (cfs)	WS EL (ft above MSL)		
	Project Pool	South St. Paul	Robert Street Bridge
0	687.2	687.2	687.2
2,000	687.2	687.2	687.2
10,000	687.2	687.2	687.6
20,000	687.2	688.2	689.3
Secondary Control			
> 12,000	686.5		

A mean effective width of the river reach was determined from aerial photographs taken in April 1971. Only the river widths of the main channel and distances of 41 sections were measured. From these the total water surface area and the total length of the river reach between UM 828 and UM 835.3 were determined as A_s = 697 acres and L = 37,060 ft, respectively. The mean river width (see Table VI-2) was calculated as

$$B = A_s/L = 802 \text{ ft} \tag{VI-1}$$

River depths in 41 cross sections were determined from the 1972 flood plain study and are shown in Table VI-1. A representative mean depth for the main channel was determined to be H = 14.9 ft.

C. Mississippi River W.S. Slope

One available HEC-2 simulation output gave a WSEL 687.06 at Station 38, and WSEL 688.24 at Station 78, at a flow rate of 20,000 cfs. The mean energy gradeline slope was computed as

$$S = \frac{688.24 + 0.04 - 687.06 - 0.04}{37,060} = 3.18 * 10^{-5} \tag{VI-2}$$

Manning's 'n' values from 0.02 to 0.06 were used in the HEC-2 study. Most sections in the river reach between UM 826 and 835.3 were assigned n = 0.03.

Water surface slopes and associated depths at flow rates below 20,000 cfs were estimated from Manning's equation and the continuity equation.

$$U = \frac{Q}{BH} = \frac{1.49}{n} H^{2/3} S^{1/2} \tag{VI-3}$$

For two flow rates Q = 20,000 and Q_x < 20,000, the equations can be restated as

$$\frac{S_x}{S_{20}} = \left(\frac{Q_x}{Q_{20}}\right)^2 \left(\frac{H_{20}}{H_x}\right)^{10/3} \left(\frac{B_{20}}{B_x}\right)^2 \left(\frac{n_x}{n_{20}}\right)^2 \tag{VI-4}$$

In the Mississippi River $B_{20} \approx B_x$ and $n_x \approx n_{20}$. Water surface slopes can therefore be calculated from a simplified equation. Table VI-3 summarizes the flow parameters.

No. of Cross Section	Surface Widths from Aerial Photo (ft)	Average Width of Reach Between Two Cross Sections (ft)	Lengths of Reaches (ft)	Surface Areas of Reaches (ft^2)	Cross Section Area (ft)	Mean Depth of Cross Section (ft)	CWSEL (ft)	Mean Depth at 687.2 (ft)
38	980	945	1070	1,011,150	11,523	11.8	687.06	11.9
39	910	915	750	686,250	11,191	12.3	687.10	12.4
40	920	885	1010	893,850	13,806	15.0	687.14	15.1
41	850	885	1130	1,000,050	11,951	14.1	687.17	14.1
42	920	920	960	883,200	11,869	12.9	687.21	12.9
43	920	930	1040	967,200	13,166	14.3	687.25	14.3
44	940	925	940	869,500	13,497	14.4	687.28	14.3
45	910	930	1070	995,100	11,014	12.1	687.32	12.0
46	950	890	1100	979,000	12,608	13.3	687.36	13.1
47	830	750	980	735,000	12,875	15.5	687.39	15.3
48	670	675	1040	702,000	12,689	(18.9)	687.42	(18.7)
49	680	680	280	190,400	10,674	15.7	687.48	15.4
50	680	770	530	408,100	16,020	(23.6)	687.52	(23.3)
51	860	910	730	664,300	15,927	18.5	687.53	18.2
52	960	880	700	616,000	9,949	10.4	687.54	10.1
53	800	725	1000	725,000	10,852	13.6	687.58	13.6
54	650	715	1000	715,000	11,174	17.2	687.60	16.8
55	780	790	1170	924,300	11,634	14.9	687.63	14.5
56	800	800	1090	872,000	13,093	16.4	687.66	15.9
57	800	750	900	675,000	19,532	(24.4)	687.71	(23.9)
58	700	695	1160	806,200	13,603	(19.4)	687.74	(18.9)
59	690	910	1140	1,037,400	13,462	(19.5)	687.82	(18.9)
60	1130	990	900	871,000	16,281	14.4	687.87	13.7
61	850	965	640	553,600	15,650	18.4	687.89	17.7
62	880	860	200	172,000	12,403	14.1	687.90	13.4
63	840	870	820	713,400	13,980	16.6	687.92	15.9
64	900	850	1060	901,000	12,827	14.3	687.94	13.6
65	800	795	830	659,850	12,800	16.0	687.99	15.2
66	790	785	1010	792,850	12,381	15.7	688.03	14.9
67	780	840	940	789,600	22,126	(28.4)	688.09	(27.5)
68	900	860	1020	877,200	25,390	(28.2)	688.10	(27.3)
69	820	810	910	737,100	23,650	(28.8)	688.11	(27.9)
70	800	710	1100	717,100	19,076	(23.8)	688.12	(22.9)
71	620	560	910	509,600	15,390	(24.8)	688.12	(23.9)
72	500	580	1360	788,800	8,939	17.9	688.12	17.0
73	660	680	600	408,000	10,809	16.4	688.12	15.5
74	700	735	1060	779,100	9,480	13.5	688.12	12.6
75	775	720	1000	720,000	9,761	12.6	688.16	11.6
76	670	700	1000	700,000	9,696	14.5	688.19	13.5
77	730	670	1000	670,000	11,851	16.2	688.23	15.2
78	610				10,960	18.0	688.24	17.0

Totals: 32,950   37,060   19,716,200

Average Width $B = \frac{\Sigma A}{\Sigma t} = \frac{19,716,200}{37.060} = 801.84$ (ft)

or $B = \frac{\Sigma b}{n} = \frac{32.950}{41} = 803.66$ (ft)

*After 1972 DNR floodplain study using HEC 2.

TABLE VI-3. Mississippi River Mean Flow Parameters Between
Metro WWTP Outlet at UM 835.3 and UM 828 and
Transverse Turbulent Diffusion Coefficients

	River Flow Rate Q_r (cfs)				
Parameter	20,000	10,000	5,000	2,000	1760
WSEL at outlet	688.2	687.5	687.3	687.2	687.2
H(ft)	15.3	14.7	14.4	14.3	14.3
B(ft)	804	804	804	804	804
U(ft/s)	1.63	0.846	0.432	0.174	0.153
S(-)	$31.8*10^{-6}$	$9.04*10^{-6}$	$2.41*10^{-6}$	$0.395*10^{-6}$	$0.306*10^{-6}$
u_*(ft/s)	.127	.0667	0.0341	0.01376	0.0121
D_h(ft^2/s)	2.02 C	1.02 C	0.51 C	0.205 C	0.180 C
$D_r(\psi)$(ft^5/s^2)	802 Cψ	195 Cψ	47.7 Cψ	7.60 Cψ	5.9 Cψ
Q_rB/u_*H^2(ft)	500,000	514,000	523,000	525,000	525,000

D. Mississippi River Transverse Turbulent Diffusion Coefficient

To apply the results of Section V, it is necessary to give a numerical
value for the transverse diffusion coefficient. Transverse turbulent dif-
fusion coefficients Dy are related to the strength of the flow induced
bed shear stresses and river geometry. The relationship

$$D = C\ u_*\ H \qquad\qquad\qquad (VI-5)$$

is often used for estimates. Therein C = coefficient, u_* = shear velo-
city, H = river depth. The value of u_* can be calculated from

$$u_* = \sqrt{\tau/\rho} = \sqrt{g\ R_h S} = \sqrt{gHS} \qquad\qquad (VI-6)$$

where τ = bedshear stress

ρ = density of water

g = acceleration of gravity

R_h = hydraulic radius

S = slope of the energy gradeline

The approximation $R_h = H$ is valid for wide rivers such as the Mississippi River.

The coefficient C is not a constant. Each river reach has its own specific value of C and only field measurements can establish a fully reliable field value.

The value of C includes the effects of river or channel aspect ratio (B/H), curvature as measured by a radius R, cross-sectional shape, contractions and expansions of the cross section. Submerged wing dams and the winding navigation channel of the Mississippi River will have their own effects on the transverse mixing coefficient.

For straight or gently meandering rivers of fairly constant width $C \approx 0.6 \pm 0.2$. In strongly winding and irregular river reaches C has been observed as high as 3.4. For a Mississippi River reach near Monticello, Minnesota, a value of $C = 2.0$ was determined by Demetracopoulos and Stefan (1982).

Buoyancy effects on transverse mixing cannot be predicted accurately with state-of-the-art information. The parameters which will control the density effects on transverse mixing are the flux of buoyancy from the effluent channel relative to the mixing power available in the stream. That ratio can be expressed as $Q_p g'/(Hu*^3)$, where g' = reduced gravity (Eq. V-3b). Experimental laboratory studies by Prych (1970) have been interpreted by Fischer (1979) to mean that buoyancy effects on transverse mixing can be ignored if the above ratio is less than five.

The transverse turbulent diffusion coefficient is calculated from Eqs. VI-5 and VI-6 as

$$D = CH\sqrt{gHS} \qquad\qquad \text{(VI-7)}$$

Because C cannot be evaluated with certainty without some field data, the equation has been evaluated as D(C) as given in Table VI-3.

The transverse turbulent diffusion factor D_r used in Eq. V-29 is evaluated as

$$D_r = \psi DH^2 U \qquad\qquad \text{(VI-8)}$$

According to Beltaos (1980), the factor ψ is stream dependent and can be evaluated from field data. A typical value for the Athabasca River in Canada is 2.56. $D_r(\psi)$ values are also given in Table VI-3.

E. Vertical Turbulent Diffusion Coefficient D_z

Vertical mixing in the Mississippi River results from turbulence produced by

(a) gravity flow and shear stress on the river bed,
(b) barge traffic,
(c) wind driven currents and waves, and
(d) natural convection due to cooling of the water.

Of interest here is the vertical mixing which will cause the underflow from the Metro WWTP outlet into the deepest part of the river to mix with the near surface waters. Each of the above four processes was briefly examined for its potential contribution.

1. Vertical Mixing by Gravity Flow

The vertical turbulent diffusion coefficient is estimated from an empirical equation of the form

$$D_z = C_v \, u* \, H \qquad\qquad (VI\text{-}9)$$

where C_v = experimentally determined coefficient on the order of 0.067.

$u*$ = shear velocity related to river flow velocity and roughness,

and H = river depth.

In a straight channel D_z is not constant but rather parabolically distributed over depth, with a maximum near mid-depth and zero near the bed and zero at the water surface. This is, however, not a crucial deviation when application to a real river is made.

More important is the consideration of the effect of a density stratification on the vertical mixing. Vertical turbulent mixing in a coflowing stream is weakened by a density stratifiction. The value of D_z given by Eq. VI-9 is reduced by a factor which depends on Richardson number defined as

$$Ri = -\frac{g}{\rho} \frac{d\rho/dz}{(du/dz)^2} \qquad\qquad (VI\text{-}10)$$

where $d\rho/dz$ = vertical density gradient

du/dz = vertical velocity gradient

48

Instead of this locally variable number a bulk Richardson parameter is easier to use in engineering studies. Such a parameter can be derived to be $Q_p g'/B u_*^3$. Open channel flow laboratory experiments by Schiller and Sayre (1973) have been interpreted by Fischer (1979) to mean that vertical mixing will be independent of density effects if the above parameter is less than one. If this condition is not satisfied, a reduction of the vertical mixing coefficient is necessary. Such a reduction may be made by considering that the vertical turbulent diffusion coefficient is reduced by a factor of ten when the stratification parameter

$$\varepsilon = \frac{1}{\rho} \frac{d\rho}{dz} \qquad (VI-11)$$

increases by a factor of ten. This was first found in oceanic studies of stratified environments as summarized by Brooks (1973) and later verified in smaller freshwater bodies.

In a river the decrease in vertical mixing with stratification can also be observed. From profiles of water temperature and salinity in the Mississippi River, it appears that a density increment of 0.001 over a 1 m height will rarely be exceeded. More typical are ε values of 10^{-4} to 10^{-6} m^{-1}, giving reduction coefficients between approximately 0.01 and 1.0 relative to the neutrally buoyant case.

A direct estimate of the reduction in vertical mixing intensity as as function of the initial (upstream) stability of the stratification and river mixing conditions was given by Schiller and Sayre (1973) based on laboratory experiments with overflows. Figure VI-1 reproduces the experimental result. The initial (before mixing) densimetric Foude number F_{OD} defined as

$$F_{OD} = \frac{U}{\sqrt{g'H}} \qquad (VI-12)$$

has been plotted against the vertical mixing coefficient $D_v/u_* H$.

The initial densimetric Froude number at the Metro WWTP outlet can only be guessed at this time because a nearfield study is missing. From field data observed during the summer of 1982, it is estimated that the strength of vertical stratification after nearfield mixing will not be in excess of 1°C and 80 mg/ℓ TDS, giving a $\Delta\rho/\rho$ of approximately 0.00034. With this value the densimetric Froude number at the beginning of the far-field will always be equal to or larger than 2.5 U (with U in ft/s), where the mean flow velocity is, of course, flow rate dependent. Using flow velocities from Table IV-3, one can estimate F_{OD} values and with the aid of Fig. VI-1 estimate the smallest possible D_v values. This is done in Table VI-4.
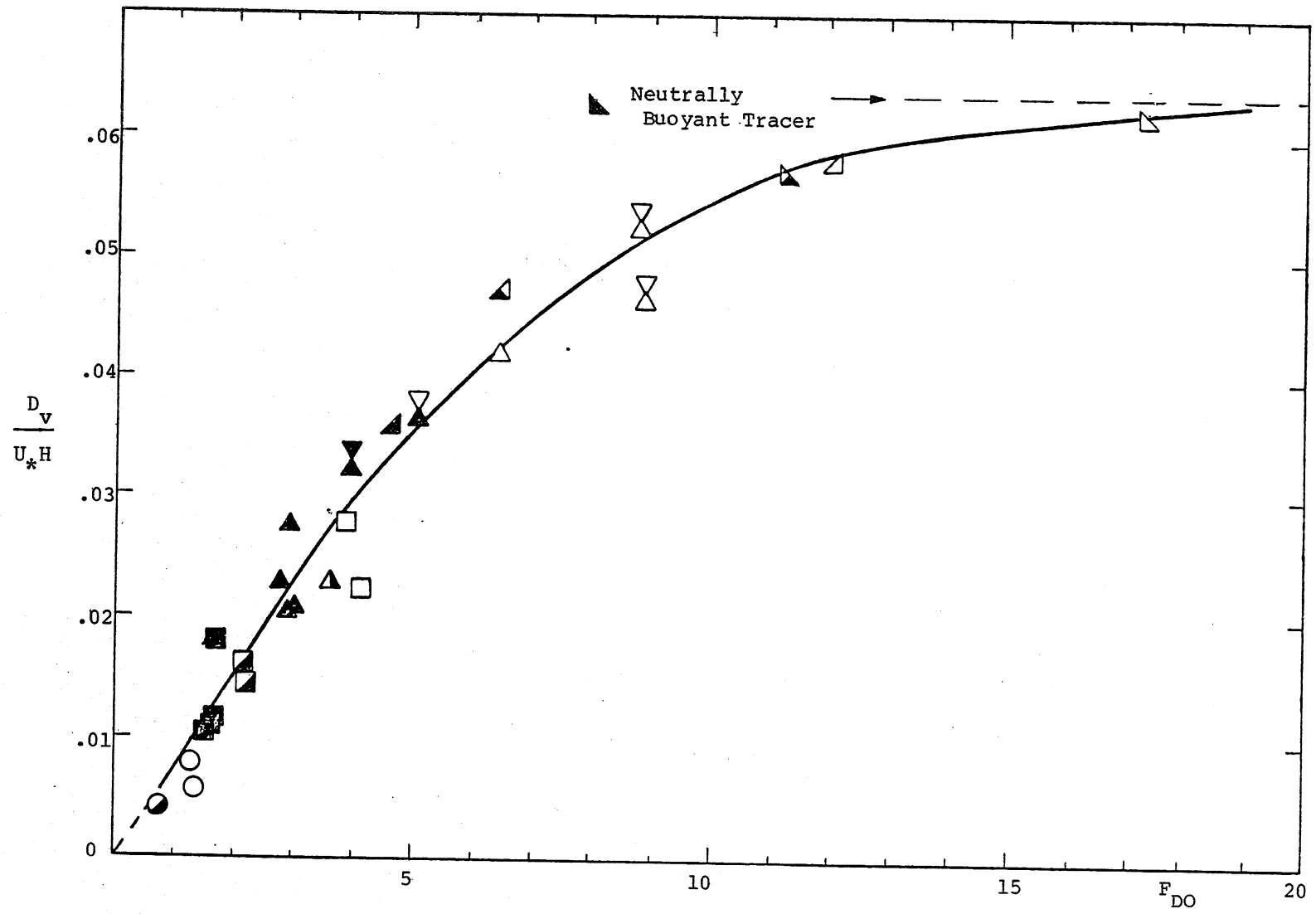
Fig. VI-1. Average values of D_v/u_*H vs. F_{DO}. (After Schiller & Sayre, 1973.) (Symbols are for different experiments.)

50

TABLE VI-4. Mississippi River Vertical Turbulent
Diffusion Coefficients

Q_r(cfs)		20,000	10,000	5,000	2,000
U(ft/s)[1]		1.63	0.85	0.43	0.17
F_{OD}(-)		4.0	2.1	1.1	0.43
u_*(ft/s)[1]		.127	.067	.034	.014
Stratified	$\dfrac{D_v}{u_*H}$	.03	.017	.008	.003
	D_v(ft^2/s)	0.06	0.016	0.004	0.0006
Neutrally Buoyant	$\dfrac{D_v}{u_*H}$	0.067	.067	.067	.067
	D_v(ft^2/s)	.14	.069	.034	.014

[1]From Table VI-3.

2. Vertical Mixing by Barges and Tugboats

A Mississippi River barge is typically 35 ft wide and 195 ft long.
Unloaded, its draft may be only 1.5 to 2 ft; when full, the draft can be 8
to 8.5 ft. "Barge tows" consist of 1 to 15 individual units and travel at
speeds of 7 to 8 mph (~ 1½ ft/s). A loaded 15 barge convoy displaces a
water volume of 870,000 ft^2. At a river cross-section of about 10,000 ft^2
this corresponds to a longitudinal water displacement of 87 ft. Three
loaded barges travelling abreast occupy 890 ft^2 of area, somewhat less than
10 percent of the river cross section.

In a stratified river the lateral displacement of the water by a barge
tow and the return flow after the passage will undoubtedly produce strong
shear flows associated with mixing.

Tugboats operating on the river have typically twin engines from 4000 to 6000 hp. A smaller switchtug used to move individual barges has typically 1000 hp.

Information on river mixing by barges and tugs found in the literature (see bibliography) relates mostly to effects on suspended sediments. However, two days of field observations and measurements showed that barge tows produce significant mixing of the stratified Mississippi River.

Conceptually, that impact can be seen by comparing the stream power of the flowing river with the power of a tug. A 5000 hp tug travelling at U = 11 ft/s will expend work at the rate of 250,000 lb/ft per linear ft of river. By comparison, the river at a flow rate of 20,000 cfs, a mean flow velocity of 1.6 ft/s and a S.W. slope of $32*10^{-6}$ will do work at a rate of only 25 lb ft/sec. To match the work done per linear ft by a barge tow, the river has to flow over low distances as shown in Table VI-5. These power considerations must lead to the expectation that barge tows and tugs will have a major impact on river mixing at typical summer flow rates .

3. Vertical Mixing by Wind and by Natural Convection

At low flow (Q < 5000 cfs), the backwater effects from Dam No. 2 cause the Mississippi River to flow rather slowly (U < 0.4 ft/s). Under those circumstances wind (waves and currents) and natural convection due to cooling of the water at the water surface may contribute significantly to the vertical mixing. These processes are however not always present and can therefore not be relief upon. For this reason they were not further explored at this time.

TABLE VI-5. River Power and Tug Power

Q(cfs)	20,000	10,000	5,000	2,000
1) $P_{river}\left(\dfrac{lb\ ft}{linear\ ft}\right)$	25	6.7	1.74	.28
2) $P_{tug}\left(\dfrac{lb\ ft}{linear\ ft}\right)$	------------- 250,000 ----------------			
River length (miles) equivalent to a 5000 hp tug	1.9	7.0	27	169

$$P_{river} = \frac{\gamma QS(1)}{U} \left(\frac{lb}{ft^3}\ \frac{ft^3}{sec}\ \frac{ft}{ft}\ sec\right)$$

$$P_{tug} = \frac{HP}{U}\ ,\ \text{values of Q, S and U from Table VI-3.}$$

VII. THEORETICAL ESTIMATES OF THE METRO WWTP EFFLUENT MIXING ZONE

A. Horizontal Mixing Zone Model

If transverse mixing (neutrally buoyant) prevals, estimates of the length of the mixing zone below the Metro WWTP outlet into the Mississippi River can be made with the aid of the closed form analytical solutions given in Section V.B.1. More accurate estimates will be possible after a streamtube model conceptually outlined in Section V.B.2 has been developed and after the required coefficients have been determined from field data.

The dimensionless river distance x' defined in Eq. V-9 and used e.g. in Figs. V-2, V-4, and V-5, can be expressed in terms of real distance x along the river.

From
$$x' = \frac{xD}{UB^2}$$

$$x = x' \frac{UB^2}{D} = \frac{x'UB^2}{Cu_* H} = \frac{Q_r Bx'}{Cu_* H^2} . \tag{VII-1}$$

The parameter $Q_r B/u_* H^2$ has been determined in Table VI3 for five flow rates. Its value at low flow rates is 525,000. Theory predicts that concentrations at the two banks are within 10 percent of the fully mixed river value at a distance $x' = 0.3$. In the Mississippi River, the distance required to achieve this is

$$x_{90\%} = \frac{(0.3)}{C} (525,000) = \frac{157,500}{C} \text{ (ft)}$$

The value of C for the Mississippi can only be guessed at present. Field measurements are necesssary to determine the actual C value of the Mississippi River reach. The effect of the very irregular river bed profile will probably be important. Since the wing dams are on alternate river sides, the river is forced to meander in its own bed. A more accurate assessment of the wingdam effects can be made by the streamtube model. That model requires information on flow velocity distribution in each cross section which has not yet been developed.

54

The C value will probably be larger than 3.0 and possibly as large as 6.0. The length of the mixing zone for neutrally buoyant effluent conditions would correspondingly be anywhere between 5 miles and 10 miles.

An estimate of the buoyancy effects on the transverse mixing coefficient requires evaluation of the parameter $Q_p g'/H u_*^3$. At river mile 835.3 (Section 78 of the 1971 DNR study) and under mean monthly July conditions: $H = 18$ ft, $Q_p \approx 360$ cfs, $g' \approx (32.2)(0.0011) = 0.035$ ft/s^2 $u_* = 0.098$ ft/s at $Q_r = 15,400$ cfs. Therefore, $Q_p g'/H u_*^3 = 740 > 5$. This indicates that under mean monthly summer conditions the buoyancy will accelerate transverse spreading. Buoyancy effects will be stronger under lower river flows. Further study of buoyancy induced transverse spreading in the Mississippi River is required.

B. Vertical Mixing Zone Model

If buoyancy and vertical mixing control the farfield of the mixing zone (Fig. III-4), then theory predicts that concentrations at the water surface and the river bottom are within 10 percent of the fully mixed river value at a distance $x'_{90\%} = 0.3$. This translates into a real distance

$$x_{90} = \frac{0.3 U H^2}{D} = \frac{0.3\, Q_r\, H^2}{C\, u_* H (HB)}$$

$$= \frac{0.3\, Q_r}{C\, u_* B} = \frac{0.3\, Q_r B}{C\, u_* H^2} \left(\frac{H}{B} \right)^2 \qquad \text{(VII-2)}$$

where $\dfrac{Q_r B}{u_* H^2}$ is given in Table VI-3,

$H/B \approx 14.3/800 = 0.018$, and

$C = D_v/u_* H$ given in Table VI-4.

One can therefore find the lengths of the farfield mixing zone controlled by vertical mixing as shown in Table VII-1. Nearfield distances have been estimated by considering a transverse underflow velocity of 0.3 ft/s and a travel distance of 500 ft, requiring about 1600 sec. The longitudinal displacement along the river during that time is estimated using velocities in Table VI-3.

TABLE VII-1. Estimates of Length of Mixing Zone Controlled by Vertical Mixing

	Q_r(cfs)	20,000	10,000	5,000	2,000	1,750
Strongly Stratified Flow	*$X_{nearfield}$	2,600	1,400	700	300	200
	$X_{farfield}$	1,600	2,800	6,100	16,200	
	X_{total}	4,200	4,200	6,800	16,500	
Weakly Stratified Flow	*$X_{nearfield}$	2,600	2,600	1,400	1,000	1,000
	$X_{farfield}$	700	700	700	700	700
	X_{total}	3,300	2,100	1,400	1,000	900

*Rough estimates.

VIII. FIELD STUDY

On July 7, 1982, and August 26, 1982, measurements were made in the
Mississippi River to trace the effluent flow from the WWTP. No artificial
tracers were added. Water temperature (T), dissolved oxygen (D.O.), speci-
fic conductance were measured in situ. Water samples were withdrawn with a
peristaldic pumping sampler and analyzed at the MWCC laboratories for
Chloride ($C\ell^-$), total dissolved solids (TDS), Zinc (Z), and Chromium (Cr).
Sewage and river water differ in all these water quality characteristics
for the following reasons:

- Sewage water has temperatures typical of the underground
  sewer system while river water, exposed to the atmosphere,
  follows strongly the seasonal variations. Differences
  can be up to 10°F at times.

- Dissolved oxygen in the WWTP effluent and the river are
  different because of BOD load, photosynthesis in the river,
  and other oxygen sources and sinks.

- Specific conductance (μmhos/cm) of water depends primarily
  on the amount of dissolved salts in the water and is therefore
  directly related to TDS.

- Total dissolved solids (TDS) are much higher in sewage than
  in river water because of inputs by industrial or domestic
  water users.

- Chloride in the form of $C\ell^-$ ion is one of the major inorganic
  anions in water and wastewater. The chloride concentration
  ($C\ell^-$) is higher in wastewater than in raw water because
  sodium chloride ($NaC\ell$) is a common article of diet and passes
  unchanged through the digestive system. It may also be added
  by industrial processes.

- Chromium salts are used extensively in industrial processes.
  Chromate compounds are frequently added to cooling water for
  corrosion control.

- Zinc enters the water from deterioration of galvanized iron
  and dezincification of brass. Zinc in water also may result
  from industrial waste.

The discharge from the Metro WWTP and the Mississippi River before
receiving the effluent have different temperatures and contain the above
materials in the concentrations shown in Table VIII-1. By looking at the

57

UM 835.5

AA ◯ MPO

UM 835.3
E   D   C   A

UM 835.2
E   D   C

+
835.0

UM 834.8
E   D   C   B

UM 834.4 E   D   C   B

(One Site at 833.1)

Feet

0   500   1000
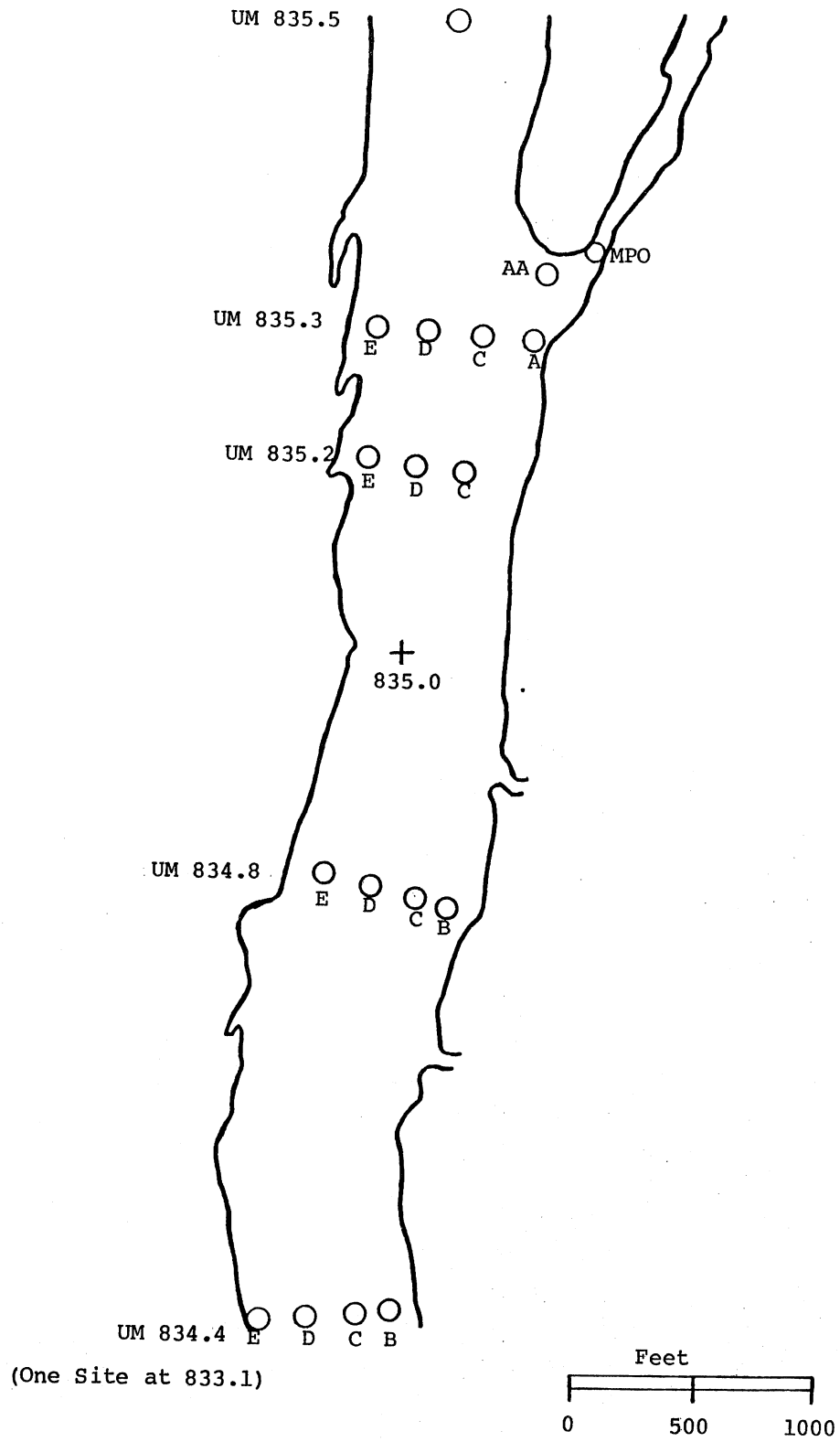
Fig. VIII-1.   Sampling sites on August 26, 1982.

excess values of concentration above the ambient river values, the effluent can be traced. T, Cℓ^-, and TDS, were found to be the most consistent tracers.

Measurements were made at 0.2 m, 1 m and every full meter below. Measurement sites are shown in Fig. VIII-1. A profile in midriver at UM 835.5 and another in midoutlet channel provided the necessary reference values shown in Table VIII-1. Measurements at the end of the outlet channel (Stations A and AA) were added to the August survey to document the sinking flow observed in July. Profiles were taken in cross sections with increasing distance from the outlet UM 835.3, UM 835.2, UM 834.8, UM 834.4 and UM 833.1.

Examples of measured vertical profiles at the end of the outlet channel divergence are shown in Fig. VIII-2. It is readily apparent that the effluent has plunged. The plunging was also visible along the water surface.

By interpolation of data, isotherms and isopleths on the river bottom and on the water surface were developed. Examples in Fig. VIII-3 show the formation of the underflow very clearly. Within less than 1,000 feet below the Metro WWTP outlet, the effluent has already reached the deepest part of the river channel.

Illustrations of cross-sectional data are given in Fig. VIII-4. The progressive mixing of the stratified river resulting from the WWTP discharge is apparent.

At river mile UM 834.4, the WWTP effluent and the river water were found pretty much well-mixed. A large portion of this mixing could be attributed to barge traffic. To illustrate this point, estimates were made of the travel time of the effluent from the outlet to the point of measurements. With this information and a record of barge passages taken during the field survey, it was then possible to determine how often a mass of water had been traversed by a tugboat before being measured at some point and time downstream.

A compilation of vertical profiles of T, D.O. and Cℓ^- by frequency of barge and tugboat passages is given in Figs. VIII-5a through III-5c. It appears that after the passage of three tugs, vertical gradients in concentration are no longer of significant levels; effluent and river water can be considered as well mixed.

TABLE VIII-1 (Part 1)

Mississippi River Mixing Zone Study, July 7, 1982
REFERENCE DATA

Depth (m)	T (°F)	T (°C)	D.O. (mg/ℓ)	Conductance (μmhos @ 25°C)	Cl⁻ (mg/ℓ)	TDS (mg/ℓ)	Zn (mg/ℓ)	Cr (μg/ℓ)
Inside Metro WWTP Outlet Channel, UM 835.3, Q_p = 340 cfs								
0.2	69.5	20.6	5.45	1080	125	558	.115	27
1.0	69.2	20.6	5.35	1080	124	542	.115	23
1.5	69.4	20.7		1080	124	558	.11	26
Avg.	69.4	20.65	5.4	1080	124	547	.112	25
Upstream River Reference, UM 835.5, Q_r = 11,100 cfs.								
	78.4	25.7	7.2	545	16.0	320	.020	1.3
Outlet Excess (Outlet Minus River)								
	-9.0	-5.05	-1.8	535	108	227	.092	23.7

TABLE VIII-1 (Part 2)

Mississippi River Mixing Zone Study, July 26, 1982
REFERENCE DATA

Depth (m)	T (°F)	T (°C)	D.O. (mg/ℓ)	Conductance (μmhos @ 25°C)	Cℓ⁻ (mg/ℓ)	TDS (mg/ℓ)	Zn (mg/ℓ)	Cr (μg/ℓ)
Inside Metro WWTP Channel, UM 835.3, Q_p = 403 cfs								
0.2	72.1	22.0	8.3	1180	119.2	631	.165	22.8
0.75	72.1	22.0	8.15	1180	123.7	615	.22	17.5
1.5	72.1	22.0	8.15	1180				
Avg.	72.1	22.0	8.2	1180	121.4	623	.193	20.2
Upstream River Reference, UM 835.5, Q = 4700 cfs								
0.2	74.0	23.1	6.85	607	16.5	291	.018	5.0
1.0	73.6	22.8	6.1	606	17.5	299	.030	5.0
2.0	73.6	22.8	6.1	606	17.7	283	.070	5.3
3.0	73.5	22.8	6.05	616		305	.017	4.5
4.0	73.5	22.8	6.0	616		296	.017	4.9
5.0	73.5	22.8	5.95	626	16.7	290	.042	4.7
6.0	73.5	22.8	5.95	626	16.7		.013	5.4
Avg.	73.5	22.8	6.0	615	17.0	296	.030	5.0
Outlet Excess (Outlet Minus River)								
	-1.4	-0.8	2.2	565	104.4	327	.163	15.2

Temp (°F)

D.O. (mg/l,

Spec. Cond.
(μmhos/cm)

Cℓ (mg/l)
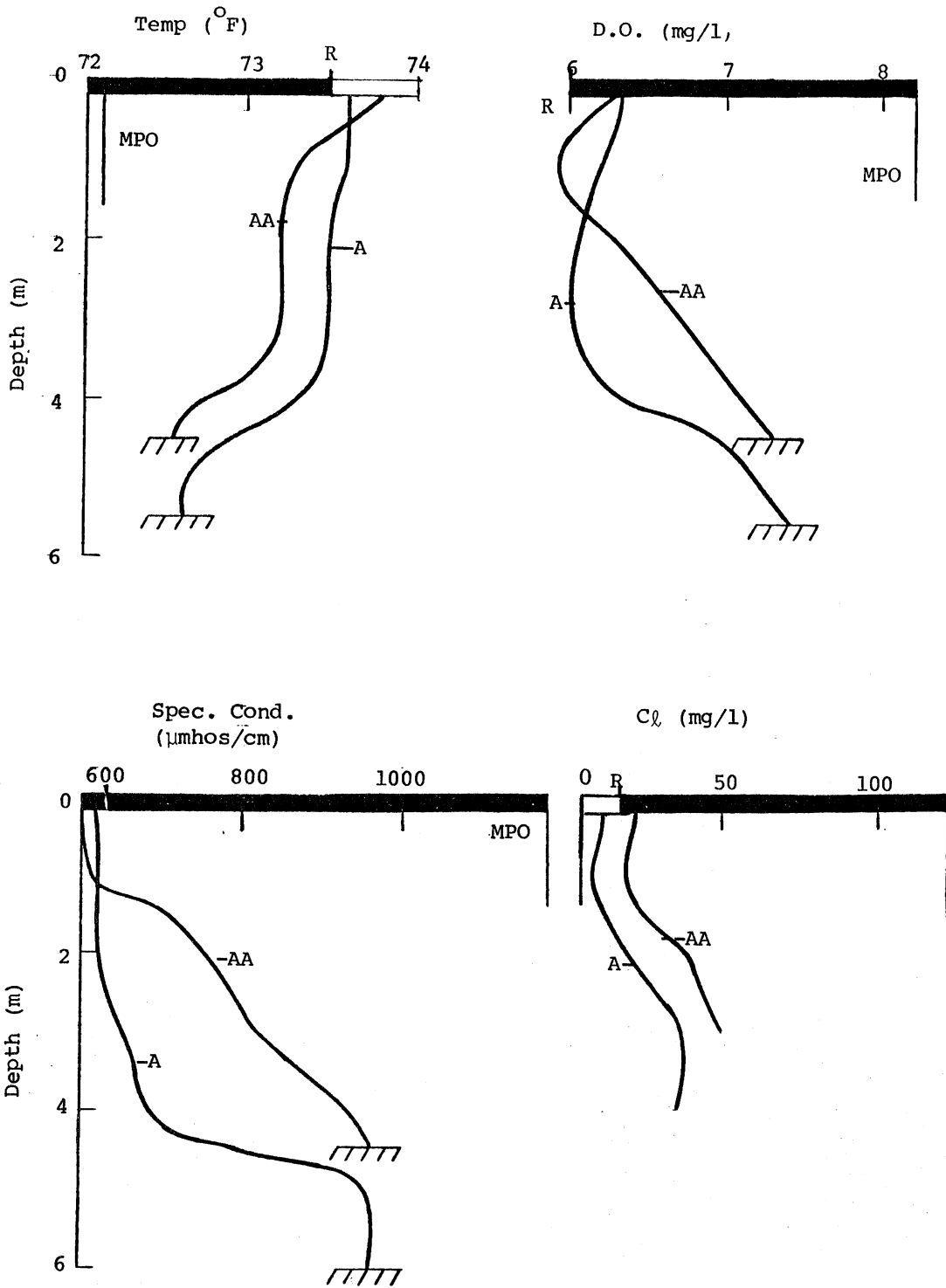
Fig. VIII-2. Water quality parameters at end of diverging
outlet channel showing plunging flow. Bars
indicate range between river reference (R) and
effluent (MPO) values. (Cont'd)

TDS (mg/l)

Zinc (mg/l)

(AA value mixxing
at 3 meters)

Chromium (mg/l)
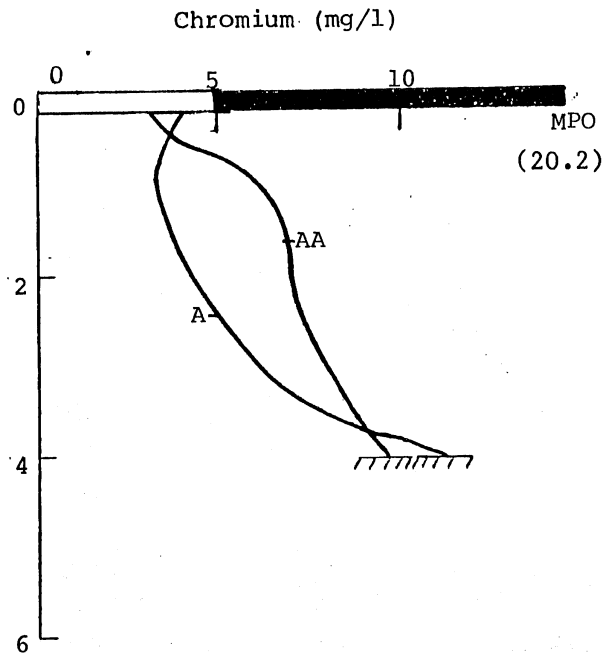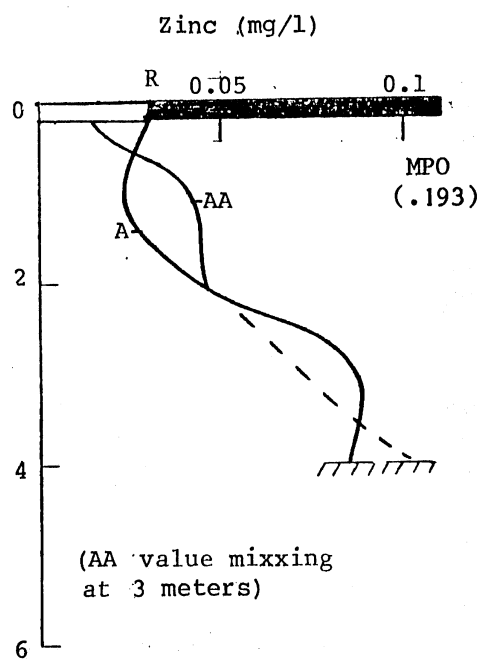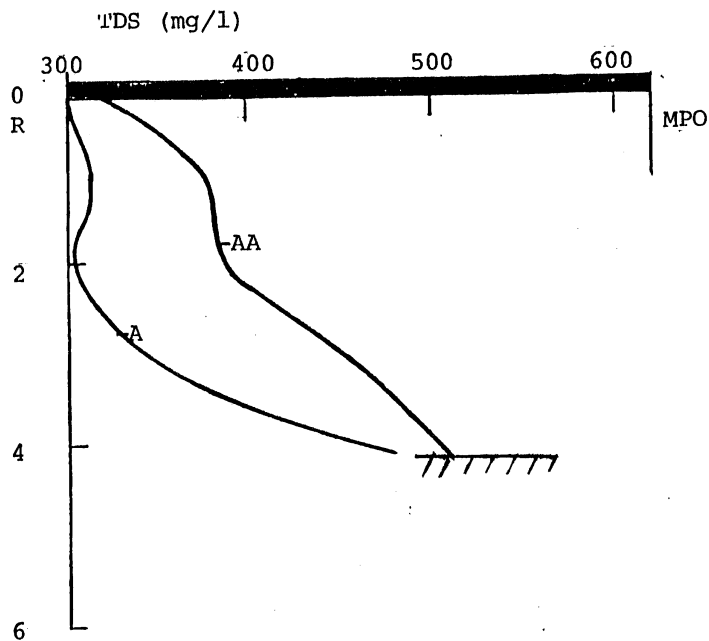
Fig. VIII-2 (Cont'd). Water quality parameters at end of diverging
outlet channel showing plunging flow. Bars indicate
range between river reference (R) and effluent (MPO)
values.

73.5

1010

4700 cfs

403 cfs

73.6

73.3

1050-1230

72.1

72.8

73.2

72.1

73.6

1350-1430

73.5

73.6

73.8

74.0

1500-1550

73.75

73.8

1610-1650 — 73.8

73.8

Bottom

1 m depth
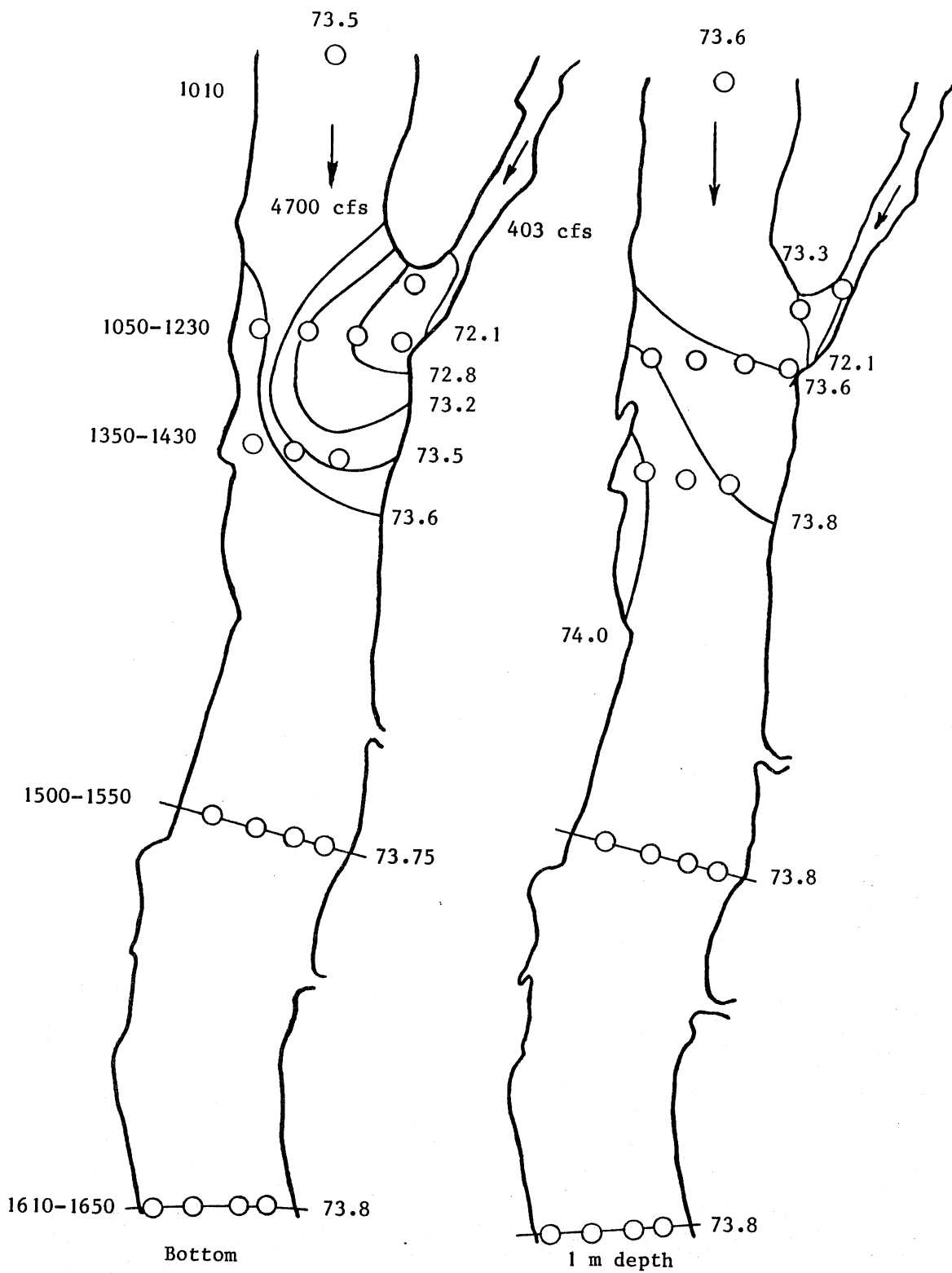
Fig. VIII-3a. Isotherms - August 26, 1982.
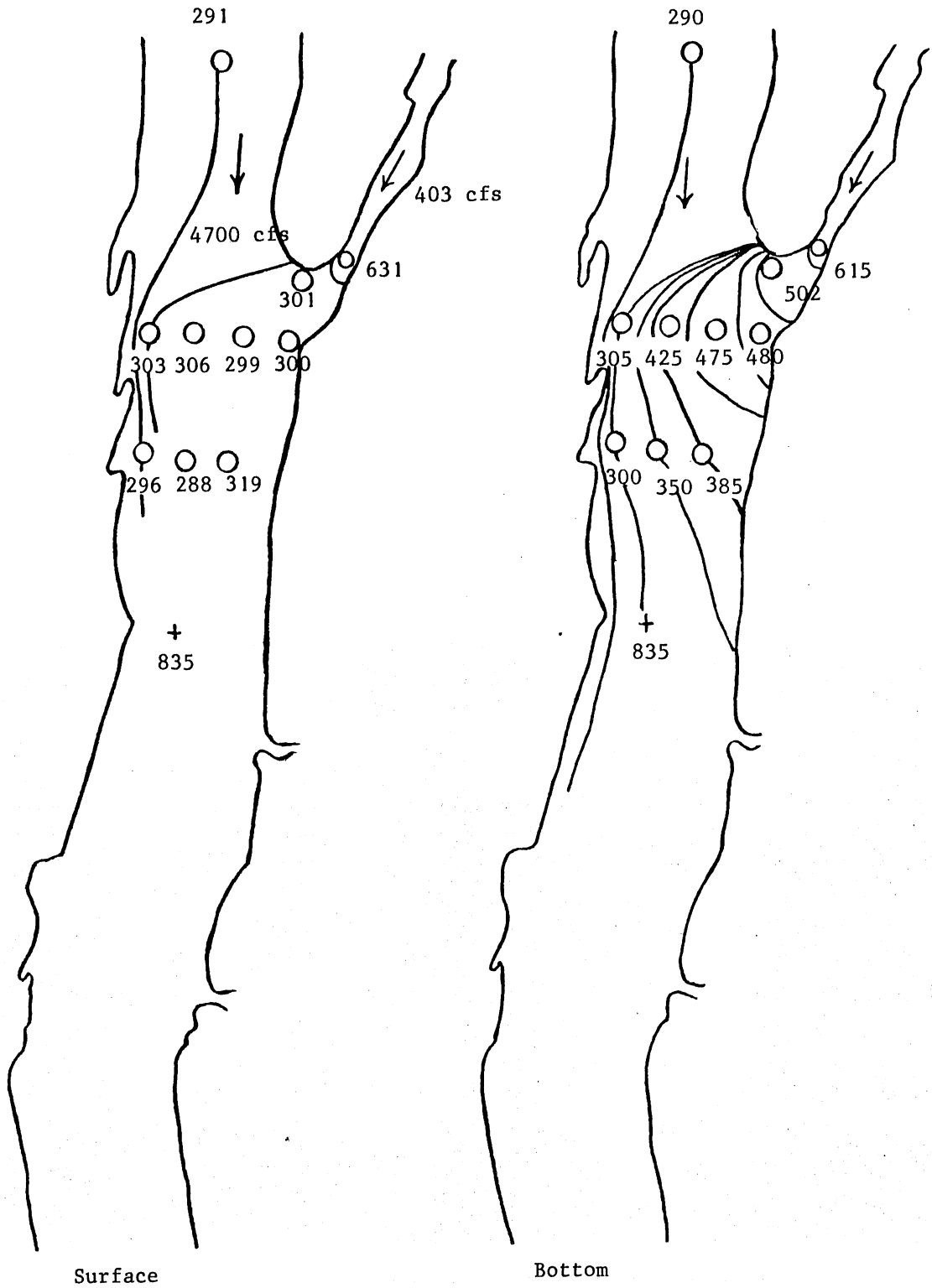
Fig. VIII-3b. TDS isopleths - August 26, 1982.
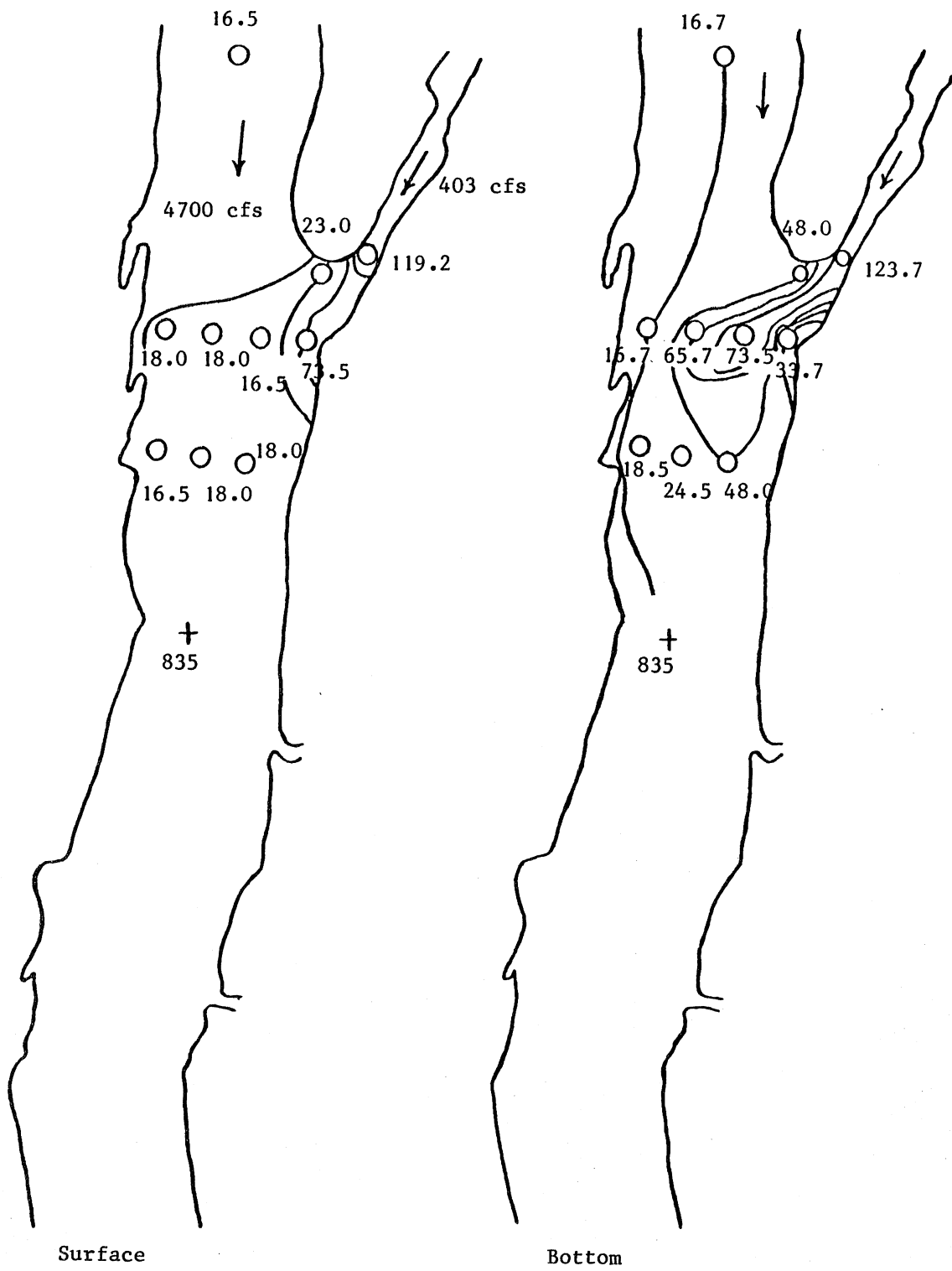
Fig. VIII-3c. Chloride isopleths–August 26, 1982.

66

6.0

6.1

↓

↓

4700 cfs

4700 cfs

403 cfs

6.3

403 cfs

8.2

6.2

8.2

7.4

7.1

6.4

6.9

6.7

6.4

6.4

Bottom

1 m depth
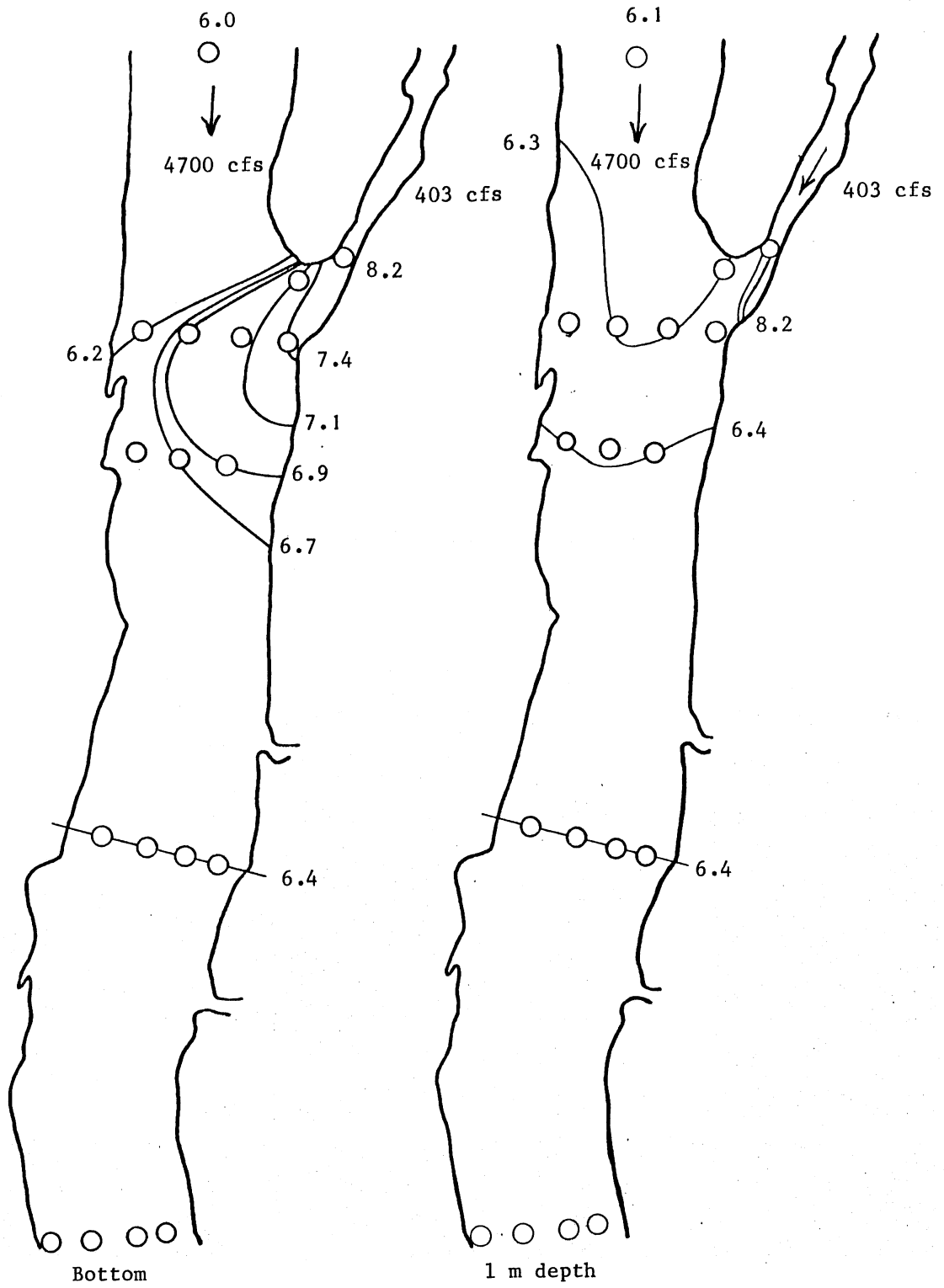
Fig. VIII-3d. Dissolved oxygen isopleths – August 26, 1982.
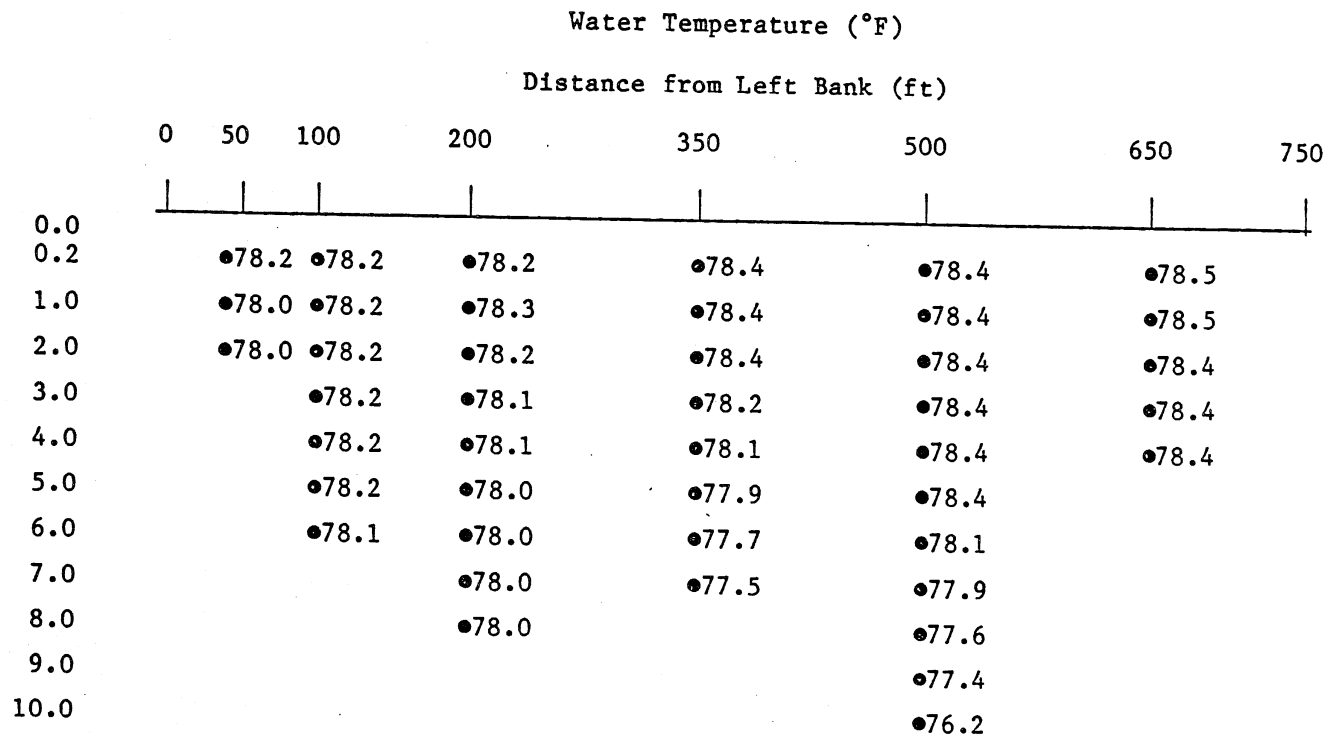
67

Water Temperature (°F)

Distance from Left Bank (ft)

Depth	0	50	100	200	350	500	650	750
0.0								
0.2		•78.2	◐78.2	•78.2	◐78.4	•78.4	•78.5	
1.0		•78.0	◐78.2	•78.3	•78.4	•78.4	•78.5	
2.0		•78.0	◐78.2	•78.2	•78.4	•78.4	•78.4	
3.0			•78.2	•78.1	◐78.2	•78.4	•78.4	
4.0			◐78.2	◐78.1	◐78.1	•78.4	◐78.4	
5.0			◐78.2	•78.0	◐77.9	•78.4		
6.0			•78.1	•78.0	◐77.7	◐78.1		
7.0				◐78.0	•77.5	◐77.9		
8.0				•78.0		◐77.6		
9.0						◐77.4		
10.0						•76.2		

	0	50	100	200	350	500	650
Meas. Time:		13:05	13:15	14:30	13:35	13:50	14:15
Travel Time:		:05	:15	:15	:15	:15	:15
Release Time:		13:00	13:00	14:15	13:20	13:35	14:00
Barge Passages:		0	0	0	0	1	0

FIGURE VIII-4a.
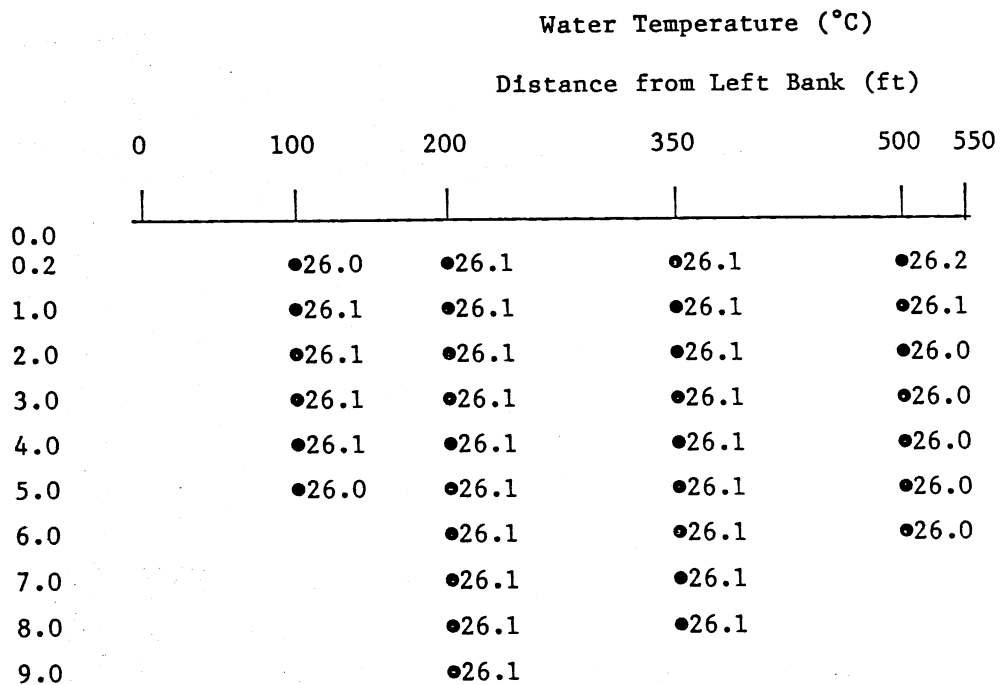
Water Temperature (°C)

Distance from Left Bank (ft)

Depth	0	100	200	350	500	550
0.0						
0.2		●26.0	●26.1	●26.1	●26.2	
1.0		●26.1	●26.1	●26.1	●26.1	
2.0		●26.1	●26.1	●26.1	●26.0	
3.0		●26.1	●26.1	●26.1	●26.0	
4.0		●26.1	●26.1	●26.1	●26.0	
5.0		●26.0	●26.1	●26.1	●26.0	
6.0			●26.1	●26.1	●26.0	
7.0			●26.1	●26.1		
8.0			●26.1	●26.1		
9.0			●26.1			

	100	200	350	500
Meas. Time:	16:35	17:36	17:15	16:55
Travel Time:	3:23	3:23	3:23	3:23
Release Time:	13:12	14:13	13:52	13:32
Barge Passages:	3	4	4	3

FIGURE VIII-4b.

69

Chloride Concentrate (mg/ℓ)

Distance from Left Bank (ft)
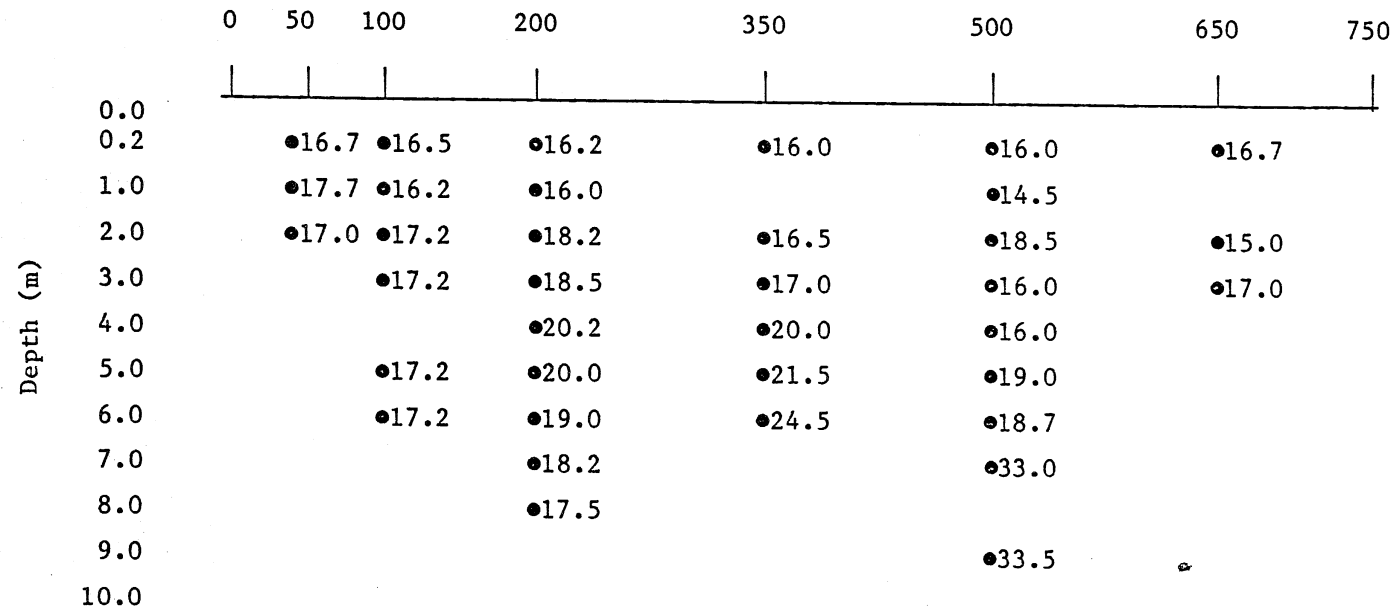
Depth (m)	0	50	100	200	350	500	650	750
0.0								
0.2		●16.7	●16.5	●16.2	●16.0	●16.0	●16.7	
1.0		●17.7	●16.2	●16.0		●14.5		
2.0		●17.0	●17.2	●18.2	●16.5	●18.5	●15.0	
3.0			●17.2	●18.5	●17.0	●16.0	●17.0	
4.0				●20.2	●20.0	●16.0		
5.0			●17.2	●20.0	●21.5	●19.0		
6.0			●17.2	●19.0	●24.5	●18.7		
7.0				●18.2		●33.0		
8.0				●17.5				
9.0						●33.5		
10.0								

Meas. Time:	13:05	13:15	14:30	13:35	13:50	14:15	
Travel Time:	:05	:15	:15	:15	:15	:15	
Release Time:	13:00	13:00	14:15	13:20	13:35	14:00	
Barge Passages:	0	0	0	0	1	0	

FIGURES VIII-4c.
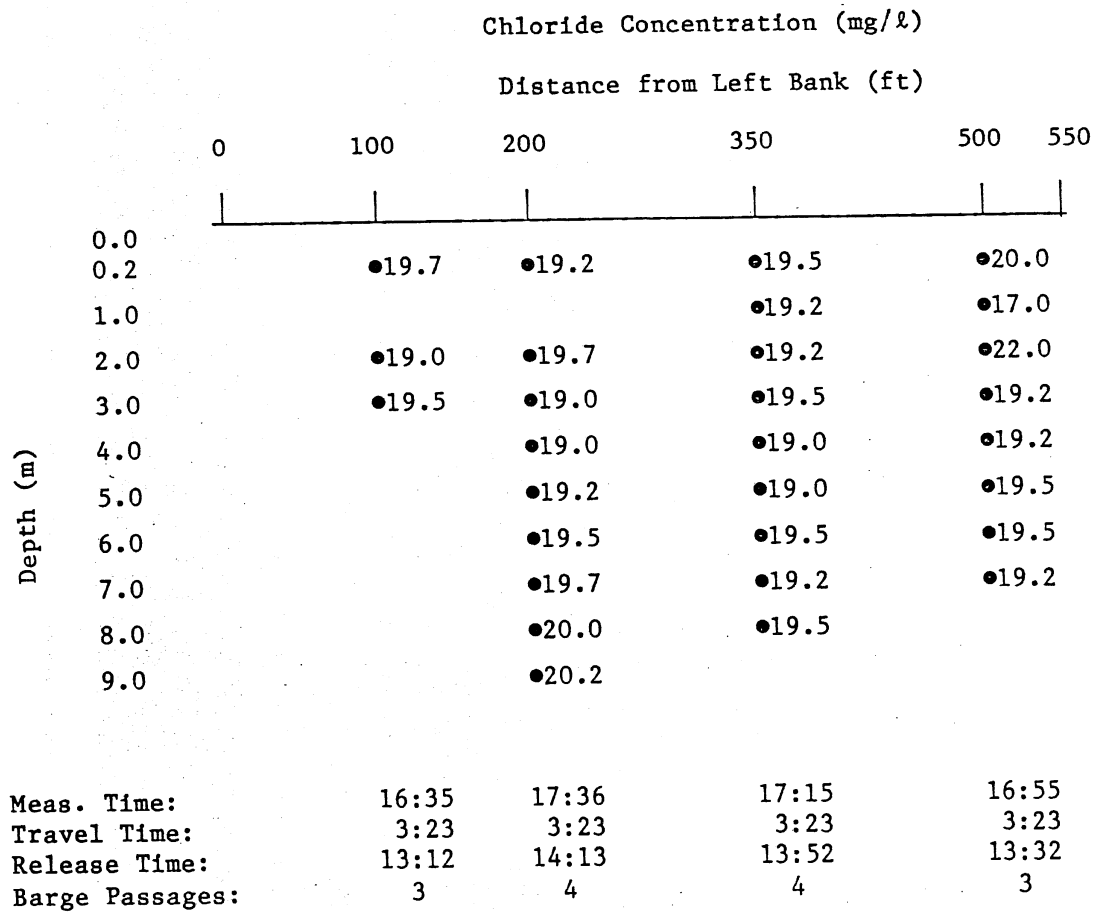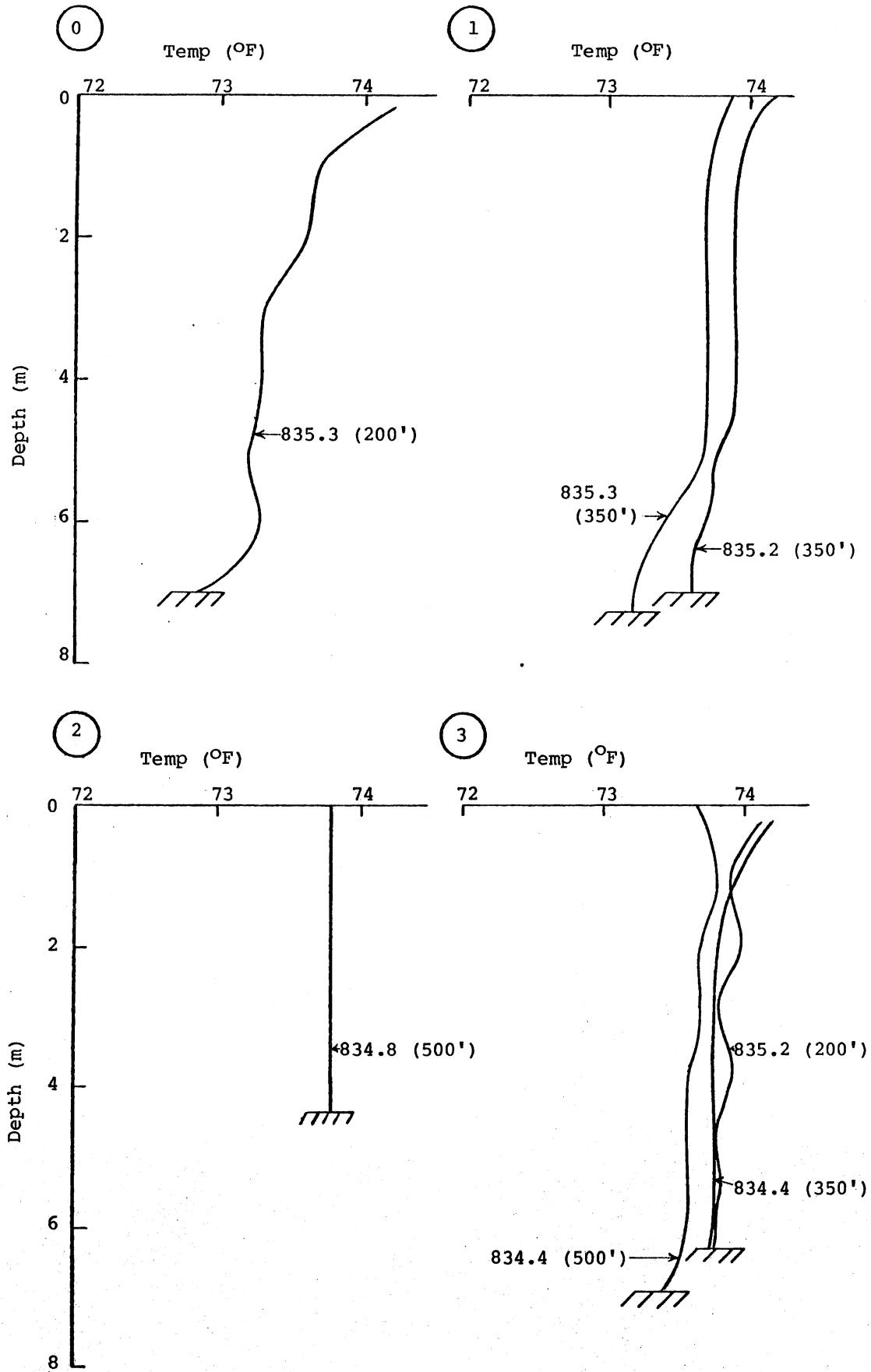
70

Chloride Concentration (mg/ℓ)

Distance from Left Bank (ft)

Depth (m)	0	100	200	350	500 550
0.0					
0.2		●19.7	●19.2	●19.5	●20.0
1.0				●19.2	●17.0
2.0		●19.0	●19.7	●19.2	●22.0
3.0		●19.5	●19.0	●19.5	●19.2
4.0			●19.0	●19.0	●19.2
5.0			●19.2	●19.0	●19.5
6.0			●19.5	●19.5	●19.5
7.0			●19.7	●19.2	●19.2
8.0			●20.0	●19.5	
9.0			●20.2		

Meas. Time:	16:35	17:36	17:15	16:55
Travel Time:	3:23	3:23	3:23	3:23
Release Time:	13:12	14:13	13:52	13:32
Barge Passages:	3	4	4	3

FIGURE VIII-4d.

71

Fig. VIII-5a. Vertical profiles of temperature as a function of
frequency of barge and tugboat passages. (Cont'd)

Fig. VIII-5a. Vertical profiles of temperature as a function
of frequency of barge and tugboat passage. (Cont'd)

73

(10) Temp (°F)
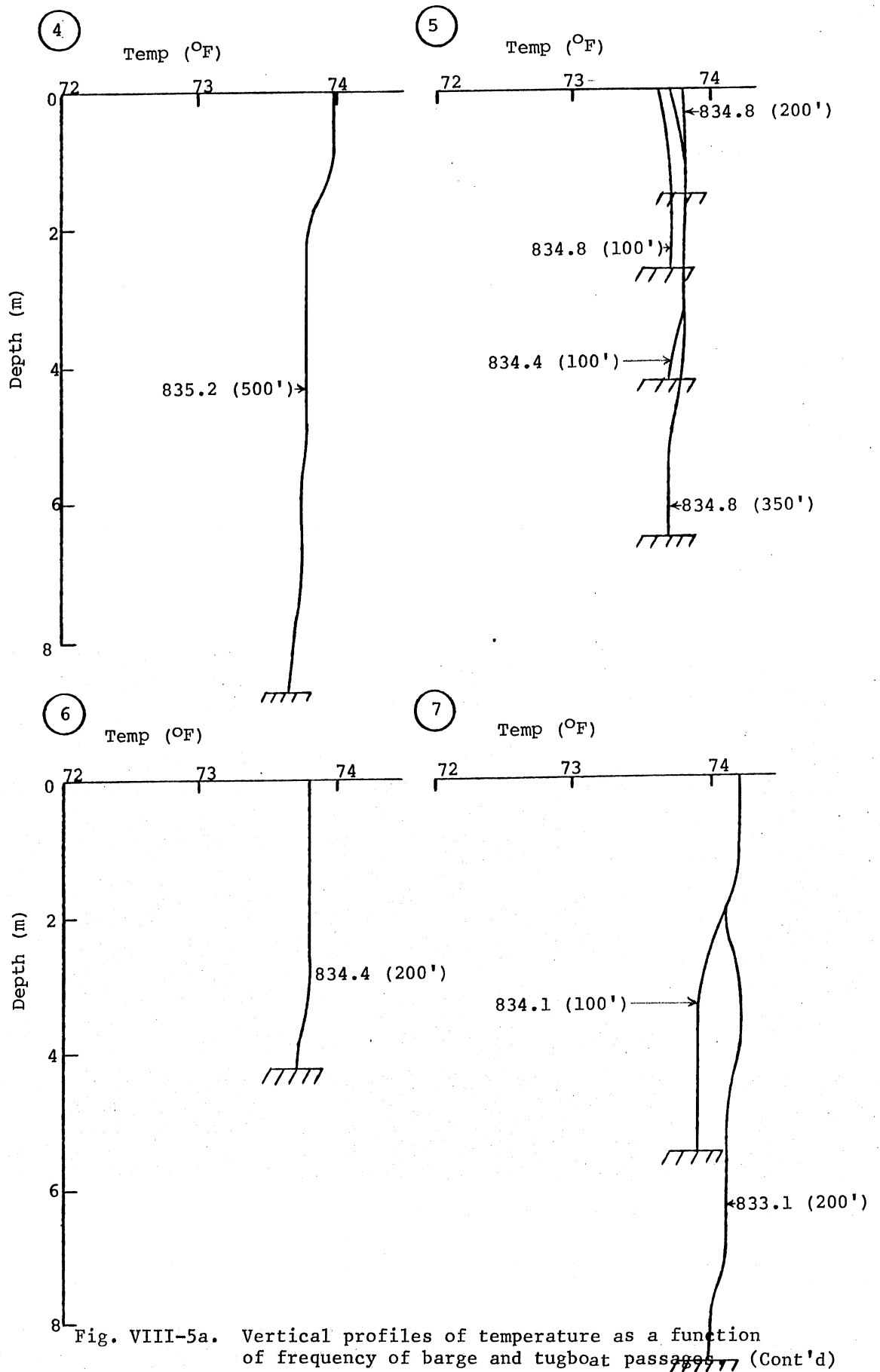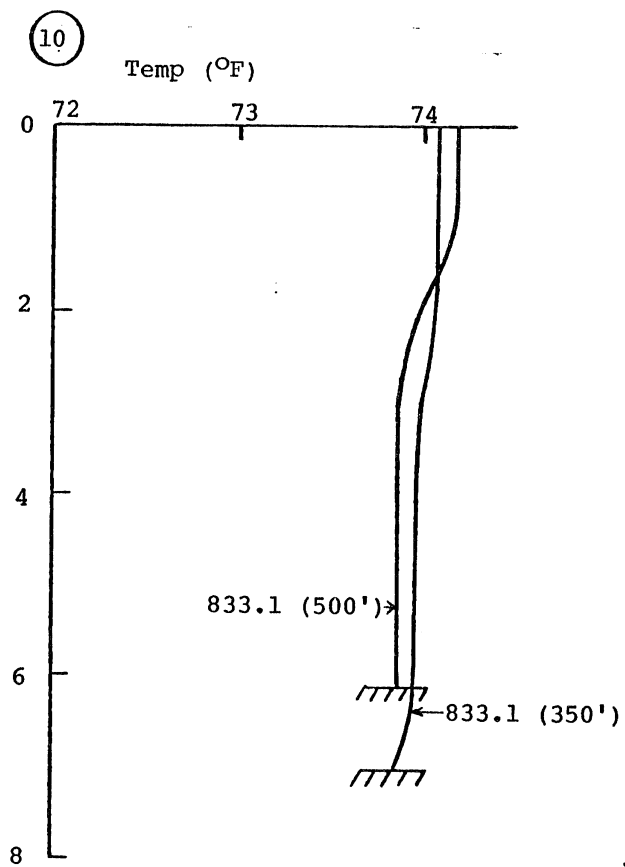
Fig. VIII-5a (Cont'd). Vertical profiles of temperature as
a function of frequency of barge and tugboat passages.

Fig. VIII-5b. Vertical profiles of chloride as a function of frequency of barge and tugboat passages. (Cont'd)

Fig. VIII-5b. Vertical profiles of chloride as a function of frequency of barge and tugboat passages. (Cont'd)

Fig. VIII-5b. Vertical profiles of chloride as a function of frequency of barge and tugboat passages. (Cont'd)

Fig. VIII-5b. Vertical profiles of chloride as a function of frequency of barge and tugboat passages. (Cont'd)

78
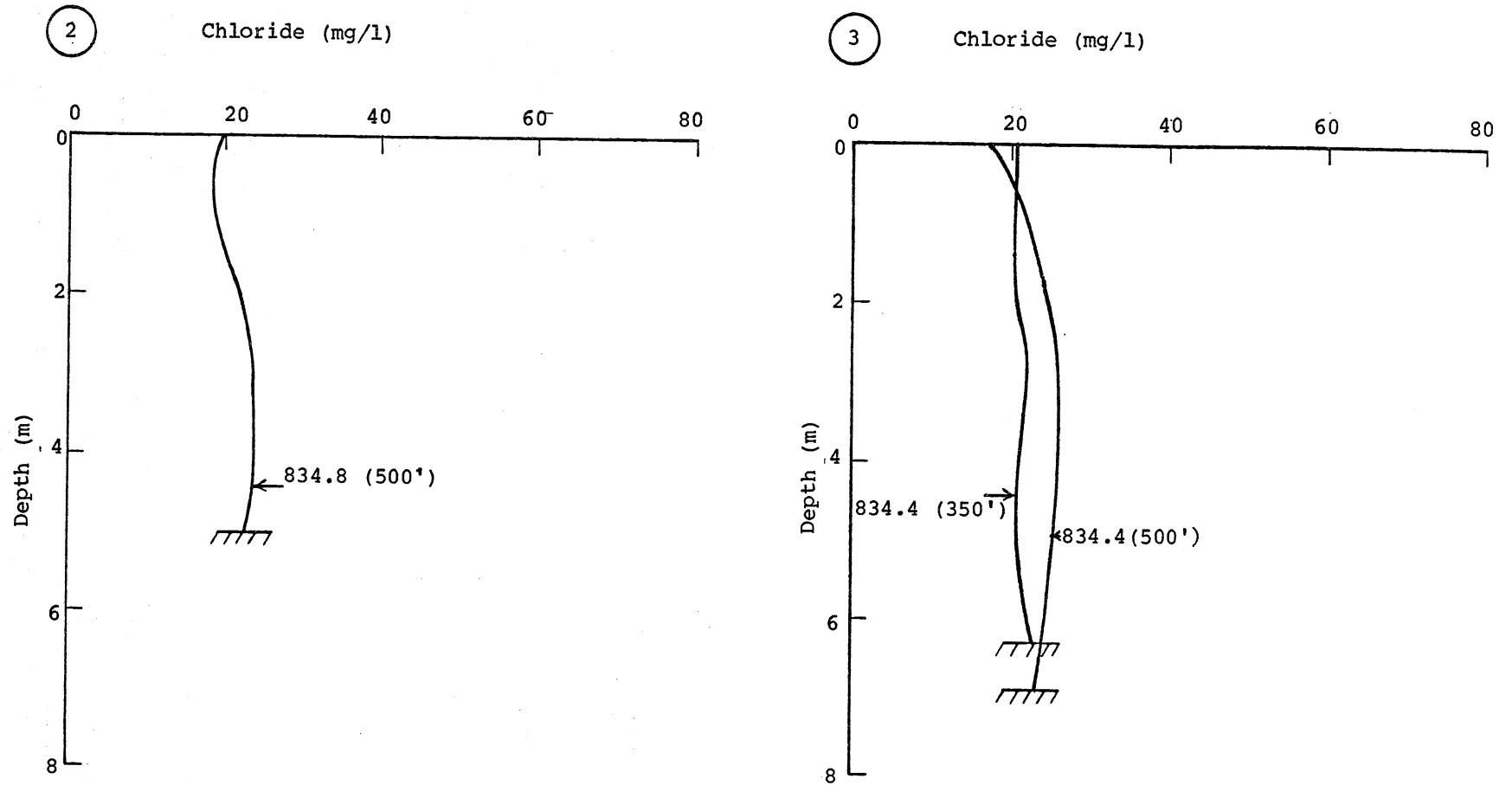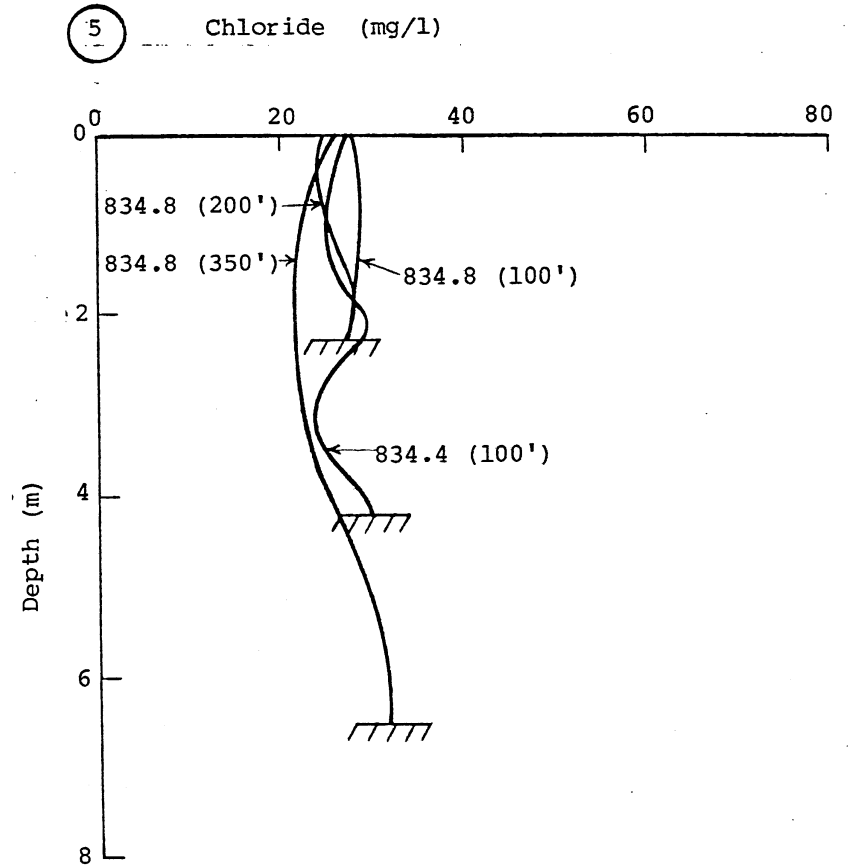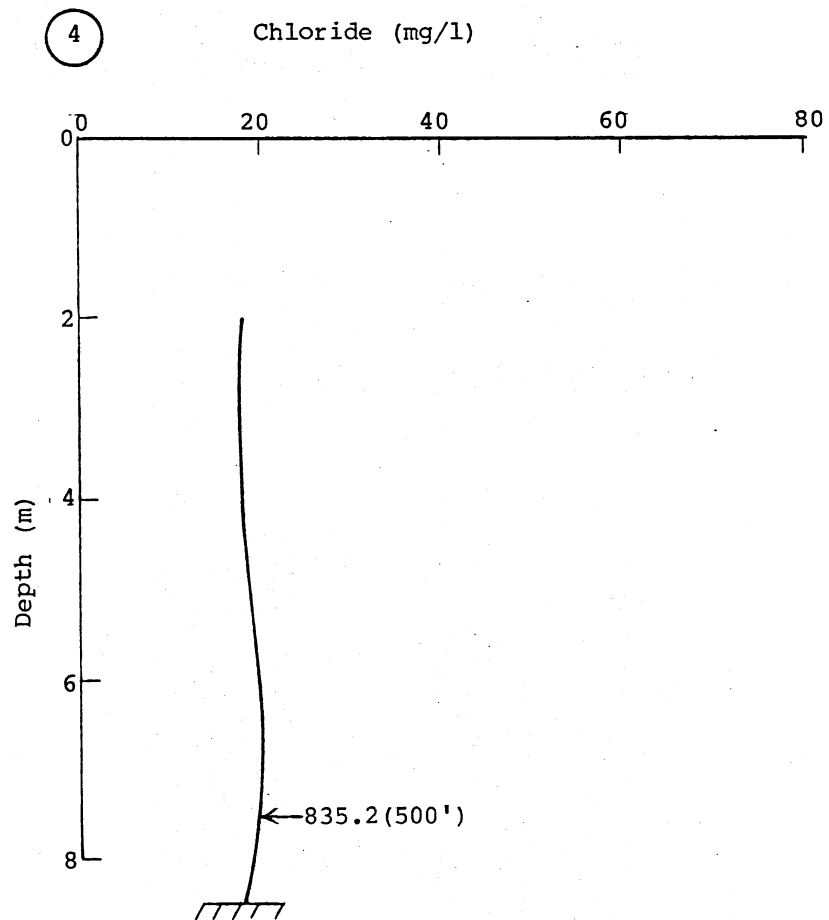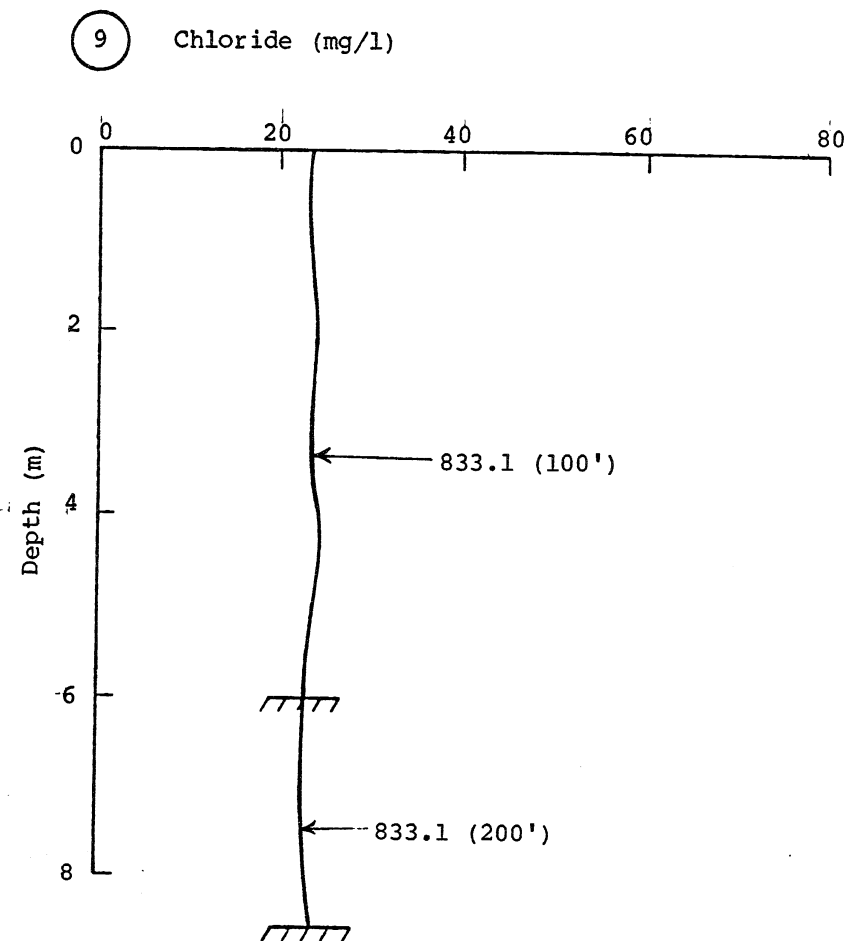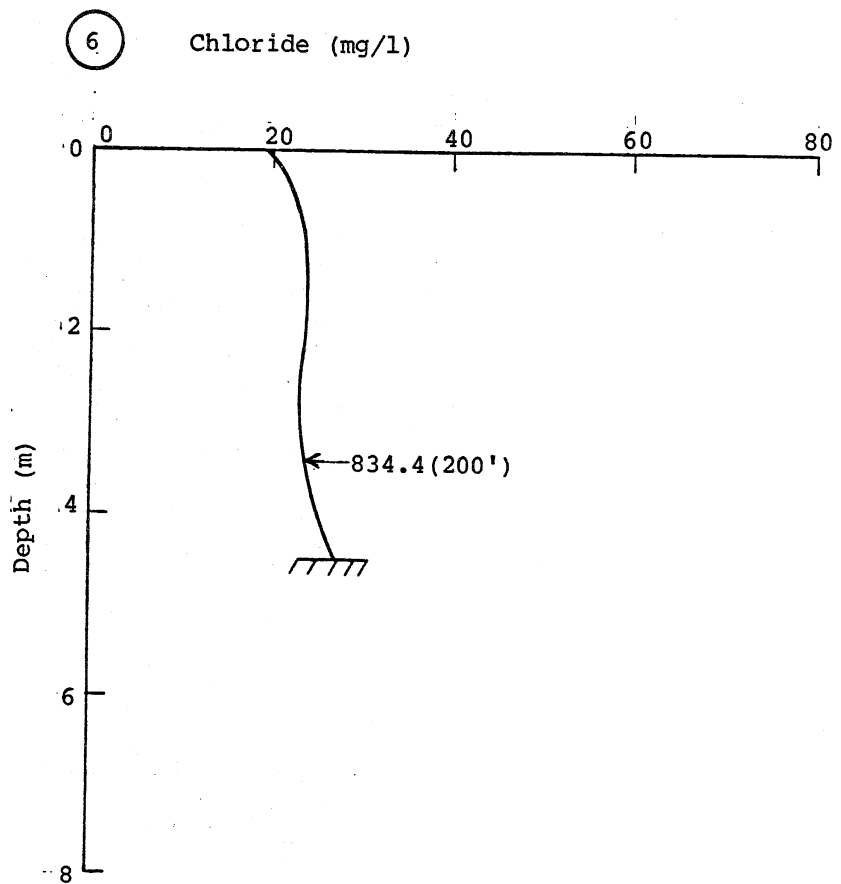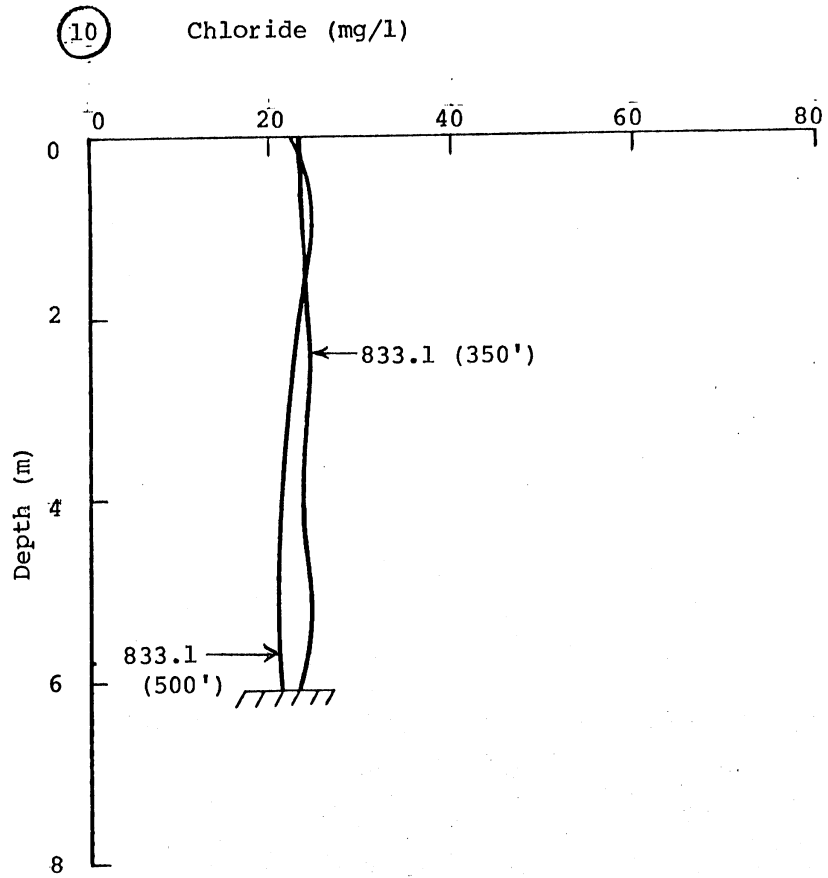
Fig. VIII-5b (Cont'd). Vertical profiles of chloride
as a function of frequency of barge and
tugboat passages.

Fig. VIII-5c. Vertical profiles of dissolved oxygen as a function of frequency of barge and tugboat passages. (Cont'd)

80
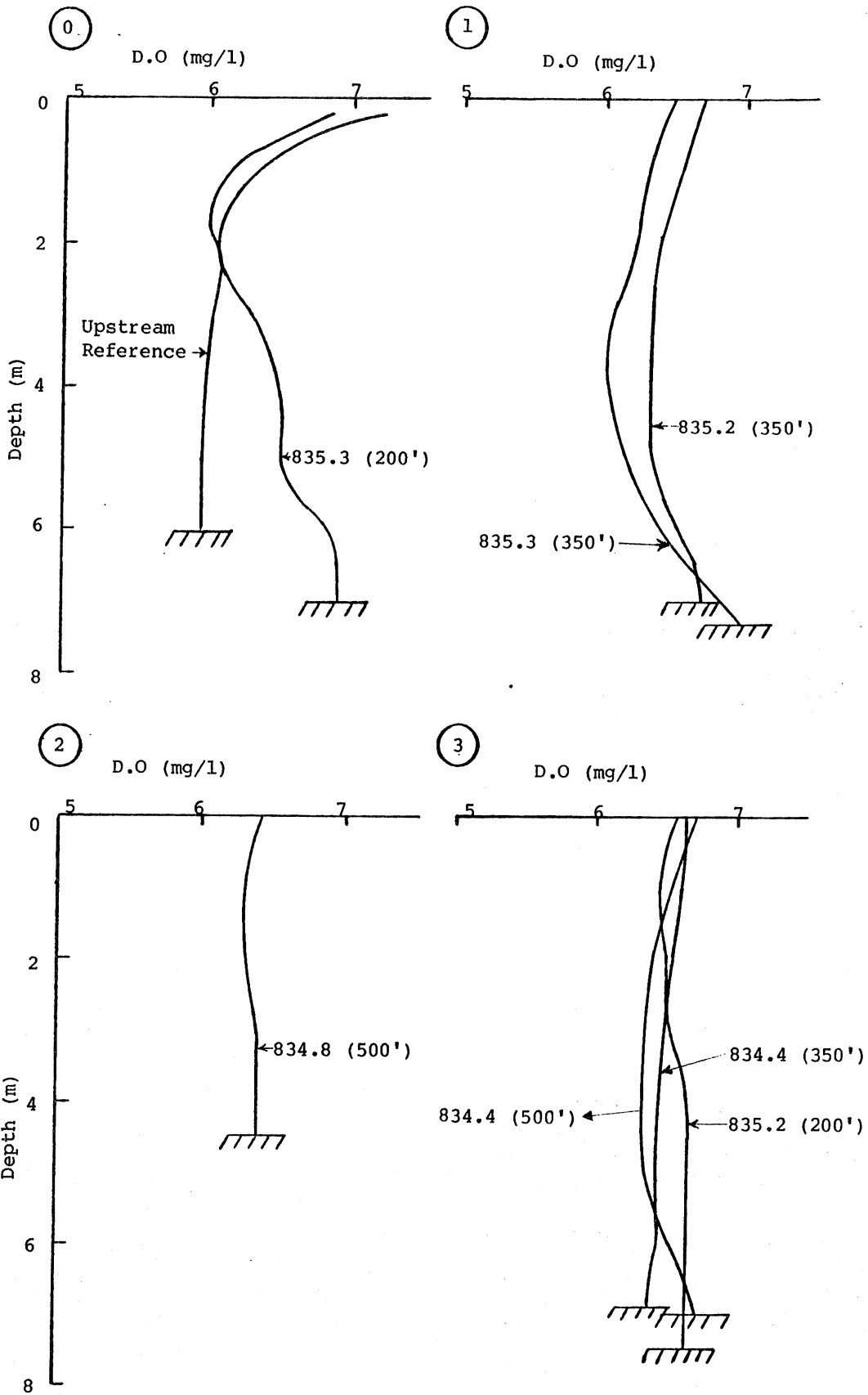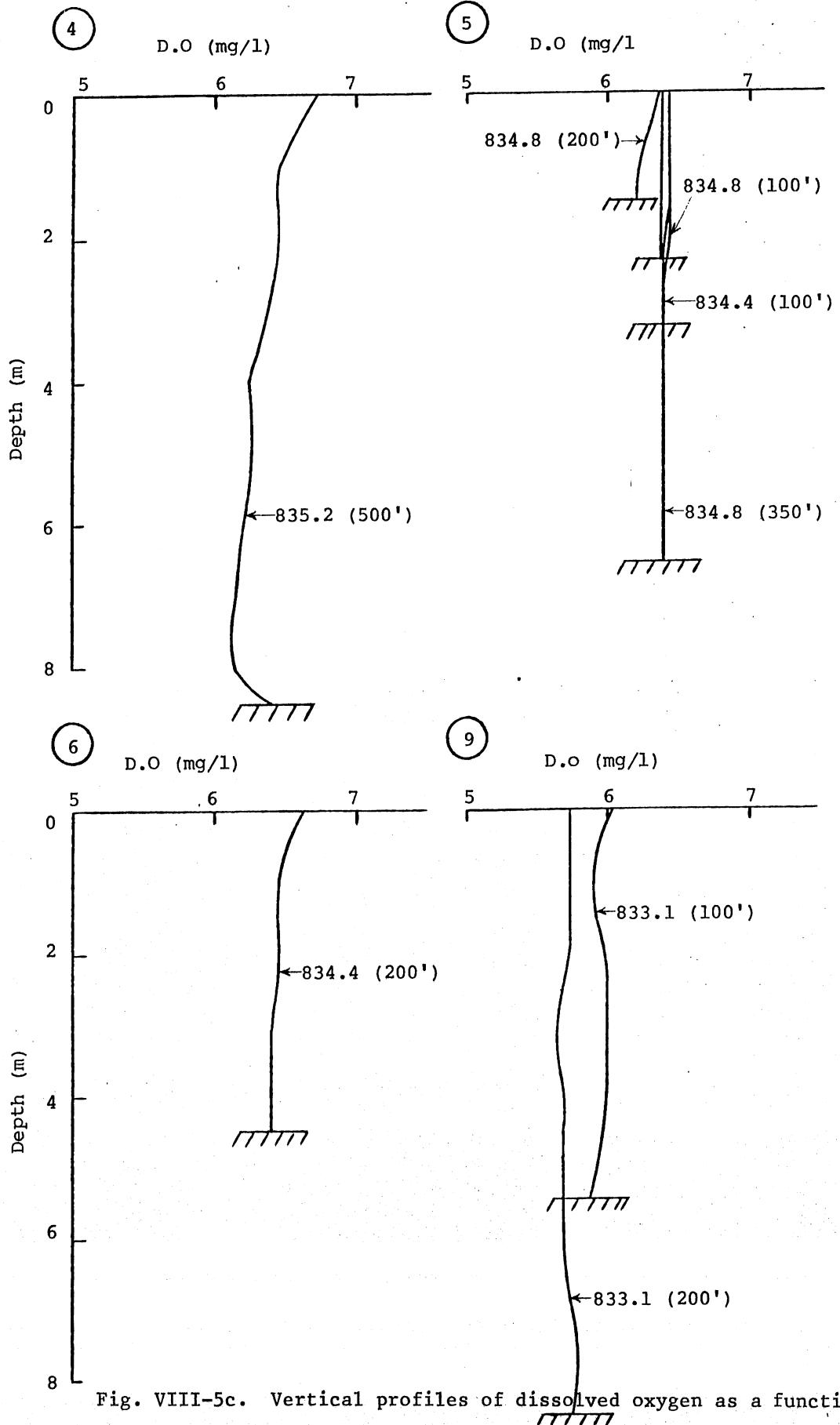
Fig. VIII-5c. Vertical profiles of dissolved oxygen as a function
of frequency of barge and tugboat passages.
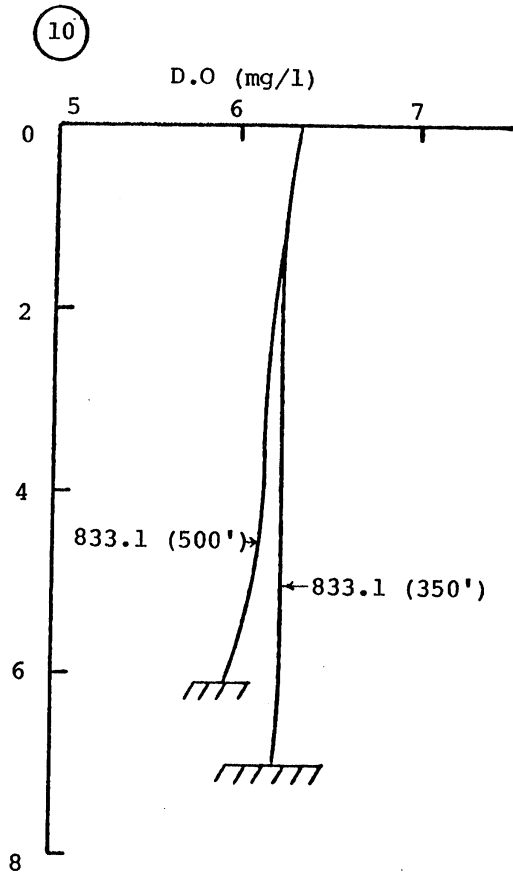
Fig. VIII-5c (Cont'd). Vertical profiles of dissolved oxygen
as a function of frequency of barge and tugboat
passages.

82

IX. SYNTHESIS OF THE SUMMER MIXING ZONE LENGTHS
OF THE METRO WWTP EFFLUENT

As a result of the theoretical considerations and two field surveys
reported in the preceding sections, the following description of the Metro
WWTP effluent zone can be given at this time:

(1) The extent of the mixing zone of the Metro WWTP effluent in the
     Mississippi River is strongly seasonally variable.

(2) The longest mixing zone of up to 5 miles length can be expected
     in fall or spring when the mixing is controlled by transverse
     spreading under neutrally buoyant conditions. Such conditions
     may also exist at very high flows during other seasons.

(3) Between May and September the Metro WWTP effluent plunges
     below the water surface before reaching the end of the
     diverging outlet channel. The effluent water therefore
     enters the Mississippi River as a submerged flow (underflow).
     Water temperatures and higher dissolved solids content in the
     effluent water relative to the oncoming Mississippi River
     water are the cause of the plunging phenomenon and the underflow.

(4) The spread of the effluent underflow across the river bottom
     appears essentially completed within 0.5 miles from the outlet
     or less the actual distance depending on river flow rate (Table
     VII-1). An analysis of the initial transverse spreading process
     (nearfield) has not been made.

(5) The river becomes vertically stratified below the outlet due
     to the sinking of the effluent into the deepest part of the
     river main channel.

(6) The most appropriate farfield model for the Metro WWTP effluent
     mixing zone in summer considers "vertical mixing" of the stra-
     tified river. (Schematic in Fig. III-4.)

(7) The vertical mixing of the stratified river (farfield) is
     accomplished by two very different mechanisms.

     (a) turbulent induced by shear on the river bed and
          secondary flow due to channel irregularities, and

     (b) barge traffic (tug boats).

(8) Gravity driven turbulent shear flow can accomplish complete ver-
     tical mixing within a distance which becomes longer and longer as

the river flow rate decreases. At flows somewhere below 4500 cfs
it becomes very difficult for the river flow to produce enough
turbulence to overcome stratification.

(9)   Vertical mixing of the stratified river is very effectively
       accomplished by barge traffic. The passage of three tug boats
       appears sufficient to reduce vertical water quality differentials
       to values within measurement accuracy. An approximate frequency
       of 1 barge tow/hr was observed.

(10)   To summarize the theoretical predictions and the field obser-
       vations, Fig. IX-1 was prepared. It gives the travel time of a
       water parcel versus river distance for several flow rates. That
       information was at first generated by computation (Table IX-1)
       and then compared to a few data points from the 1976/77
       Mississippi River dye study (Fig. IX-2). The calculated and
       observed velocities which are represented by the slopes of the
       lines in the time versus distance plots of Fig. IX-1 and IX-2 are
       in reasonable agreement.

(11)   It appears that for river flows below 6,000 cfs barge traffic
       controls the vertical mixing, whereas for river flows above
       20,000 mixing is predominantly by shear flow. Between 6,000
       and 20,000 cfs both are likely to make a significant contribution
       (Fig. VIII-1).

On the time versus distance diagram (Fig. IX-1) the theoretical esti-
mates of summer mixing zone lengths from Table VII-1 have been added for
a strongly stratified flow.

Also added were the distances (mixing lengths) corresponding to three
barge tow passages at a frequency of one per hour, one per two hours, and
one per three hours. These become the actual mixing zone lengths when
river flow is low and tugboats control the mixing.

Also shown in Fig. IX-1 (as circles) are the mixing zone lengths
observed in July and August, 1982, at river flows of 11,400 and 5,100 cfs,
respectively.

To facilitate the interpretation of Fig. IX-1, mixing zone lengths as
a function of river flow rate have been extracted and plotted in Fig. IX-3.
The values are the theoretical prediction from Table VII-1 with an adjust-
ment for the field observations made in summer of 1982. Figure IX-3 repre-
sents the best estimate of the Metro WWTP effluent mixing zone length in
summer, which can at present be given. Further studies of vertical mixing
in the Mississippi River are recommended to refine this result.

TABLE IX-1. Computation of Travel Time versus River Distance

Cross Section*	Distance (ft)	River Mile	Q = 10,000 cfs U ft/sec	L/U sec	Travel Time Q = 10,000 cfs sec	hrs	min	Q=5000 cfs hrs	min	Q=1750 cfs hrs	min
78	0	835.4	.91								
77	1000	835.2	.84	1140	1140		20		40	1	50
76	2000	835.0	1.03	1170	2210		40	1	20	3	30
75	3000	834.8	1.02	980	3190		50	1	40	5	00
74	4060	834.6	1.05	1020	4210	1	10	2	20	6	40
73	4660	834.5	.93	600	4810	1	20	2	40	7	35
72	6020	834.2	1.12	1330	6140	1	42	3	25	9	40
71	6930	834.0	.65	1030	7170	2	00	4	00	11	20
70	8030	833.8	.52	1880	9050	2	30	5	00		
69	8940	833.6	.42	1940	10990	3	00	6	00		
68	9960	833.4	.39	2520	13510	3	45	7	30		
67	10900	833.2	.45	2240	15750	4	20	8	40		
66	11910	833.0	.80	1620	17370	4	50	9	40		
65	12740	832.9	.78	1050	18420	5	10	10	20		

*1972 DNR flood plain study using HEC-2.
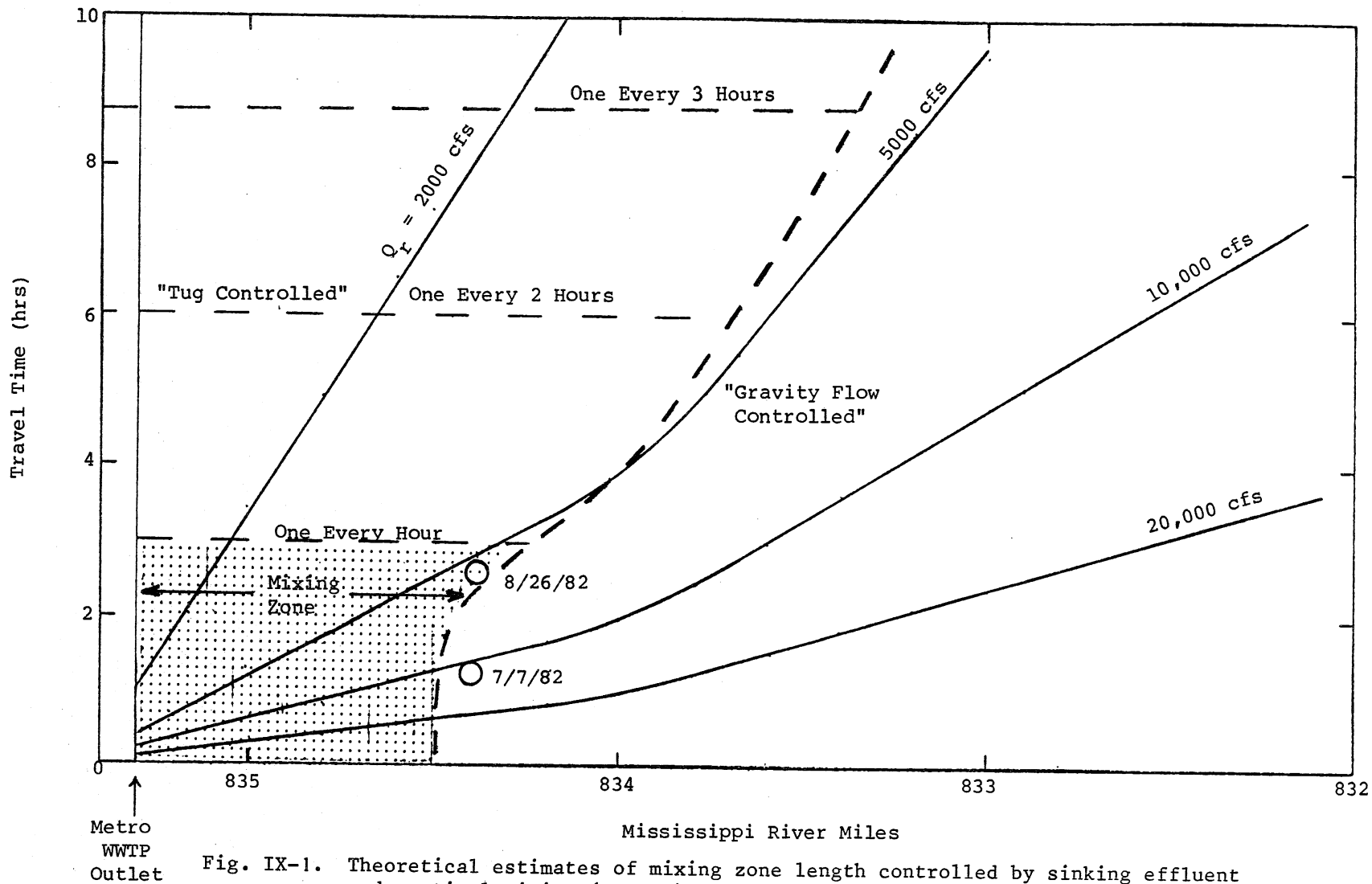
Fig. IX-1. Theoretical estimates of mixing zone length controlled by sinking effluent and vertical mixing (summer).
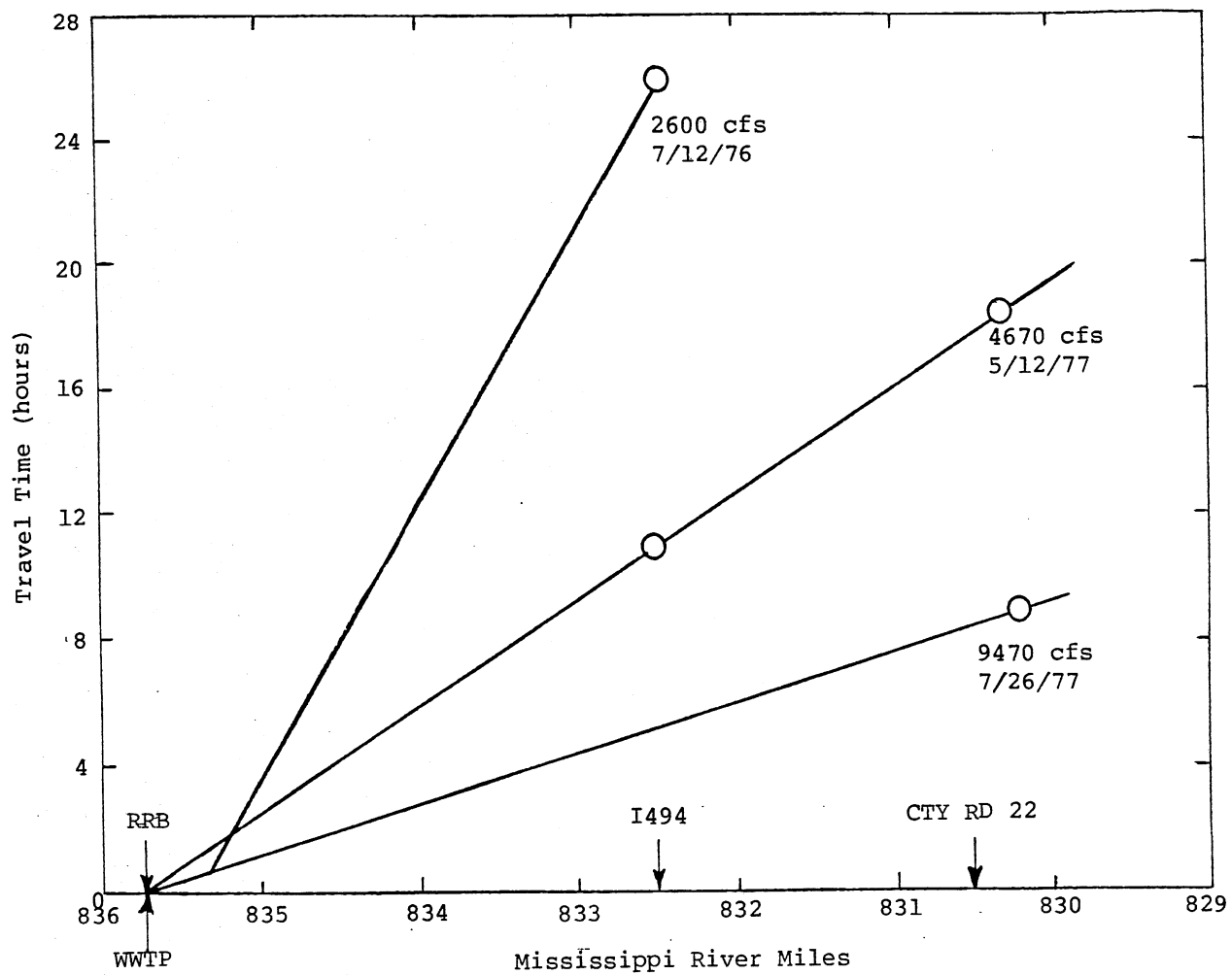
Fig. IX-2. Travel time versus distance diagram derived from 1976/77 Mississippi River dye studies.
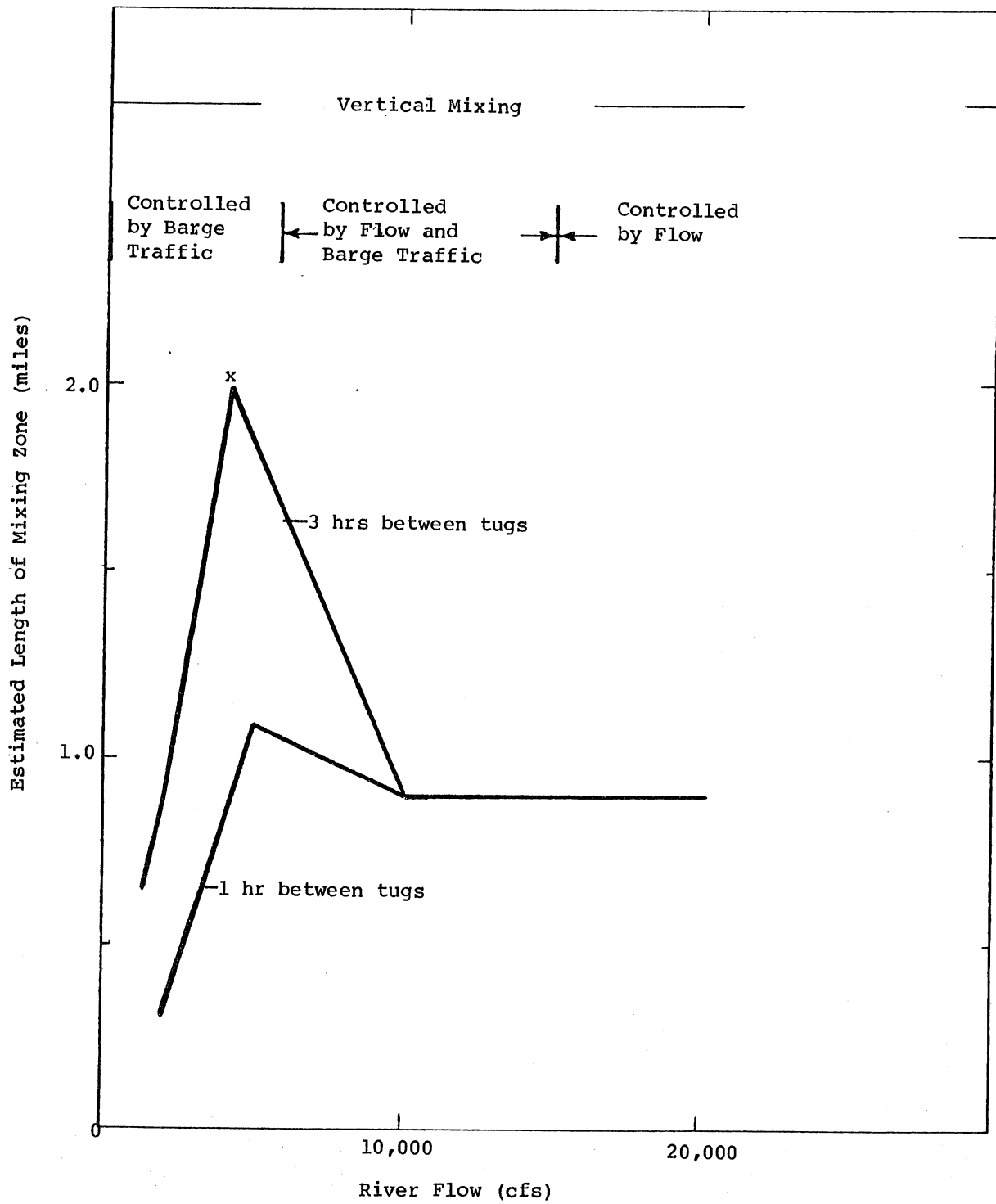
Fig. IX-3. Estimated summer mixing zone length of Metro WWTP
effluent into Mississippi River.

ACKNOWLEDGEMENTS

89

BIBLIOGRAPHY

Beltaos, S. Transverse Mixing Tests in Natural Streams, Journal Hydraulics Division, ASCE, Vol. 106, No. HY10, Oct. 1980, pp. 1607-1625.

Beltaos, S., Closure to "Transverse Mixing Tests in Natural Streams," Journal Hydraulics Division, ASCE, Vol. 107, No. HY12, Dec. 1981, pp. 1738-1746.

Bhowmik, N., Adams, R., Ronini, A., Guo, C-Y, Kisser, D., and Sexton, M., "Resuspension and Lateral Movement of Sediment by Tow Traffic on the Upper Mississippi and Illinois Rivers," Contract Report 269, Illinois State Water Survey, September, 1981.

Brooks, Norman H., "Dispersion in Hydrologic and Coastal Environments," U.S. EPA, Ecological Research Series, EPA-660/3-73-010, Aug., 1973.

Chen, Jing-Chang. Studies on Gravitational Spreading Currents, W. M. Keck Lab., Report No. KH-R-40, California Institute of Tech., Pasadena, Calif., March, 1980, 433 pp.

Demetracopoulos, A. D and Stefan, H. G. Transverse Turbulent Diffusion of a Cooling Water Discharge in a Wide and Shallow River, Journal Hydraulics Division, ASCE, 1982.

Eheart, James W. Two-Dimensional Water Quality Modeling and Waste Treatment Optimization for Wide, Shallow Rivers, Ph. D. Thesis, Univ. of Wisconsin, Madison, 1975, 355 pp.

Environmental System Engineering Institute, "Mixing Effects Due to Boating Activities in Shallow Lakes," NTIS No. PB-285 493, ESEI Technical Report No. 78-10, June, 1978.

Fischer, H. G., List, E. J., Koh, R.C.Y., Imberger, J., and Brooks, N. H. Mixing in Inland and Coastal Waters, Academic Press, 1979, 483 pp.

Harleman, D.R.F. Stratified Flow, Chapt. 26, in Handbook of Fluid Dynamics, V. L. Streeter, Ed., Wiley & Sons, 1960, p. 26-1 to 26-21.

Herricks, E. E. and Bantzer, C. J., "Effects of Barge Passage on the Water Quality of the Kaskaskia River," Environmental Engineering Series No. 60, Civil Engineering Studies, University of Illinois, Urbana, Illinois, December, 1980.

Holley, E. R. and Abraham, G. Laboratory Studies on Transverse Mixing in Rivers, Journal of Hydraulic Research, Vol. 11, No. 3, 1973, pp. 219-253.

Holley, E. R. and Abraham, G. Field Tests on Transverse Mixing in Rivers, Journal Hydraulics Division, ASCE, Vol. 99, No. 12, Dec., 1973, pp. 2213-2331.

Hoopes, J. A., Wu, D. S., and Villemonte, J. R. Mixing Zone Studies of the Sewage Discharge from the Waukesha Municipal Sewage Treatment Plant into the Illinois-Fox River at Waukesha, Wisc., Project Report, Department of Civil and Environmental Engineering, Univ. of Wisconsin-Madison, Feb., 1976, 139 pp.

Johnson, J. H., "Effects of Two Traffic on the Resuspension of Sediments and on Dissolved Oxygen Concentrations in the Illinois and Upper Mississippi Rivers under Normal Pool Conditions," Technical Report Y-76-1, U. S. Army Engineer Waterways Experiment Station, Environmental Effects Laboratory, Vicksburg, Mississippi, 1976, 181 pp.

Kaleris, V. and Schatzmann, M. Cooling-Water Dispersion under the Influence of Groynes, Third Conference on Waste Heat Management and Utilization, Miami Beach, Fla., May 11-13, 1981.

Karaki, S. and Van Hoften, J., "Resuspension of Bed Material and Wave Effects on the Illinois and Upper Mississippi Rivers Caused by Boat Traffic," CER 74-75SKJU9, Colorado State University, Ft. Collins, Colorado, Nov., 1974.

Lau, Y. Lam and Krishnappan, B. G. Modeling Transverse Mixing in Natural Streams, Journal Hydraulics Division, ASCE, Vol. 107, Feb. 1981, pp. 209-226.

Link, L. E., Jr. and Williamson, A. N., Jr., "Use of Automated Remote Sensing Techniques to Define the Movement of Two-Generated Suspended Material Plumes on the Illinois and Upper Mississippi Rivers," Army Engineer Waterways Experiment Station, Vicksburg, Mississippi, 1976, 71 pp.

McCutcheon, S. C. Vertical Velocity Profiles in Stratified Flows. Proc. Symp. on Surface Water Impoundments, ed. by H. G. Stefan, ASCE, Oct., 1981, pp. 1229-1238.

Paily, P. P. Mixing Zone Analysis for River Plumes, Journal Environmental Engineering Divsion, ASCE, Vol. 107, No. EE4, Aug., 1981, pp. 731-746.

Prych, E. A. Effects of Density Differences on Lateral Mixing in Open Channel Flows, W. M. Keck Lab. Report No. KH-R-21, Calif. Institute of Technology, Pasadena, Calif., May, 1970, 225 pp.

Rodi, W., Paulovic, R. N., and Srivatsa, S. K. Prediction of Flow and Pollutant Spreading in Rivers, Universität Karlsruhe, Report SFB 80/T/184, Sept., 1980.

Schatzmann, M. and Naudascher, E. Design Criteria for Cooling Water Outlet Structures, Journal Hydraulics Division, ASCE, Vol. 106, No. HY3, March, 1980, pp. 397-408.

Schiller, E. J. and Sayre, W. W. Vertical Temperature Profiles in Open Channel Flow, Journal Hydraulics Division, ASCE, Vol. 101, No. HY6, June, 1975.

Schiller, E. J. and Sayre, W. W. Vertical Mixing of Heated Effluents in Open Channel Flow, Iowa Institute of Hydraulic Research, Iowa City, Iowa, IIHR Report No. 148, September, 1973, 146 pp.

Somlyódy, L. An Approach to the Study of Transverse Mixing in Streams, Journal of Hydraulics Research, Vol. 20, No. 2, 1982, pp. 203-220.

Stefan, H. G. and Gulliver, G. S. Effluent Mixing Zone in a Shallow River, Journal Environmental Engineering Division, ASCE, Vol. 104, No. EE2, April, 1978, pp. 199-213.

Villemonte, J. R., Hooper, J. A., Wu, D. S., and Lillesand, T. M. Remote Sensing in the Mixing Zone. University of Wisconsin, Madison, Department of Civil and Environmental Engineering, Institute for Environmental Studies, Remote Sensing Program, Report No. 22, August, 1973 and Proc. Int'l. Symp. on Remote Sensing of Water Resources, AWRA, Burlington, Ontario, June, 1973.

Webel, Gisbert. Turbulente Quervermischung in Gerinneströmungen, Universität Karlsruhe, Rep. SFB 80/ET/205, April, 1982, 116 pp.

Yotsukura, N. and Sayre, W. W. Transverse Mixing in Natural Channels. Water Resources Research, Vol. 12, No. 4, Aug., 1976, pp. 695-704.

LIST OF TABLES

APPENDIX A.   Evaluation of Eq. V-12
(Point source with K'=0)

x'	$\frac{1}{(\pi x')^{1/2}}$	C/C_o		
		y'=0	y'=1	y'=1/2
0	(∞)	(∞)	0	0
0.005	7.9789	7.98	0	0
0.01	5.6419	5.64	0.000	0.011
0.02	3.9894	3.99	0.000	0.175
0.04	2.821	2.82	0.011	0.591
0.06	2.303	2.30	0.071	0.813
0.08	1.995	1.99	0.175	0.915
0.10	1.784	1.78	0.293	0.961
0.15	1.457	1.46	0.550	0.990
0.20	1.262	1.28	0.723	0.9996
0.30	1.030	1.10	0.895	1.0
0.40	0.892	1.038	0.961	1.0
0.50	0.7979	1.014	0.989	1.0

APPENDIX C — Evaluation of Eq. V-24

(Line Source with $K' = 0$, $Q_p/Q_r = 0.2$, $C_p = 5\,C_o$)

		c/c_p		
x'	$\dfrac{1}{\sqrt{4x'}}$	$y'=0$	$y'=1$	$y'=1/2$
0.005	7.07	0.9545	0	0
0.01	5.00	.8427	0	0.017
0.02	3.53	0.6827	0	0.0666
0.03	2.89		0	0.1082
0.04	2.5	0.5205	0.004	0.1378
0.06	2.04	0.4363	0.021	0.1716
0.08	1.76	0.3829	0.043	0.1866
0.10	1.58	0.3453	0.0664	0.1924
0.15	1.29	0.2850	0.1155	
0.20	1.118	0.2482	0.1486	
0.30	0.912	0.218	0.1803	
0.40	0.791	0.208	0.1930	
0.50	0.707		0.1974	